ISBN 978-82-326-5010-1 (printed ver.)
ISBN 978-82-326-5011-8 (electronic ver.)
ISSN 1503-8181

NTNU
Norwegian University of
Science and Technology

Salman Zaferanlouei

Doctoral thesis

Doctoral theses at NTNU, 2020:332

NTNU
Norwegian University of Science and Technology
Thesis for the Degree of
Philosophiae Doctor
Faculty of Information Technology and
ElectricalEngineering
Department of Electric Power Engineering

NTNU

Doctoral theses at NTNU, 2020:332

Salman Zaferanlouei

Integration of Electric Vehicles into Power Distribution Systems– The Norwegian Case Study

Using High-Performance Multi-Period AC Optimal Power Flow Solver

NTNU
Norwegian University of
Science and Technology

Salman Zaferanlouei

Integration of Electric Vehicles into Power Distribution Systems– The Norwegian Case Study

Using High-Performance Multi-Period AC Optimal Power Flow Solver

Thesis for the Degree of Philosophiae Doctor

Trondheim, October 2020

Norwegian University of Science and Technology
Faculty of Information Technology and Electrical Engineering
Department of Electric Power Engineering

NTNU
Norwegian University of
Science and Technology

NTNU
Norwegian University of Science and Technology

Thesis for the Degree of Philosophiae Doctor

Faculty of Information Technology and Electrical Engineering
Department of Electric Power Engineering

© Salman Zaferanlouei

ISBN 978-82-326-5010-1 (printed ver.)
ISBN 978-82-326-5011-8 (electronic ver.)
ISSN 1503-8181

Doctoral theses at NTNU, 2020:332

Printed by NTNU Grafisk senter

Preface

This work has been initiated by the Open and Autonomous Digital Ecosystems (OADE) project, and conducted entirely at the Department of Electric Power Engineering, NTNU, Trondheim. The main supervisor is Professor Magnus Korpås, head of the research group of Electricity Markets and Energy Systems Planning (EMESP), NTNU, and the co-supervisors are Professor John Krogstie, head of department of Computer Science, IDI, NTNU, and Associate Professor Hossein Farahmand, EMESP, NTNU.

The PhD was financed by the Faculty of Information Technology and Electrical Engineering, NTNU. k-sted:632015 NTNU-Prosjektnr: 81770798/RSO.

This work is intended to demonstrate the challenges of integration of electric vehicles with smart grid and suggest economical and sustainable approaches in order to resolve them.

Dedication

To my parents

Acknowledgment

Undertaking PhD studies is like climbing at extreme altitude. Sometimes it might get windy, sometimes there might be with a blizzard, and sometimes it is sunny, with a lot of enjoyment. When you feel you are at the top, you suddenly feel utterly relaxed. During these five years, it was my pleasure to meet such nice people and experience a unique atmosphere in IEL.

I would like to express my highest appreciation and thanks to my main supervisor Magnus Korpås. Your attitude is exemplary. You have exactly what a PhD supervisor requires to motivate students. You were the one who directed this project towards high-performance computing, which fostered my desire to explore the structure of the sparse ACOPF matrices. Moreover, thanks to my first co-supervisor John Krogstie for providing me a master student (Jan Ørstavik, department of computer science, IDI, NTNU) to extend my ideas out of power systems realm. Indeed, it was a great collaboration.

I would also like to thank my associate professors: Hossein Farahmand and Vijay Venu Vadlamudi, for sitting with me and spending time listening to my arguments. Your support will never be forgotten.

During these years, I have held scientific discussions with Iver Bakken Sperstad and Venkatachalam Lakshmanan (researchers at SINTEF Energy Research), Jamshid Aghaei (Professor at Shiraz University), Pedro Crespo Del Granado (Senior Researcher, NTNU), Iromi Ranaweera (Senior Lecturer at the Faculty of Engineering, University of Ruhuna), Antonio Zecchino (Research Scientist at EPFL, Switzerland), Naser Hashemipour (PhD student, Shiraz University, Iran), Sigurd Bjarghov (PhD student, IEL), and Paolo Pisciella (Researcher, INDØK). Your comments and your scientific perspectives were invaluable.

Special thanks to Anders Gytri for fast responses to my requests regarding the extra computational assets, to Åshild and Bodil for their follow up of administration tasks, and to Ida Fuchs for her consistent follow up on my ongoing innovation project.

I want to thank my friends in Trondheim: Venkat, SigurdJ, Tin, Markus, ErlendE, ErlendK, Espen, SigurdB, Astrid, Hossein, Naghme, MartinH, MartinK, HK, Emre, Iromi, Philipp, Antonio, Kjetil, Vladi, Christos, Nik, Tarik, Stella, Yasser, Z, Malene, Tom, Mani, Juana, Ahmad, Naser, Ingrid, Vanja, Julia, Mahmood, Unni, Huda, and Sanaz.

I also have some friends back in Iran who where were source of motivation and moral support. In years to come we will be together again: Mehdi, Nader, Morteza, Hadi, HamedH, Morvarid, Saeed, Iman, Afshin, Shiva, Kazem, Ghasem, Roozbeh, and HamedZ.

I have had the opportunity to work with many master's students: Adrian Cruz, Frida Berglund, Guro Sæther, Jan Ørstavik, Jørgen Erdal, Manuel Pérez Bravo, Martin Lillebo, Oda Andrea Hjelme, Line Nyegaard, Sondre Harbo, and Sigurd Bjarghov. I hope you enjoyed research and collaboration with me and our group.

I would like to give my special thanks to my flatmates Mostafa and Daash-Mehdi.

Finally I would like to thank Marie, who supported me during the moments of distress.

Abstract

With the massive increase in the integration of Electric Vehicles (EVs), their share of energy consumption has shifted from fossil fuels to electricity. This shift in turn heavily relies on the safe, reliable and cost-efficient operation of electricity distribution networks. Traditionally, grids were built to transfer electricity from the generation side to the consumer at the endpoint, and neither designed to be smartly controlled, nor to integrate battery storage, photovoltaic solar panels (PV), wind energy and shiftable loads on the consumer side. The shift toward an active controllable distribution grid with active end-users requires new methods and tools for planning and operation. With this perspective, the aim of this PhD thesis is to develop a tool to integrate and optimise a large number of Stationary Energy Storage Systems (SESS) and EVs in the distribution grid.
The thesis has provided several key contributions:

C 1. Develop a high-performance and memory-efficient multi-period AC optimal power flow solver called "BATTPOWER", integrating a large number of intertemporal constraints. BATTPOWER takes advantage of several methods and sparse structures to speed-up the solution proposal significantly, as it: 1) incorporates the analytical first and second partial derivatives of constraints and objective functions with respect to all optimisation variables, 2) explores the sparsity structures of partial derivatives, 3) reorders the Jacobian matrix of the KKT structure, and 4) uses a sparse Schur-Complement algorithm for the multi-period structure of the KKT matrix.

C 2. Convert a large-scale local distribution grid into a standard research format, and simulate the integration of a large fleet of EVs. The simulation results reveal that the maximum share of EVs it could accommodate is around 20% (220 EVs out of 1113 estimated passenger cars) through an uncoordinated (dumb) charging strategy with no grid reinforcement.

C 3. Propose a centralised charging scheduling strategy using multi-period AC optimal power flow and integrating operational grid constraints which it solves the large-scale local distribution network (974 buses, 1023 lines, 2 generators and 1113 EVs) within 790 seconds.

C 4. Simulation results using the proposed centralised charging scheduling strategy reveal that the local grid could accommodate 36% (400 EVs out of 1113) without considering grid operational constraints. However, it manages to schedule all EVs (100%) though consideration of operational grid constraints in the optimisation problem.

C 5. Simulation results of the combined EV and PV cases signify the increasing growth of EV and PV penetration simultaneously with similar growing rates can lead to: 1) a more stable voltage profile, 2) lower line/transformer overloading problems, and 3) higher social-welfare and, lower and cost-efficient operation.

Moreover, from the game theoretical perspective, an Agent-Based Modelling (ABM) simulation is conducted to investigate the increasing impact of a large-scale EV fleet on the power system. In this mode the agents' incentives are: 1) to maximise state of charge (SOC), 2) to maximise SOC and minimise electricity price, and 3) no incentive (when they arrive, they charge). The EV agents are modelled through different charging strategies. Their different behaviour indicates how these incentives might affect their charging at different times and locations. This could be a useful tool for policymakers and researchers alike who like to estimate the variability of future demand.

In addition, a low-voltage area hosting 54 end-users is analysed by using real power measurements obtained from smart meters in load flow analysis. The possibility of a fast charger in the low voltage grid has been assessed, and an optimal location for fast charging is proposed. The optimisation model aims to minimise the grid loss along with voltage fluctuations. The results show that the EV-hosting capacity of the grid is sufficient for a majority of the end-users, but the weakest power cable in the system will be overloaded at around 20% EV penetration level. The network tolerated an EV penetration of 50% with regard to the voltage levels at all end-users.

Finally, the scenarios of EV and home batteries are compared with the objective of investigating the economic potential of utilising PV and storage at an end-user level. This is performed with a dynamic programming algorithm to minimise the electricity costs under four different grid tariff structures. When utilising an EV battery together with rooftop PV, the cost is reduced by a maximum of 19.2%, whereas a home battery installation together with PV reduces the cost by a maximum of 14.4%.

Overall, this PhD thesis primarily provides a mathematical backbone for an efficient solution of Multi-Period AC Optimal Power Flow (MPOPF), which could be taken as a stage for further development and future computationally efficient control systems. In addition, it looks into a path toward the sustainable operation and planning of power systems, more specifically focused on the electrification of the transport sector in combination with PV.

Contents

Preface iii

Dedication v

Acknowledgment vii

Abstract ix

List of Tables xviii

List of Figures xx

Abbreviations xxi

1 Introduction 1

1.1 Motivation 1

1.2 EV charging scheduling 2

1.2.1 Incorporating the Grid Operational Constraints 2

1.2.2 Without Grid Operational Constraints 8

1.3 Agent-Based Modeling 13

1.4 Reinforcement Learning 13

1.5 Multi-Period AC Optimal Power Flow (MPOPF) 14

1.5.1 Research Gaps 15

1.6 Research Questions 15

1.7 Tasks 16

1.8 Contributions 16

1.9 List of Publications 17

2 Contributions 21

2.1 BATTPOWER Toolbox: Memory-Efficient and High-Performance MultiPeriod AC Optimal Power Flow Solver—Part I: Mathematical Concepts 21

2.1.1 Analytical Gradients 22

2.1.2 Sparse Matrix Operations 22

2.1.3 Reordering 24

2.1.4 Schur-Complement 26

2.2 BATTPOWER Toolbox: Memory-Efficient and High-Performance MultiPeriod AC Optimal Power Flow Solver—Part II: Case Study 26

2.2.1 Analytical Derivatives 26

2.2.2 Schur-Complement 28

2.3 BATTPOWER Application: Large-Scale Integration of EVs in an Active Distribution Grid —Norwegian Case Study 28

2.4 Computational Efficiency Assessment of Multi-Period AC Optimal Power Flow including Energy Storage Systems 30

2.5 Integration of PEV and PV in Norway Using Multi-Period ACOPF—Case Study 31

2.5.1 Centralised Charge Profile vs Uncoordinated Charge Profile 31

2.5.2 Share of Load on a LV Transformer 31

2.6 Optimal Scheduling of Plug-in Electric Vehicles in Distribution Systems Including PV, Wind and Hydropower Generation 35

2.7 Agent Based Modelling and Simulation of Plug-in Electric Vehicles Adoption in Norway 37

2.8 Impact of Large-Scale EV Integration and Fast Chargers in a Norwegian LV Grid 40

2.8.1 Load Flow Analysis 40

2.8.2 Optimal Placement of Fast Charger and Reactive Power Provision 41

2.9 Value Comparison of EV and House Batteries at End-user Level under Different Grid Tariffs 42

3 Response to Research Questions and Tasks **45**

3.1 Answer to Research Questions 45

3.2 Description of Tasks 47

3.3 Relationships Between Papers 49

4 Conclusion **53**

4.1 Recommendations for Future Research 55

Papers **73**

Paper I ***BATTPOWER Toolbox: Memory-Efficient and High-Performance MultiPeriod AC Optimal Power Flow Solver—Part I: Mathematical Concepts*** **77**

Paper II ***BATTPOWER Toolbox: Memory-Efficient and High-Performance MultiPeriod AC Optimal Power Flow Solver—Part II: Case Study*** **95**

Paper III ***BATTPOWER Application: Large-Scale Integration of EVs in an Active Distribution Grid —Norwegian Case Study*** **105**

Paper IV *Computational Efficiency Assessment of Multi-Period AC Optimal Power Flow including Energy Storage Systems* **123**

Paper V *Integration of PEV and PV in Norway Using Multi-Period ACOPF—Case Study* **131**

Paper VI *Optimal Scheduling of Plug-in Electric Vehicles in Distribution Systems Including PV, Wind and Hydropower Generation* **139**

Paper VII *Agent Based Modelling and Simulation of Plug-in Electric Vehicles Adoption in Norway* **147**

Paper VIII *Impact of large-scale EV integration and fast chargers in a Norwegian LV grid* **157**

Paper IX *Value Comparison of EV and House Batteries at End-user Level under Different Grid Tariffs* **165**

Appendix **173**

Appendix A Permutation Matrix and Reordering **175**

List of Tables

1.1 Taxonomy of the EV charging scheduling strategies, with grid operational constraints, since 2009 6

1.2 Taxonomy of the EV charging scheduling methods, without grid operational constraints, since 2009 11

2.1 Total time (TotalTime = No.of Iter. × TimePerIter) elapsed to calculate: 1) Analytical (hand-coded) derivatives, and 2) Numerical derivatives 27

2.2 [a) total energy production, b) active system loss, and c) system cost] in three different operational modes. 29

2.3 Computational time for different solvers and with the same convergence criteria 30

2.4 Variation of R_1 and R_2 for different EV-PV penetration levels for one-cycle 0800 - 0800 34

2.5 Variation of R_3, R_3, and minimised cost of power import for different EV-PV penetration levels 34

2.6 Statistics for 40-day simulation statistics with 1500 agents with different charging strategies 39

2.7 Total costs for customer for different scenarios and tariff structures. All numbers are given in NOK. 43

A.1 Properties of Permutation Matrix 176

List of Figures

2.1 Total time (TotalTime = No.of Iter. × TimePerIter) for solution of the linear KKT systems of (2.11) solved by Schur-Complement algorithm proposed in the part I paper vs direct sparse LU solver, applied on IEEE 118 27

2.2 70% EV and 100% PV penetration in the distribution grid. Charge behaviour and SOC of the EVs located at the residential area: a) with the proposed algorithm, and b) with dumb-charging method. . 32

2.3 LV network (230 V) supplied by the transformer-DT1. 36

2.4 Voltage variation at the critical nodes of the network with optimal charging and dumb charging (Black: H50, Red: H23, Blue: H02, Green: H16 and Brown: H33). 50% EV and 50% PV in the network. 36

2.5 Total power demand from 1500 EVs during 40 days with charging based on SOC. 38

2.6 Total power demand from 1500 EVs during 40 days with charging strategy based on SOC and price. 39

2.7 Largest load ratio value reached for all buses in the system, all EV penetration cases 40

2.8 Lowest voltage magnitudes reached for all buses in the system, all EV penetration cases 41

2.9 Fast charger with/without RPC at feeder G4 42

2.10 Relative annual cost for different scenarios, all compared to the base case cost. 44

3.1 Overview of: (a) research questions, and (b) tasks 49

3.2 The relationships between the papers in this thesis. 51

List of Abbreviations

ABM	Agent-Base Modeling
ACOPF	AC Optimal Power Flow
AMS	Advanced Metering Systems
DSO	Distribution System Operator
EV	Electric Vehicle
G2V	Grid to Vehicle
HV	High Voltage
IP	Interior Point
KKT	Karush–Kuhn–Tucker
LV	Low Voltage
MPOPF	Multi-Period AC Optimal Power Flow
MV	Medium Voltage
NLP	Non-Linear Programming
NLP	Nonlinear Programming
PV	Photo-Voltaic solar panel
RES	Renewable Energy Systems
SESS	Stationary Energy Storage Systems

V2G	Vehicle to Grid

Chapter 1

Introduction

1.1 Motivation

In recent years, a large increase in electric vehicle (EV) sales has been observed due to decreasing battery prices, larger production volumes and increasing restrictions due to climate policies [1]. Norway in particular has the highest EV share in the world, with 10% of the total car parks being fully electric, numbering 260,000 cars [2]. With a market share of 43% of all new sales, this growth is expected to continue. EV charging is anticipated to create congestion in distribution grids, and the Norwegian regulator estimates that 1.2 billion euros can be saved through the smart coordination of EV charging [3].

Currently, most EV chargers start charging at the nominal capacity until the EV battery is full or the set point has been reached. In the future, we assume that EV charging can be controlled according to the wishes of the EV owner, a feature that to some extent already exists. Many potential charging schemes are suggested in the literature, such as charging “queues”, “bandwidth sharing” and price signals [4–6]. However, these approaches often ignore power system aspects or strongly simplify them. By considering EV charging as part of a Multi-Period AC Optimal Power Flow (MPOPF) problem, optimal charging schedules considering system feasibility can be achieved, while still minimising costs.

There are three main motivations to write this PhD thesis:

I. **Sustainability:** Large-scale introduction of Renewable Energy Sources (RES) (PV and wind), Energy Storage Systems (ESS), and EV will influence the way that the electricity grid operates, especially the distribution grid. We need computationally fast and tractable toolboxes to ensure more sustainable developments, by more accurately tracking nodal voltage fluctuations and losses in the electricity network, thus providing lower cost of operation and higher social welfare.

II. **Economics:** According to NVE [7] and Nordpool [8], the total electric power generated and average electricity price in Norway, 2018, was around 147 TWh and 419 NOK/MWh respectively. Thus, the total electric power revenue is around 61.6 billion NOK. If it is possible to save 1% by operating the RES, ESS and EVs more reliably and efficiently, then it could amount to 615 million NOK.

III. **Reliability:** The 2018 NVE annual report [9] indicated that the Energy Not Supplied (ENS) in Norway in 2017 was 14.3 GWh. Papers [10], [11] present the costs for the average interruption duration in Norway. If the assumptions have been made in these studies hold for 2017, then the annual cost of power interruption is as much as the operational costs of today [10] i.e. around 1600 MNOK/year. Thus, in order to operate the network securely and stably, accurate operational models are required.

1.2 EV charging scheduling

In this section, the literature studies considering EV charging scheduling are reviewed and investigated in order to find research gaps and raise the main thesis research questions. The literature on the subject is divided into two subcategories: 1) EV charging scheduling incorporating the grid operational constraints, and 2) EV charging scheduling without considering grid operational constraints.

1.2.1 Incorporating the Grid Operational Constraints

The approaches to EV charging scheduling incorporating the grid operational constraints are reviewed chronologically in this subsection. The following are the main papers published in this subject from 2009 to 2020.
Reference [12] developed a management tool to charge large-scale EVs through three ways: 1) dumb charging, 2) dual tariff policy, and 3) smart charging. A medium-size Medium Voltage (MV) grid is chosen for the benchmark study. The level of efficiency of each method has been identified and assessed until the grid operational constraints have reached their limit. A MV network, located in Portugal, was exploited as a benchmark environment. Operational constraints and grid loss are observed in the different test scenarios. An optimisation framework to coordinate charging of EVs is suggested by [13] to minimise the power loss and maximise the main grid load factor. The stochastic programming approach is used to cover the uncertain nature of household load. The IEEE 34-node radial network is used for simulation of the distribution network.

Reference [14] suggested a load management plan for EV charging coordination. The method is Real-Time Smart Load Management (RT-SLM) control strategy based, which updates every 5 min and minimises total cost of generation and loss. The method is applied on a small test case. Reference [15] formulated an optimisation framework by assigning price-elastic load to EV charging and considering optimal power flow as the balance constraint and cost of production as the objective function. The optimisation model is applied to a small-scale IEEE 14-bus system. A Smart Load Management (SLM) system is proposed by [16] for the coordination of large-scale EV chargers in distribution feeders. The SLM approach is tested for a 1200 bus test system consisting of low-voltage residential networks. The authors of [17] studied the effect of large-scale EV penetration on two large distribution networks: area (a) with a large low-voltage area with 6,000 residential users, and area (b) a medium-voltage industrial and a low-voltage residential area with over 61,000 users. They ran power flow and studied the power losses with different levels of penetration of EV. However, there is no discussion of the computational complexity of the proposed work.

Two EV-charging controller methodologies, a local EV charger controller and a centralised EV charger controller are introduced and compared by [18]. They suggested that although the network and communication infrastructure needed to implement the local control method would be far less than that of the centralised control case, the centralised controller gives a more reliable operational outcome in the case of high EV penetration. Reference [19] proposed an EV charging algorithm which maximises power delivered to all EVs in a distribution grid with consideration of voltage and line/transformer capacities. However, there is no battery model and loss minimisation through the optimisation horizon. Reference [20] suggested a joint optimal power flow and EV-charging framework that considers an OPF problem with EV charging over time. This nested optimisation problem is solved through a decomposition approach which has lower computational complexity than that of the centralised interior point solvers. The approach is implemented on the IEEE 14-bus.

Reference [21] presented a hierarchical decomposition approach to coordinate the charging and discharging behaviours of EVs. The upper-level objective is to minimise the total cost of the distribution grid with control of the dispatchable EV aggregators and generators. The lower-level objective aims to follow the decisions made by the upper level and design charge and discharge strategies for individual EVs in a specified dispatching period. The IEEE 118 bus is used to validate the proposed method. Reference [22] suggested an integrated Distribution Locational Marginal Pricing (DLMP) method in order to mitigate congestion actuated by EVs. In the proposed approach, nodal prices are cleared by solving the social welfare optimisation of the distribution grid. Reference [23] proposed a stochastic simulation technique to investigate the impact of EV charging demand on the distribution network. The daily feeder load, EV charging time, and state of charge are derived from real measurements and survey data. Reference [24] suggested a simple decentralised random access framework to schedule EV charging. They discussed the advantage of implementation of a simple decentralised algorithm in the paper. Reference [25] proposed an unbalanced three-phase multi-period AC optimal power flow optimisation problem which allocates individual variables to each EV and controls the charging rate and times of charge of EVs over a 24-hour time horizon. The cost function is to minimise the total cost subjected to operational constraints. The proposed formulation is solved through the Non-Linear Programming (NLP) solver of MATLAB, called FMINCON. Moreover, it is applied to an 85 bus test case, 74 single-phase, and 11 three-phase case study. A multi-objective and multi-layer planning algorithm to accommodate a large number of EVs in the distribution network is suggested by [26]. It includes uncertainties in the distribution grid, and aims to minimise greenhouse gas emissions and system cost during the planning horizon, defined in terms of multi-objective mixed integer nonlinear programming and solved based on a Non-Dominated Sorting Genetic Algorithm (NDSGA).

Reference [27] proposed a Mixed-Integer Linear Programming (MILP) model for EV charging coordination in an unbalanced distribution network. The proposed method takes into account the distributed generators and operational constraints. The linear proposed model is solved using commercial MLIP solvers. The proposed model is tested on a 394-bus distribution system. However, there is no discussion of the computational complexity of the proposed problem in the paper. Reference [28] proposed a method for real-time management of EV charging procedures such that it flattens the peak load, increases the number of rechargeable EVs, and activates the network operational constraints. The approach integrates: 1) the scheduling algorithm, 2) power flow equations, and 3) operational constraints. Simulations are conducted on a real medium-sized Italian electricity distribution grid. The size of the simulated grid is unknown in the paper. Reference [29] studied a fast receding horizon optimisation problem by linearisation of voltage drop in the network. Two objectives have been considered: 1) maximisation of total EVs charging in the network, and 2) cost of charging. Higher efficiency in exploiting the existing lines/transformers in the distribution network is observed in the simulation results of the proposed method.

Reference [30] proposed a two-stage energy exchange planning strategy for a multi-micro-grid system incorporating EVs as storage devices. The proposed method brings down the electricity cost and prevents frequent transition between charge and discharge modes. Reference [31] proposed: 1) a centralised control algorithm which uses limited data to manage EV-charging stations to mitigate grid operational constraints, and 2) an OPF-based method. The first method is implemented on two real and large distribution grid cases with 351 and 428 customers. The proposed control algorithm works based on the selection of time of charge and considers the transformer overloading. The objective function for the OPF-based method is to minimise the number of EV disconnections. However: 1) there is no discussion of the computational complexity of each method in the paper, and 2) the OPF-based method is not designed as a multi-period form and the presented model does not have a storage model. Reference [32] investigated the optimal value of the power factor in order to find the optimal allocated number of and sizing of solar parking lots for the EVs. The objective is to minimise the total cost of the formulated problem over the optimisation horizon. The problem is solved using quantum annealing (QA). Reference [33] proposed an efficient multi-objective hierarchical optimisation scheme to accommodate more renewable connections. Simulations are performed to illustrate the method on a real Australian distribution network with 560 buses.

Reference [34] studied the problem of the placement of the EV charging station. The transportation network graph and electric network graph are considered in the study. Authors developed a java-based software to assess the interaction between costumers. They demonstrated that the charging station placement is associated with the heatmap of the traffic flow. Reference [35] proposed a partial decomposition based on Lagrange relaxation method for EV charging in the case of a transmission-constrained power system. The proposed method can help to: 1) reduce total generation cost, and 2) alleviate the transmission grid congestion. The method is tested on IEEE-RTS1979. Reference [36] proposed a decentralised EV-charging protocol using the Frank-Wolfe method. They discuss the computational complexity of centralised methods in the paper, especially when the problem size is scaled up. They claim that the proposed method has high performance and call upon low computational infrastructure from EV controllers. Reference [37] proposed two smart-charging strategies with the objectives of: 1) minimisation of total daily cost, and 2) peak-to-average ratio. The proposed strategies are tested through a 37-bus distribution system. The solution is based on a heuristic-based method. Reference [38] suggested a queuing method for the charging of EVs. The impacts of the state of charge and battery charge behaviour are investigated on the EV service time. The nonlinear problem (NLP) is written in GAMS and solved with a MINOS5.1 solver. The proposed method is tested on 69 bus radial distribution system. The authors of [39] presented a mathematical model for charging load using a queuing model by a neural network. The charging load is integrated with operational limits in order to find optimal operation and the smart charging schedule of the EV-charging station. The model is tested with a 69 bus distribution network. The nonlinear problem is written in GAMS and solved through the

MINOS5.1 solver.
Reference [40] introduced a fast-solving method for coordinated charging of EVs based on linearisation of branch power flow. They implemented their work on IEEE 33 bus distribution network. Reference [41] proposed a scheduling method for EV charging by introducing three preference types: radical, conservative and balanced users. They suggested that this could be an economic incentive scheduling method for an optimisation framework. Reference [42] developed a model predictive control-based approach to solve the joint problem of EV charging scheduling and power control. The objective is to minimise both EV charging cost and energy generation cost while satisfying the daily household and EV power demand. The authors of [43] proposed a horizon optimisation control framework in order to schedule the operation of the distribution network in an efficient manner. The main objective of the proposed optimisation is to abide by the operational constraints to ensure the secure operational scheduling. The operational constraints are voltage bounds and rated power bounds. The optimisation problem is based on multi-period three-phase Optimal Power Flow (OPF) which can be solved by a classic NLP solver. A Cost Constrained Variable (CCV) method is adopted for the operational cost of each Distributed Energy Resource(DER) such as Battery Energy Storage Systems (BESS), EV, and PV in the LV network. However, the implemented method is tested on a small-scale Distribution Network (DN). The computational complexity of the proposed method is not discussed in the paper. Reference [44] presented a game theoretical platform for energy consumers in order to compete for locational marginal prices. They extracted the nodal marginal prices through running optimal power flow on the IEEE 24 bus system. A multi-objective optimisation framework has recently been proposed by [45] and is solved using a differential evolution method to mitigate voltage unbalance in high EV penetration scenario. Table 1.1 summarises the literature review regarding the EV charging scheduling considering grid operational constraints since 2009.

Table 1.1: Taxonomy of the EV charging scheduling strategies, with grid operational constraints, since 2009

Paper	Grid Operational Constraint	Case Size	Computational Test and Argument	Scalability Tests	A[a]	Method
[12]	Yes	Medium Size Exact size not reported Medium Voltage (MV)	Test:No Argument:No	No	No	Load flow analysis
[13]	Yes	IEEE-34 Radial network	Test:No Argument:Yes	No	No	Load flow analysis Dynamic programming
[14]	Yes	449 bus: IEEE31 for MV 22× 19 bus LV	Test:Yes Argument:partial	No	No	Heuristic algorithm Load flow analysis Real-time smart load management

[a] A: Incorporating all the systems elements (battery storage and grid) together spatially and temporally.

Paper	Grid Operational Constraint	Case Size	Computational Test and Argument	Scalability Tests	A[a]	Method
[15]	Yes	IEEE 14-bus	Test:No Argument:No	No	Yes	MPOPF Joint OPF-charging optimization
[16]	Yes	1200 bus: IEEE31 for MV 22× 53 bus LV	Test:No Argument:No	LargeCase	No	Heuristic algorithm Load flow analysis Smart load management
[17]	Yes	Large case Not clear in number of bus/line	Test:No Argument:No	LargeCase	No	Load flow analysis
[18]	Yes	Not clear in Number of bus/line 74 residential customers	Test:No Argument:No	No	No	3-phase load flow
[19]	Yes	Not clear in number of bus/line 134 residential customers	Test:No Argument:partial	No	No	Linear programming 3-phase load flow Heuristic algorithm
[20]	Yes	IEEE 14-bus	Test:Yes Argument:Yes	No	Yes	MPOPF Decomposition method Nonsmooth separable programming
[21]	Yes	Modified IEEE 118-bus	Test:No Argument:partial	No	Yes	MPOPF Hierarchical decomposition AMPL/IPOPT AMPL/CPLEX
[22]	Partially DC approx No voltage	RBTS bus 4 [46]	Test:No Argument:Partial	No	No	Integrated distribution locational Marginal pricing (DLMP) DCOPF
[23]	Yes	IEEE 13-bus TPC 25-bus	Test:No Argument:No	No	No	Stochastic Analyses Three-phase load flow Monte Carlo simulation
[24]	Yes	[12]	Test:No Argument:Partial	No	No	Heuristic Method Decentralized random access
[25]	Yes	85 bus: 11 3-phase bus 74 1-phase Customer bus	Test:No Argument:Yes	No	Yes	MPOPF FMINCON MATLAB Three-phase Unbalanced load flow
[26]	Yes	38-bus 12.66-kV	Test:No Argument:No	No	Yes	MPOPF Non-dominated sorting genetic algorithm Load flow equations
[27]	Yes	394 bus: 34 bus MV 360 bus LV	Test:No Argument:No	No	Yes	MPOPF Unbalanced system Mixed-integer linear programming CPLEX
[28]	Yes	Size:unknown Real medium-size Italian electricity Distribution grid	Test:Yes Argument:Yes	No	Yes	Real-time management Power flow analysis Heuristic Method
[29]	Yes	real distribution network Melbourne 114 customers	Test:No Argument:Yes	No	Yes	DC-equivalent model Linear approximation Receding horizon
[30]	Yes	Not clear 5 microgrid systems 100EV in each	Test:No Argument:No	No	No	Decentralized scheduling Dual variable Two-stage optimisation
[31]	Yes	Not clear No number bus/line large distribution grid 351 and 428 customers	Test:No Argument:No	No	No	OpenDSS 3-phase power flow Heuristic Method
[32]	Yes	28-bus	Test:No Argument:No	No	No	Quantum annealing Power flow equations Heuristic Method Planning problem

[a] A: Incorporating all the systems elements (battery storage and grid) together spatially and temporally.

Paper	Grid Operational Constraint	Case Size	Computational Test and Argument	Scalability Tests	A[a]	Method
[33]	Yes	560 bus	Test:Yes Argument:Yes	No	No	Multi-objective hierarchical 3-phase power flow PSO Heuristic method
[34]	Yes	IEEE 118-bus	Test:No Argument:No	No	No	Power flow Bayesian game
[35]	Partially PTDF method No voltage	IEEE-RTS1979	Test:No Argument:No	No	No	Partial decomposition Lagrange relaxation method Power flow distribution factor Linearised method
[36]	Yes	IEEE 13-bus 123-bus	Test:No Argument:Yes	Partially	Yes	Frank–Wolfe method Decentralised method Linearised distribution Unbalanced distribution grids
[37]	Yes	37-bus dist. grid	Test:No Argument:No	No	Yes	Heuristic method Power flow analysis
[38]	Yes	69-bus dist. grid	Test:No Argument:No	No	Yes	Power flow equations MINOS5.1 solver GAMS
[39]	Yes	69-bus dist. grid	Test:No Argument:No	No	Yes	Power flow equations MINOS5.1 solver GAMS Neural Network
[40]	Yes	IEEE 33-bus 354-bus dist.	Test:Yes Argument:Yes	No	Yes	Branch power flow Balanced dist. grid Unbalanced dist. grid Linearization methods
[41]	Yes	IEEE-33-bus	Test:No Argument:No	No	No	Power flow analysis Multi-objective scheduling
[42]	Yes	Case9 Case14 Case30 Case118mod	Test:Yes Argument:Yes	Partially NolargeCase	Yes	MPC Optimal power flow Semi-definite relaxation
[43]	Yes	LV European Net Small scale	Test:No Argument:No	No	Yes	MPOPF Three-Phase Cost Constrained Variable
[44]	Yes	IEEE 24 bus	Test:No Argument:No	No	Yes	Linearised ACOPF Game theory Locational marginal prices
[45]	Yes	Not clear	Test:No Argument:No	No	No	differential evolution method Multi-objective optimisation Voltage unbalance 3-phase power flow Heuristic Method

[a] A: Incorporating all the systems elements (battery storage and grid) together spatially and temporally.

1.2.2 Without Grid Operational Constraints

The approaches to EV charging scheduling which have not considered the grid operational constraints are reviewed chronologically from 2009 to 2020 in this subsection.

The authors of [47] considered a method for the management of EV loads which aims to save costs. This is performed with a rolling horizon stochastic dynamic programming algorithm. In [48], a unidirectional V2G is proposed through an aggregator, which combines the capacity of many EVs to participate in the energy market through bidding. A bidding algorithm is proposed in this work for unidirectional regulation of an aggregator, with the objective of profit maximisation and constraints of optimal system load and optimal price. Reference [49] introduced three optimal charging algorithms in order to minimise the impact of EV charging on the distribution network. The authors compared the computational burden of each method with each other. A real-time dispatching EV method is introduced and applied to a 9 bus case test.

Reference [50] analysed the impact of EV charging on a local residential distribution transformer. Reference [51] presented an optimisation load demand for EV charging scheduling. The proposed method is discussed with respect to travel pattern and willingness of customers. The impact of EV charging load on flattening the national demand profile in the UK has been investigated with numerical results. It is found that a smooth load profile may be obtained at all EV penetration levels if the fast-charging mode is activated. Reference [52] proposed a two-stage charging control strategy to shift transformer load and charge EVs with a high performance. They implemented the suggested strategy on 24 residential houses. Reference [53] proposed: 1) a globally optimum EV charging scheduling with the objective of minimisation of total costs of all EVs, and 2) a locally optimal point for EV charging and discharging to minimise the total cost of EVs in the contemporary ongoing EV set in the local area. The benefit of the proposed algorithm is that the globally scheduling model is scalable for a large number of EVs and the local scheduling model is not.

Reference [54] introduces a process to involve EV aggregators in the electricity market. The scheduling of EV charging and discharging is in coordination with the Distribution System Operator (DSO). It is shown that the system would be able to intake higher EV penetration without expanding the supply side. Reference [55] proposes a decentralised algorithm to optimally schedule EV charging by the exploitation of the elasticity of EV load to fill the valleys in electric load profiles. The authors of [56] and [57] proposed optimal EV coordination strategies with cost-benefit analysis. The charging load of EV on the distribution grid is calculated with a modified Latin Hypercube Sampling (LHS) method in order to capture the stochastic features of EVs. A two-stage optimisation model for optimal charge of EV is proposed for minimising load peak and load fluctuations. The optimal charging of EVs is benchmarked on data collected in the Beijing–Tianjin–Tangshan Region (BTTR) China.

Reference [58] suggested a stochastic framework for EV charge demand. It provides: 1) an accurate forecast of the load, and 2) a decomposition model of load, with demand flexibility. The numerical results suggested that the proposed method performs more accurately than the standard load prediction techniques. Reference [59] estimated the EVs' consumption through a stochastic model for the type-of-trip and corresponding charging need. The suggested method demonstrated how the type-of-trip and charge opportunities affect the load profiles and load shifting of EVs. Reference [60] suggested a decentralised and packetised approach to EV charge management. The advantages of a packetised approach are discussed in the paper. The authors of [61] suggested an algorithm in order to estimate V2G capacity using real-time EV scheduling. The effective usage of EVs as a distributed storage system is suggested and demonstrated in the paper. Reference [62] investigated the implementation of stochastic dynamic programming on the optimisation of charging and frequency regulation capacity bids of an EV in a distribution grid. A Markov decision problem is formulated in order to calculate an EV's expected cost over a charging horizon. Reference [63] proposed an online coordinated charging decision (ORCHARD) algorithm for minimisation of the energy cost. They proved that ORCHARD is strictly feasible such that it completes all charging demands in due time.

Reference [64] proposed a new cellphone application algorithm, implemented to predict the energy demand at EV-charging stations. The total time for data analysis is reported to be within a few seconds. The prediction algorithm is based on the fast machine learning-based time series. Two applications are designed on top of the prediction algorithm where they predict: 1) the expected available energy at the outlet, and 2) the expected charging finishing time. Reference [65] proposed a layered distributed charging load for controlled charging of EVs based on the Lagrangian relaxation and an auxiliary problem principle. The proposed method is suitable for large populations of EVs and gains an advantage in reducing the generation cost. However, load flow equations are not considered as a part of the formulation.

Reference [66] reviews the online EV-charging scheduling methods, which focus on uncertainty and randomness of EV arrival and departure along with state of charge and energy demand, as proposed in the literature. Some promising future research directions have been discussed regarding the stochastic modelling of EVs. Reference [67] presented a two-stage modeling framework to extract the data from real EV charging events. The real data are collected from the Plugged-in Midlands (PiM) project. A Fuzzy-based model is developed to exploit the collected data and use as a tool for further prediction. The created model is applied to a case study with real charging and weather data from three locations in the UK. Reference [68] proposed a model predictive control algorithm for coordinated efficient charging of EVs to minimise the cost and impact of EVs to the power grid. Reference [69] presented experimental results of EV operation for offline Uninterruptible Power Supply (UPS). Two power outage detection algorithms have been introduced and analysed with voltage and current control strategies. Reference [70] suggested a two-stage dynamic programming framework to find the optimal charging strategy using short-term data prediction and long-term historical data. The simulation results suggest that the proposed method reduces energy costs within the simulation horizon.

Reference [71] proposed a high-efficient mathematical model for the optimal routing and charging of EVs. It aimed to: 1) find the best route for each EV, 2) satisfy the welfare of all passengers, 3) maximise the energy efficiency subject to defined constraints, and 4) explore the impact of EVs on the electric distribution grid as a prediction tool. The solution method was based on a mixed-integer quadratically constrained programming problem. Two modes of offline and real-time optimisation algorithms are suggested. Reference [72] presented a recharging plan for EVs to optimise the cost of charge and prevent congestion problems using a dynamic stochastic optimisation method. A stochastic linear programming approach is formulated in the paper. Stochastic variables are taken to be load, electricity price and DER generation. The authors of [73] proposed a bilevel optimisation in a system of commercial buildings integrated to DSO. The objectives are: 1) to increase load penetration with maximisation of the system load factor, and 2) to reduce energy cost for the buildings. The advantages and disadvantages of the proposed bilevel optimisation have been tested on a 33-node distribution test feeder connected to several commercial buildings.

Reference [74] modeled a large population of grid-connected EVs, where EVs can be a grid service provider with model-based control and discrete charging rate. A linear quadratic regulator to provide a load-following service through tracking a power signal is developed. Reference [75] investigated the price scheduling problem of EVs. Some central charging stations have been controlled by an aggregator with two objectives: 1) EV owner comfort, and 2) cost minimisation of charging stations. The advantages and disadvantages of suggested method have been discussed. Table 1.2 sums up the literature review conducted in this subsection regarding the EV charging scheduling considering grid operational constraints since 2009.

Table 1.2: Taxonomy of the EV charging scheduling methods, without grid operational constraints, since 2009

Paper	Grid Operational Constraint	Case Size	Computational Test and Argument	Scalability Tests	A[a]	Method
[47]	No	—	Test:No Argument:No	No	No	EV load management
[48]	No	—	Test:No Argument:No	No	No	Aggregator Demand response Vehicle-to-grid (V2G)
[49]	No	9-bus dist. grid 18-bus	Test:No Argument:partial	No	No	Losses minimization Load factor
[50]	No	6 house + 6 EV No grid	Test:No Argument:No	No	No	Monte Carlo Simulation Fleet study Transformer life

[a] A: Incorporating all the systems elements (battery storage and grid) together spatially and temporally.

Paper	Grid Operational Constraint	Case Size	Computational Test and Argument	Scalability Tests	A[a]	Method
[51]	No	—	Test:No Argument:No	No	No	Load modeling Quadratic programming Load demand
[52]	No	Distribution transformer feeds: 24 residential houses	Test:No Argument:No	No	No	fuzzy logic control Two-stage charging control Aggregator Optimizer
[53]	No	—	Test:No Argument:No	No	No	Convex optimization Optimal scheduling
[54]	No	IEEE-RTS [76]	Test:No Argument:No	No	No	Aggregator Mixed-integer linear programming
[55]	No	—	Test:No Argument:No	No	No	Controllable electric load Decentralized algorithm Valley-filling
[56] - [57]	No	No grid Beijing–Tianjin –Tangshan Region BTTR	Test:No Argument:No	No	No	Latin hypercube sampling method Two-stage optimization
[58]	No	—	Test:No Argument:No	No	No	Stochastic model Load forecasting Queueing theory
[59]	No	—	Test:No Argument:No	No	No	Irecharging price sensitivity Type-of-trip
[60]	No	—	Test:No Argument:No	No	No	Decentralised approach Packetized approach
[61]	No	—	Test:No Argument:No	No	No	Real-time EV scheduling Building Energy Management V2G
[62]	No	—	Test:No Argument:No	No	No	Approximation algorithms Dynamic programming Frequency regulation Markov decision
[63]	No	—	Test:No Argument:Yes	No	No	Online coordinated charging
[64]	No	—	Test:No Argument:Yes	No	No	Cellphone application algorithm Fast machine learning-based Kernel methods
[65]	No	IEEE-RTS [77]	Test:No Argument:No	No	No	Auxiliary Problem Principle Lagrangian Relaxation aggregator
[66]	No	—	Test:No Argument:No	No	No	Online Charging Scheduling Review paper
[67]	No	No grid three area: Nottinghamshire Leicestershire West Midlands	Test:No Argument:No	No	No	Two stage modeling framework Fuzzy-based model Heuristic Method
[68]	No	—	Test:Yes Argument:Yes	No	No	Model Predictive Control Optimal charging control
[69]	No	—	Test:No Argument:No	No	No	Kalman filter Power outage detection algorithms Uninterruptible power supply Heuristic method
[70]	No	—	Test:No Argument:No	No	No	Two-stage dynamic programming Optimal charging strategy
[71]	No	—	Test:No Argument:No	No	No	Mixed-integer Quadratically constrainted
[72]	No	—	Test:No Argument:No	No	No	Recharging plan Dynamic stochastic optimisation Stochastic linear programming
[73]	No	33-node Distribution test feeder	Test:Yes Argument:Yes	No	No	Bilevel optimisation MATLAB and YALMIP

[a] A: Incorporating all the systems elements (battery storage and grid) together spatially and temporally.

Paper	Grid Operational Constraint	Case Size	Computational Test and Argument	Scalability Tests	A[a]	Method
[74]	No	—	Test:No Argument:No	No	No	Aggregator Linear quadratic control Partial differential equations
[75]	No	Not clear Micro-grid	Test:Yes Argument:Yes	No	No	Price scheduling Aggregator Pareto optimality

[a] A: Incorporating all the systems elements (battery storage and grid) together spatially and temporally.

1.3 Agent-Based Modeling

Agent-Based Modeling (ABM) is a game-theoretical based approach towards the understanding and analysis of the outcome of interactive games, in which it is a game for energy cost in the context of the power systems. This method could be a potentially strong tool in order to predict future demand size and time. Here we briefly summarise the literature in this discipline.

Reference [78] proposed an agent-based model of a fleet of EVs in order to analyse: 1) EV fleet evolution, 2) EV energy demand simulations, and 3) transport simulations. The daily behaviour of the EV and the energy required to charge the EV are determined. A power system model is combined with a charging control algorithm to study the impact of EVs on the electricity network and simultaneously provide insight into EV load patterns and changes in transport behaviour. Reference [79] proposed a multi-agent EV charging control method that considers the network impacts. A realistic and urban distribution network is simulated and evaluated with the proposed method. The authors of [80] investigated two practical mechanisms as extensions of second price auction: 1) the EV agent submits a number of bids, such as one for each of the different energy quantities, and 2) the elastic-supply progressive second price, where the EV agent submits a two-dimensional bid for the price and the desired energy quantity. The analysis is further investigated with numerical results. Reference [81] proposed a model for EVs to participate in frequency regulation in an electricity market. A hierarchical game is proposed for this purpose. Reference [82] proposed an EV-charging navigation framework with simultaneous grid and transport constraints. The proposed framework coupled the power system with the transportation system through the charging and navigation of massive EVs. A non-cooperative game theoretical formulation is proposed for EVs to compete for charging power.

1.4 Reinforcement Learning

Recent studies have attempted to bypass the classical view of power systems, especially by using machine learning methods.

Reference [83] proposed a model-free approach, based on reinforcement learning (RL). A Markov Decision Process (MDP) was formulated in the RL environment. The RL algorithm controls the whole set of EVs at once. Reference [84] suggested a multi-agent deep reinforcement learning algorithm for demand-side management of distributed EV charging stations plus PV and BESS systems. The paper argues that the classic solution of an EV scheduling problem (centralised optmisation) is not computationally capable of handling a large number of variables and constraints, while machine learning methods can handle the run-time time-varying dynamic data of the scheduling problem of multiple EV charging stations simultaneously. Reference [85] presented an agent-based control system for the coordination of EV charging in the distribution grid. Search techniques and neural networks are used for the coordination of EVs and a series of laboratory experiments are conducted for V2G tests.

1.5 Multi-Period AC Optimal Power Flow (MPOPF)

The optimal power flow is a non-linear and non-convex problem which was first introduced in the 1960s [86]. Although it is considered to be a classic power systems problem among researchers, depending on the technical applications and operational dimensions, it may be adapted to various versions such as the Multi-Period AC Optimal Power Flow (MPOPF), introduced by [87], and may become intractable and computationally very demanding even after around 60 years [88], [89].

Many researchers have been attempting to either simplify MPOPF by linearising the main problem [90–92], or by making it more reliable by finding the global optimum point with different convex relation approaches such as [93], semidefinite programming (SDP) relaxations [94], [95] and second-order cone programming [96]. Moreover, MPOPF is suggested as a potential online operational tool [97] for use in the near future.

Since the non-linear ACOPF problems require non-linear solvers to be called, several NLP solvers are used to solve MPOPF problems; these are primarily developed based on IP methods, such as MIPS [98], IPOPT [99] KNITRO [100], and recently BELTISTOS [101], in which the only tailored algorithm to solve MPOPF problems is BELTISTOS. An extensive review of both MPOPF problem formulations and solution methods can be found in [88, 102].

It is well-known from the literature [103], [104] that the solution of linear Karush–Kuhn–Tucker (KKT) systems and calculation of gradients are the two most computationally expensive aspects in solving a MPOPF problem. Thus, the authors of [105], [106] proposed a fast solver to exploit the sparsity of a MPOPF structure (both KKT systems and gradients) and speed up the solution. These are papers I and II, located in chapters I and II of this thesis. They comprise the main contribution of the thesis.

1.5.1 Research Gaps

There are several research gaps which previous references have not considered with respect to the MPOPF and EV scheduling:

- Principally, they disregarded the computational tractability and scalability of the proposed method. With few exceptions, there is no discussion of how fast the proposed method can be.
- The proposed methods are applied and tested with either a small-scale test case or medium-scale test case.
- The grid operational constraints have often been disregarded. However, while there are some studies which considered them, there is limited discussion on how computationally efficient they are.
- The non-linear balance constraints of ACOPF have been simplified in most of the cited studies. Therefore, the power loss either is not considered as a part of the global solution or simplified in the method.

1.6 Research Questions

The thesis is defined with some research questions, which can be summarised here:

RQ 1. With only "passive charging", the deployment of EVs will be limited by grid constraints. Can "smart-charging" overcome this problem?

RQ 2. How many additional EVs can be served by fast-charging points with a "smart-charging" regime compared to "passive charging"?

  C 1. Without any reinforcements of the grid.

  C 2. Without any reduction in driving range.

RQ 3. How much grid reinforcements is needed with smart vs passive-charging to fulfill increasing targets for an EV fleet as a replacement for gasoline and diesel cars?

RQ 4. Could integration of PV mitigate the impact of increasing EV penetration on the distribution grid?

1.7 Tasks

With respect to the research questions, some tasks have been defined in this PhD thesis.

Task 1. Develop a smart-charging algorithm/scheme with the objective to compare and analyse how many additional EVs can be served by a smart-charging method.

Task 2. Develop a simulator for the combined power-and-transport system that can measure the consequences of conditions C 1. and C 2. in RQ 2. of smart and passive-charging for a realistic case study.

Task 3. Simulate the combined system with an increasing number of charging points (and cars), and measure the "saturation point" with respect to the requirements in RQ 2..

Task 4. Develop a power flow solver that takes into account the operational grid constraints, grid losses and also local generations.

Task 5. Investigate the impact of growing penetration of EVs and PVs together in the distribution grid.

1.8 Contributions

The main contributions of this thesis are itemised in the list provided below. Note that the order of items and papers is related to the comprehensiveness of the work.

- Introduction of a high-performance and memory-efficient multiperiod ACOPF solver called "BATTPOWER" for both the operational scheduling of energy storage, and charging scheduling of EVs, in the first and second paper [105], [106]: chapter I and chapter II of this thesis.
- Demonstration of an application of the BATTPOWER solver, with simulation of a Norwegian large-scale distribution grid (1023 lines, 974 buses and 2 generators) along with the high penetration of EVs, in the third paper [107]: chapter III of this thesis.
- Introduction of first and second analytical derivatives of equality and inequality constraints along with objective function into a primal-dual interior point (IP) method solver in order to speed up the computational performance in the fourth paper [108]: chapter IV of this thesis.

- A MPOPF structure is introduced in the fifth paper [109]: chapter V of this thesis, in order to take into account grid operational constraints for a basic operational tool. A detailed cost analysis is performed, when PV-EV penetration is altered from 0% until 100%.

- The impact of large-scale penetration of EVs and PVs is investigated on a medium sized distribution grid using MPOPF in the sixth paper [110]: chapter VI of this thesis. However: 1) the computational performance is not studied, and 2) the case study is a medium sized distribution grid with (146 lines 147 buses, and 2 generators).

- An agent-based modeling of EVs has been developed in order to simulate the future power demand side in different locations from a given number of EVs. Simulations have been conducted for the city of Trondheim and the results have been discussed in the seventh paper [111]: chapter VII of this thesis. The PhD candidate has partially contributed in this work, since the simulations have been conducted with the master's student Sondre Harbo[1].

- The impact of increasing EV penetration level in a local low-voltage Norwegian grid has been investigated using real power measurement data. Hourly measured Advanced Metering System (AMS) data for one year have been collected from an area connected to a substation transformer. A method is proposed to find the best location for installation of the fast charger, with respect to the grid operational constraints. Further details can be found in the eighth paper [112]: chapter VIII of this thesis. The PhD candidate has partially contributed in this work, since the simulations have been conducted with the master's student Martin Lillebo[1].

- The economic potential of utilising PV and batteries (either EV or SESS), for an electricity prosumer, has been investigated subject to different grid tariff billing formats. The optimisation is run using dynamic programming for an end user equipped with: 1) PV solar panel, 2) SESS/EV, and 3) Base case with no battery and PV. The results are discussed in detail in the ninth paper [113]: chapter IX of this thesis. The PhD candidate has partially contributed to this work, since the simulations have been conducted with the master's student Sigurd Bjarghov[1].

1.9 List of Publications

The following is a list of publications contributed during the PhD:

---

[1] For more details, please see co-authorship forms attached as a part of the submission package.

I. S. Zaferanlouei, H. Farahmand, V. Vadlamudi, and M. Korpås, “BATTPOWER Toolbox: Memory Efficient and High-Performance MultiPeriod AC Optimal Power Flow Solver—Part I: Mathematical Concepts,” submitted for review, 2020.

II. S. Zaferanlouei, H. Farahmand, V. Vadlamudi, and M. Korpås, “BATTPOWER Toolbox: Memory Efficient and High-Performance MultiPeriod AC Optimal Power Flow Solver—Part II: Case Study,” submitted for review, 2020.

III. S. Zaferanlouei, V. Lakshmanan, S. Bjarghov, H. Farahmand and M. Korpås, “BATTPOWER Application: Large Scale Integration of EVs in a Local Distribution Grid—Norwegian Case Study,” submitted for review, 2020.

IV. S. Zaferanlouei, M. Korpås, J. Aghaei, H. Farahmand and N. Hashemipour, “Computational Efficiency Assessment of Multi-Period AC Optimal Power Flow including Energy Storage Systems,” in 2018 International Conference on Smart Energy Systems and Technologies (SEST), Sep. 2018, pp. 1– 6. DOI: 10.1109/SEST.2018.8495683.

V. S. Zaferanlouei, M. Korpås, H. Farahmand and V. V. Vadlamudi, “Integration of PEV and PV in Norway Using Multi-Period ACOPF—Case study,” in 2017 IEEE Manchester PowerTech, ISSN: null, Jun. 2017, pp. 1–6. DOI: 10.1109/PTC.2017.7981042.

VI. S. Zaferanlouei, I. Ranaweera, M. Korpås and H. Farahmand, “Optimal Scheduling of Plug-in Electric Vehicles in Distribution Systems Including PV, Wind and Hydropower Generation, eng. Energynautics GMBH, 2016,” ISBN: 978-3-9816549-3-6.

VII. S. Flinstad Harbo, S. Zaferanlouei and M. Korpås, “Agent Based Modelling and Simulation of Plug-In Electric Vehicles Adoption in Norway,” in 2018 Power Systems Computation Conference (PSCC), Jun. 2018, pp. 1– 7. DOI: 10.23919/PSCC.2018.8442514.

VIII. M. Lillebo, S. Zaferanlouei, A. Zecchino and H. Farahmand, “Impact of large-scale EV integration and fast chargers in a Norwegian LV grid,” The Journal of Engineering, vol. 2019, no. 18, pp. 5104–5108, 2019, ISSN: 2051-3305. DOI: 10.1049/joe.2018.9318.

IX. S. Bjarghov, M. Korpås and S. Zaferanlouei, “Value comparison of EV and house batteries at end-user level under different grid tariffs,” in 2018 IEEE International Energy Conference (ENERGYCON), Jun. 2018, pp. 1– 6. DOI: 10.1109/ENERGYCON.2018.8398742.

The following is a list of publications contributed during the PhD, but which not relevant to the main thesis topic:

I. [114]: F. Berglund, S. Zaferanlouei, M. Korpås and K. Uhlen, (2019). “Optimal Operation of Battery Storage for a Subscribed Capacity-Based Power Tariff Prosumer—A Norwegian Case Study,” Energies, 12(23), 4450.

II. [115]: G. Sæther, P. Crespo del Granadob, S. Zaferanlouei, “Peer-to-Peer electricity trading in an Industrial site:Value of buildings flexibility on peak load reduction,” Working Paper, NTNU, 2020.

Chapter 2

Contributions

The following chapters in this thesis, from chapter I until chapter IX include the main papers contributed during the PhD study and research. Therefore, in order to smooth the follow-up and give a concise overview to the readers, this chapter is intended to summarise the main contributions made in each paper. In this respect, the author has attempted to write the following sections as simply and concisely as possible. Further details can be found in the original papers.

2.1 BATTPOWER Toolbox: Memory-Efficient and High-Performance MultiPeriod AC Optimal Power Flow Solver—Part I: Mathematical Concepts

The BATTPOWER solver is the main contribution of this thesis, which was developed to fulfill the Task 4. and Task 1. in the section 1.7 of chapter 1.
The contributions made in this project are the following:

I. Derive the first and second partial analytical derivatives of constraints and objective function to be used in the KKT conditions (the necessary optimality conditions: the partial derivatives of Lagrangian w.r.t. all variables should be equal to zero).

II. Explore the sparsity structure of each constraint, and their subsequent derivatives in the multi-period form.

III. Introduce a new re-ordering for the Hessian of KKT conditions such that the new format can be solved with a Schur-Complement algorithm.

IV. Introduce a Schur-Complement algorithm tailored for the re-ordered KKT structure.

2.1.1 Analytical Gradients

The first and second analytical derivatives of nonlinear and linear inequality constraints $\mathbf{H}(\mathbf{X})$[1], nonlinear and linear equality constraints $\mathbf{G}(\mathbf{X})$ and objective function$F(\mathbf{X})$ are extracted and can be found in Appendix A of this paper, (see chapter I).

$$\mathbf{G}_{\mathbf{X}} = \frac{\partial \mathbf{G}}{\partial \mathbf{X}} \tag{2.1a}$$

$$\mathbf{H}_{\mathbf{X}} = \frac{\partial \mathbf{H}}{\partial \mathbf{X}} \tag{2.1b}$$

$$F_{\mathbf{X}} = \frac{\partial F}{\partial \mathbf{X}} \tag{2.1c}$$

$$\mathbf{G}_{\mathbf{XX}} = \frac{\partial}{\partial \mathbf{X}}(\mathbf{G}_{\mathbf{X}}^{\top}\boldsymbol{\lambda}) \tag{2.1d}$$

$$\mathbf{H}_{\mathbf{XX}} = \frac{\partial}{\partial \mathbf{X}}(\mathbf{H}_{\mathbf{X}}^{\top}\boldsymbol{\lambda}) \tag{2.1e}$$

$$F_{\mathbf{XX}} = \frac{\partial}{\partial \mathbf{X}}(F_{\mathbf{X}}^{\top}) \tag{2.1f}$$

2.1.2 Sparse Matrix Operations

In general, the analysis of computational complexity of sparse matrices and vectors (algebraic operations) is dependent on the sparsity structure of each matrix in the operation. This means that if we know the sparsity structure of each matrix beforehand, then it is possible to write a specific tailored algorithm to complete this operation much faster than a general algorithm written to solve any type of structure. However, the tailored algorithm might not work for general problems. Why then might a tailored algorithm solve a specific sparsity structure faster?

I. Memory allocation of sparse matrices. If the memory required before and after each operation is determined, then the operation can be performed faster.

II. Operational Performance. A tailored algorithm can be extended according to the type of expected successive operations. If the type of operations is determined, then specific libraries could be developed in order to lower the computational costs.

---

[1] Note that all vectors and matrices are shown with bold and non-italic notation: **BOLD**

An example is provided in the following to simplify the concept:

Example 2.1.1 *Let* $A = \begin{bmatrix} 0 & a \\ b & 0 \end{bmatrix}$ *and* $B = \begin{bmatrix} c & 0 \\ 0 & d \end{bmatrix}$, *then the computational complexity of* $A \times B$ *is compared when:*

- *A and B are full matrices.*
- *A and B are sparse matrices.*

If we define a flop as one addition, subtraction, multiplication, or division of two floating-point numbers, then the number of flop counts is a criterion for the assessment of computational performance.

Full matrix operation: *The operation is performed with 12 flops.*

$$\begin{bmatrix} 0 & a \\ b & 0 \end{bmatrix} \times \begin{bmatrix} c & 0 \\ 0 & d \end{bmatrix} = \begin{bmatrix} 0 \times c + 0 \times a & 0 \times 0 + a \times d \\ b \times c + 0 \times 0 & b \times 0 + 0 \times d \end{bmatrix} \tag{2.2}$$

Sparse matrix operation: *Representation format: Coordinate list (COO). The operation is performed with 2 flops.*

$$\begin{aligned} &\overbrace{\begin{bmatrix} 0 \\ 1 \end{bmatrix} \begin{bmatrix} 1 \\ 0 \end{bmatrix}}^{(incices\ of\ i\ and\ j)} \quad \overbrace{\begin{bmatrix} a \\ b \end{bmatrix}}^{(vector\ of\ values)} \times \overbrace{\begin{bmatrix} 1 \\ 0 \end{bmatrix} \begin{bmatrix} 0 \\ 1 \end{bmatrix}}^{(incices\ of\ i\ and\ j)} \quad \overbrace{\begin{bmatrix} c \\ d \end{bmatrix}}^{(vector\ of\ values)} \\ &= \overbrace{\begin{bmatrix} 0 \\ 1 \end{bmatrix} \begin{bmatrix} 1 \\ 0 \end{bmatrix}}^{(incices\ of\ i\ and\ j)} \quad \overbrace{\begin{bmatrix} a \times d \\ b \times c \end{bmatrix}}^{(vector\ of\ values)} \end{aligned} \tag{2.3}$$

A full matrix operation is compared with a sparse matrix operation in Example 2.1.1. A full matrix operation is carried out with 12 flops, while a sparse matrix operation is performed with 2 flops. Note that operation performed in both Eqs. (2.2) and (2.3) are assumed to be performed using a user-defined library.
Although Example 2.1.1 compares the full matrix operation with sparse matrix, the library developed to operate and execute sparse matrix operations is not

strictly similar in each case. This is because sparse matrix representations are not necessarily similar. Moreover, sparse matrices have different structures depending the usage; therefore, it is possible to define and develop a tailored algorithm depending upon various types of structures.

2.1.3 Reordering

A novel reordering format and subsequent permutation matrices have been developed for the first time in this thesis. Equation (2.4) is the well-known Jacobian of KKT equation in chapter I of this thesis, where it is reordered to the arrowhead coefficient matrix of Eq. (2.11).

$$\overbrace{\begin{bmatrix} \begin{bmatrix} \mathbf{M}_1 & & \\ & \ddots & \mathbf{M}_T \end{bmatrix} & \mathbf{G}_{\mathbf{X}}^{\top} \\ \begin{bmatrix} \widetilde{\mathbf{G}}_{\mathbf{x}_1} & & \\ & \ddots & \widetilde{\mathbf{G}}_{\mathbf{x}_T} \\ \overline{\mathbf{G}}_{\mathbf{x}_1} & & \\ & \ddots & \overline{\mathbf{G}}_{\mathbf{x}_T} \\ \overline{\mathbf{G}}^{s}_{\boldsymbol{\tau}_1} & & \\ & \ddots & \overline{\mathbf{G}}^{s}_{\boldsymbol{\tau}_T} \end{bmatrix} & \mathbf{O} \end{bmatrix}}^{\mathbf{A}} \overbrace{\begin{bmatrix} \Delta\mathbf{x}_1 \\ \vdots \\ \Delta\mathbf{x}_T \\ \Delta\widetilde{\boldsymbol{\lambda}}_1 \\ \vdots \\ \Delta\widetilde{\boldsymbol{\lambda}}_T \\ \Delta\overline{\boldsymbol{\lambda}}_1 \\ \vdots \\ \Delta\overline{\boldsymbol{\lambda}}_T \\ \Delta\overline{\boldsymbol{\lambda}}^{s}_1 \\ \vdots \\ \Delta\overline{\boldsymbol{\lambda}}^{s}_T \end{bmatrix}}^{\mathbf{X}} = \overbrace{\begin{bmatrix} -\mathbf{N}_1 \\ \vdots \\ -\mathbf{N}_T \\ -\widetilde{\mathbf{g}}(\mathbf{x}_1) \\ \vdots \\ -\widetilde{\mathbf{g}}(\mathbf{x}_T) \\ -\overline{\mathbf{g}}(\mathbf{x}_1) \\ \vdots \\ -\overline{\mathbf{g}}(\mathbf{x}_T) \\ -\overline{\mathbf{g}}^{s}(\boldsymbol{\tau}_1) \\ \vdots \\ -\overline{\mathbf{g}}^{s}(\boldsymbol{\tau}_T) \end{bmatrix}}^{\mathbf{B}} \tag{2.4}$$

Basic properties of permutation matrices are used to convert the structure of Eq. (2.4) to a new structure depicted in Eq. (2.11). These properties are elaborated in Appendix A of this thesis. Four properties of a permutation matrix are introduced in Table A.1. If we have a linear algebraic equation $\mathbf{AX} = \mathbf{B}$, similar to Eq. (2.4), where $\mathbf{A} \in \mathbb{R}^{n\times n}$ is the coefficient matrix, $\mathbf{X} \in \mathbb{R}^{n\times 1}$ is the vector of variables, and $\mathbf{B} \in \mathbb{R}^{n\times 1}$ is the righthand side, in order to obtain Eq. (2.11) the following procedure is performed:

I. Vector of variables $\mathbf{X}$ is taken as the reference vector, for permutation index:

$$\begin{bmatrix} \Delta\mathbf{x}_1 & \dots & \Delta\mathbf{x}_T & \Delta\widetilde{\boldsymbol{\lambda}}_1 & \dots & \Delta\widetilde{\boldsymbol{\lambda}}_T & \Delta\overline{\boldsymbol{\lambda}}_1 & \dots & \Delta\overline{\boldsymbol{\lambda}}_T & \Delta\overline{\boldsymbol{\lambda}}^{s}_1 & \dots & \Delta\overline{\boldsymbol{\lambda}}^{s}_T \end{bmatrix}^{\top} \tag{2.5}$$

Therefore, index of $i = \{1, \dots, n\}$ which indicates the variables in vector $\mathbf{X}$, (vector (2.5)) can be extended as vector (2.6). Now the permutation vector of $\Xi = (\xi_{i=1}, \ldots, \xi_{i=n})$ can be defined, see Appendix A for basic definitions. Vector of index i of vector (2.5) is written as:

$$\begin{aligned}\Big[& i = \{1\} \quad \ldots \quad i = \{N_x\} \quad i = \{N_x + 1\} \quad \ldots \quad i = \{N_x + N_{gn}\} \\ & i = \{N_x + N_{gn} + 1\} \quad \ldots \quad i = \{N_x + N_{gn} + N_{gl}\} \\ & i = \{N_x + N_{gn} + N_{gl} + 1\} \quad \ldots \quad i = \{N_x + N_{gn} + N_{gl} + N_{gs}\}\Big]^{\top}\end{aligned} \tag{2.6}$$

II. Permutation vector of Ξ (a new index) is defined to reorder Eq. (2.5) to form Eq. (2.7). For example, if $i = \{1, 2, 3, 4\}$, permutation could be $\Xi = \{3_{i'=1}, 2_{i'=2}, 4_{i'=3}, 1_{i'=4}\}$. In order to obtain (2.7), Ξ is defined as the vector (2.8).

$$\left[\Delta \mathbf{x}_1 \ \Delta \widetilde{\boldsymbol{\lambda}}_1 \ \Delta \overline{\boldsymbol{\lambda}}_1 \ldots \Delta \mathbf{x}_T \ \Delta \widetilde{\boldsymbol{\lambda}}_T \ \Delta \overline{\boldsymbol{\lambda}}_T, \quad \Delta \overline{\boldsymbol{\lambda}}^s_1 \ldots \Delta \overline{\boldsymbol{\lambda}}^s_T\right]^{\top} \tag{2.7}$$

$$\begin{aligned}\Xi = \Big[& \xi_{\{i'=1\}} = \{1\} \quad \xi_{\{i'=2\}} = \{N_{gn} + 1\} \quad \xi_{\{i'=3\}} = \{N_x + N_{gn} + 1\} \\ & \ldots \\ & \xi_{\{i'=N_x+N_{gn}+N_{gl}-n_{gn}-n_{gl_T}\}} = \{N_x\} \\ & \xi_{\{i'=N_x+N_{gn}+N_{gl}-n_{gl_T}\}} = \{N_x + N_{gn}\} \\ & \xi_{\{i'=N_x+N_{gn}+N_{gl}\}} = \{N_x + N_{gn} + N_{gl}\} \\ & \xi_{\{i'=N_x+N_{gn}+N_{gl}+1\}} = \{N_x + N_{gn} + N_{gl} + 1\} \\ & \ldots \\ & \xi_{\{i'=N_x+N_{gn}+N_{gl}+N_{gs}\}} = \{N_x + N_{gn} + N_{gl} + N_{gs}\}\Big]^{\top}\end{aligned} \tag{2.8}$$

III. When the vector Ξ is defined, then permutation matrix $\mathbf{P}$ can be constructed according to Eq. (A.1) in Appendix A. If $\mathbf{P}$ is multiplied to the equation $\mathbf{AX} = \mathbf{B}$, then:

$$\mathbf{PAX} = \mathbf{PB} \tag{2.9}$$

If the properties of permutation matrices are used here, which are elaborated in Table A.1 of Appendix A, then:

$$\mathbf{PAPP}^{-1}\mathbf{X} = \mathbf{PB} \tag{2.10}$$

Thus, the Eq. (2.4) is converted to the well-known arrowhead structure of (2.11), using (2.10). Term **PAP** reorders the rows and columns of the coefficient matrix, term $\mathbf{P}^{-1}\mathbf{X} = \mathbf{P}^{\top}\mathbf{X}$ reorders the vector of variables, and term **PB** reorders the righthand side.

$$\overbrace{\begin{bmatrix} \Upsilon_1 & & & & \boldsymbol{\rho}_1^\top \\ & \Upsilon_2 & & & \boldsymbol{\rho}_2^\top \\ & & \ddots & & \vdots \\ & & & \Upsilon_T & \boldsymbol{\rho}_T^\top \\ \boldsymbol{\rho}_1 & \boldsymbol{\rho}_2 & \dots & \boldsymbol{\rho}_T & 0 \end{bmatrix}}^{\mathbf{PAP}} \overbrace{\begin{bmatrix} \delta\boldsymbol{\omega}_1 \\ \delta\boldsymbol{\omega}_2 \\ \vdots \\ \delta\boldsymbol{\omega}_T \\ \delta\boldsymbol{\lambda} \end{bmatrix}}^{\mathbf{P}^\top\mathbf{X}} = \overbrace{\begin{bmatrix} \boldsymbol{\zeta}_1 \\ \boldsymbol{\zeta}_2 \\ \vdots \\ \boldsymbol{\zeta}_T \\ \boldsymbol{\Gamma} \end{bmatrix}}^{\mathbf{PB}} \tag{2.11}$$

2.1.4 Schur-Complement

A high-performance and memory-efficient sparse Schur-Complement algorithm is introduced in this paper in order to solve the multi-period structure of the KKT systems for both stationary SESS and EV. The proposed algorithm consists of two sub-algorithms:

I. Alg. 1) Schur-Complement factorisation.

II. Alg. 2) Forward and backward substitution.

2.2 BATTPOWER Toolbox: Memory-Efficient and High-Performance MultiPeriod AC Optimal Power Flow Solver—Part II: Case Study

This paper extends the Part I's paper with a numerical analysis to support the arguments in the mathematical background. The computational performance of first and second analytical partial derivatives of constraints and objective function are compared with those of numerical derivatives in order to show the scalability of the proposed algorithm. Moreover, the computational performance of the proposed Schur-Complement algorithm is compared with a direct LU solver.

2.2.1 Analytical Derivatives

Table 2.1 shows the total time elapsed to calculate the analytical derivatives and of the numerical ones. The numerical gradients are calculated based on the central finite difference method.

Since analytical derivatives are an accurate model of the partial derivatives of functions, further accuracy comparison with the finite numerical method applied here is neglected. The computational performances of analytical derivatives are significantly higher than numerical derivatives.

Table 2.1: Total time (TotalTime = No.of Iter. × TimePerIter) elapsed to calculate: 1) Analytical (hand-coded) derivatives, and 2) Numerical derivatives

				Analytical			Numerical		
Case	T	n_y	iter	$F_{\mathbf{X}}$(s)	$\mathbf{G_X}+\mathbf{H_X}$(s)	$\mathscr{L}^{\gamma}_{\mathbf{XX}}$(s)	$F_{\mathbf{X}}$(s)	$\mathbf{G_X}+\mathbf{H_X}$(s)	$\mathscr{L}^{\gamma}_{\mathbf{XX}}$(s)
Case9	2	5	13	0.03	0.13	0.14	0.43	0.98	140.07
Case9	10	5	23	0.08	0.36	0.37	11.32	30.62	22815.29
IEEE30	2	5	12	0.04	0.25	0.18	1.01	2.16	682.70
IEEE30	10	5	16	0.05	0.24	0.25	16.73	49.12	79712.78
IEEE118	2	5	22	0.04	0.19	0.20	7.41	18.07	24557.09
IEEE118	10	5	37	0.09	0.62	0.82	158.21[1]	572.09 [1]	4599735[1]
PEGASE1354	2	5	23	0.05	0.61	0.78	85.54[1]	496.18 [1]	7185888 [1]
PEGASE1354	10	5	33	0.10	3.77	5.15	588.06[1]	3530 [1]	51550941[1]

[1] Estimated total time: The time elapsed for one iteration multiplied to the iteration that would take to converge

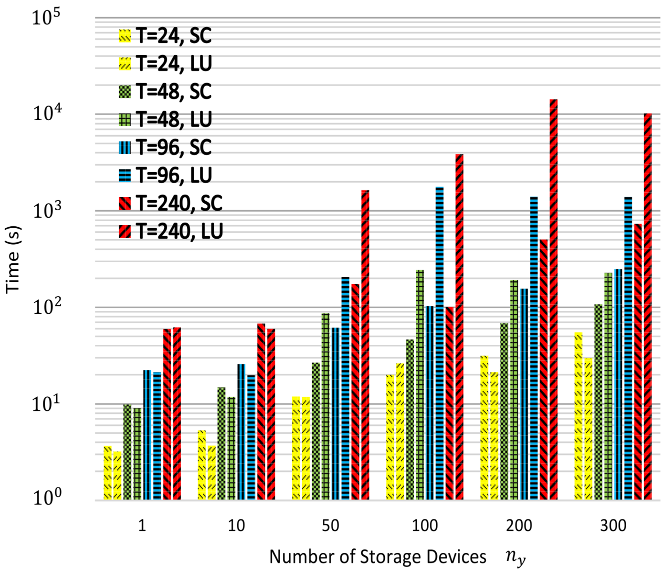

Figure 2.1: Total time (TotalTime = No.of Iter. × TimePerIter) for solution of the linear KKT systems of (2.11) solved by Schur-Complement algorithm proposed in the part I paper vs direct sparse LU solver, applied on IEEE 118

2.2.2 Schur-Complement

The computational performance of the proposed sparse Schur-Complement algorithm is compared with a direct sparse LU solver in this paper with two application modes, SESS and EV modes.

Figure 2.1 depicts the computational time needed to solve Eq. (2.11) of case IEEE118 with Schur-Complement and a direct sparse LU solver for the number of storage devices n_y =1, 5, 10, 20, 50, and 100; each case takes into account time horizons of T = 24, 48, 96, and 240. As $n_y > 10$ the Schur-Complement solver has higher performance which increases considerably when $T > 24$. Note that the direct sparse-LU solver is dominant again when $n_y > 300$, for the reason that $n_y > \mathcal{K}$ where $\mathcal{K} \propto N_{\Upsilon_t} = 2n_b + 2n_g + 4n_y + n_{gn} + n_{gl_t}$, where n_b, n_g, n_y, n_{gn} and n_{gl_t} are respectively the number of buses, generators, storage devices, grid non-linear equalities and grid linear equalities at time t. Put simply, when $n_y > 300$, the number of storage devices is larger than a certain number which is proportional to the size of blocks of Υ_t in (2.11). More results can be found in chapter II of this thesis.

2.3 BATTPOWER Application: Large-Scale Integration of EVs in an Active Distribution Grid —Norwegian Case Study

This work was developed to: 1) find responses to RQ 1., RQ 2. and RQ 3. in the section 1.6, and 2) fulfill the Task 1., Task 2., and Task 3. in the section 1.7 of chapter 1.

The contribution made in this paper can be summarised as:

I. Propose a fast and scalable centralised optimisation model: An optimal charge scheduling of EVs with consideration of grid operational constraints (Multi-period AC Optimal Power Flow (MPOPF) with grid operational constraints).

II. Apply the proposed method on a large real case study. The case study is the largest local case study ever explored in research as a Norwegian distribution network, with 974 buses, 1023 lines, 2 generators, 856 consumers, and 1113 EVs.

III. Compare the cost-effectiveness of the proposed method with: 1) an uncoordinated charge method, and 2) a centralised charge method without considering the grid operational constraints (MPOPF without grid operational constraints).

Table 2.2 compares three different strategies of EV charge scheduling. These strategies are tested for: 1) daily energy consumption, 2) system loss, 3) system cost, 4) daily/yearly saving, and finally 5) robustness of each method to charge EVs without interruption. It should be kept in mind that: 1) these values are only based on energy price (summation of hourly energy consumed multiplied to by hourly spot price for the period under study), which might be considerably higher than what has been presented here, and 2) the saving value, which is calculated subject to the assumption that the spot price is flat during midnight in the Norwegian system, as can be seen in [8]. If the Danish spot price is adopted in this calculation, then the saving would be much higher, due to the fact that Danish spot price is considerably more volatile than Norwegian one.

Numerical results suggest that: 1) Uncoordinated charge method has slightly higher operational costs than the centralised charge scheduling method, which can be negligible. However, the maximum number of EVs for which uncoordinated charging can be accommodated in the current grid infrastructure without reinforcement is only 20%, and 2) centralised charge scheduling strategies with and without consideration of grid operational constraints have almost identical operational cost. However, the latter can only accommodate 36% of EVs without grid reinforcement.

Table 2.2: [a) total energy production, b) active system loss, and c) system cost] in three different operational modes.

Method	4	5	6	7	8	9
1	118.64	9.0	75,819	–	–	220 EV (20%)
2	118.74	8.6	73,974	1,846 – 2.4 %	673,790	400 EV (36%)
3	118.74	8.6	74,636	1,184 – 1.6 %	432,160	1113 EV (100%)

[1] Dumb Charging.
[2] MPOPF without operational limits.
[3] MPOPF with operational limits.
[4] Daily Energy Consumption (MWh).
[5] LOSS (MWh).
[6] System Cost (NOK).
[7] Daily Saving (NOK)–(%).
[8] Yearly Saving (NOK).
[9] Max EV hosting Capacity.

2.4 Computational Efficiency Assessment of Multi-Period AC Optimal Power Flow including Energy Storage Systems

This work was developed to fulfill the Task 1. in the section 1.7 of chapter 1. Computational efficiency of an MPOPF incorporating energy storage systems (intertemporal constraints) is accessed for the first time during this PhD study in the fourth paper, chapter IV of this thesis. The purpose of study was to develop a scalable MPOPF structure subject to large-scale case studies. Thus, we introduced the analytical first and second partial derivatives of Lagrangian w.r.t. all variables into MPOPF formulation to accelerate the solution of large-scale case studies. Moreover, the proposed problem could potentially be an open-box platform for further research, to: 1) solve other types of power system problems within the introduced package, and 2) introduce power system components inside the current formulation.

Table 2.3 shows the overall results of a 3 bus case study, where the proposed method incorporated the analytical derivatives. Many types of NLP solvers have been tested and compared with the proposed method. The proposed method converges almost 10 times faster than the commercial solvers in this table.

Table 2.3: Computational time for different solvers and with the same convergence criteria

Implemented environment	Solver	Computational time (sec)
MATLAB	FMINCON	0.411
GAMS	CONOPT	0.408
GAMS	CONOPT4	0.592
GAMS	COUENNE	0.637
GAMS	IPOPT	0.538
GAMS	IPOPTH	0.517
GAMS	KNITRO	0.461
GAMS	MINOS	0.413
GAMS	PATHNLP	0.472
GAMS	SNOPT	0.385
MATLAB	The Proposed Method	0.056

It should be kept in mind that anlaytical derivatives are the accurate value of a calculated gradient; therefore, it does not make sense to compare the calculated values with other types of method. However, it makes sense to compare numerical gradients with analytical ones to check how accurate they might be.

Key findings in this paper:

I. Introduction of analytical first and second partial derivatives of Lagrangian w.r.t. all variables.

II. The MPOPF model is extended to a open-box stage. There is a potential to use this platform for other types of application and solve similar related problem with specific features: 1) fast enough, and 2) accurate.

2.5 Integration of PEV and PV in Norway Using Multi-Period ACOPF—Case Study

This work was developed: 1) to find responses for RQ 1., RQ 2., RQ 3., and RQ 4. in section 1.6, and 2) to fulfill the Task 1., Task 3. and Task 5. in section 1.7 of chapter 1.

The integration of Distributed Energy Resources (DER) and Renewable Energy Systems (RES) will pose substantial challenges in the electricity distribution networks. The impact of large-scale EV penetration along with consideration of wind turbine, hydropower, and Photovoltaic (PV) solar panels on the distribution grid is analysed through two methods: 1) uncoordinated (dumb) charging of EVs, and 2) centralised EV charging using a MPOPF method. Details regarding the mathematical formulations and data input can be found in chapter V of this thesis.

2.5.1 Centralised Charge Profile vs Uncoordinated Charge Profile

Figure 2.2 illustrates the behaviour and SOC of individual EVs located on the secondary side of a transformer. A comparison of the results of the MPOPF algorithm with those of the dumb-charging scenario is also provided in this figure. From figure 2.2-a, it can be seen that charging occurs at the lowest marginal price around hours 25-31. However, for the dumb-charging scenario, the charging occurs at the arrival time. Figure 2.2-b illustrates the charge rate per hour: kW (kWh/h) for the dumb-charging scenario, which can be up to 13 kW per charging point. On the other hand, the mean charging rate of coordinated charge control is significantly lower (between 2-3 kW) than a dumb-charging method, which poses lower stress on the distribution grid lines/transformers, both in terms of voltage and load ratio.

2.5.2 Share of Load on a LV Transformer

Tables 2.4 and 2.5 present more detailed results. Two ratio terms are defined: R_1, in Eq. (2.12) which is the ratio of summation of total PV generations to the summation of consumers' energy demand in one cycle; R_2, in Eq. (2.13) which is the

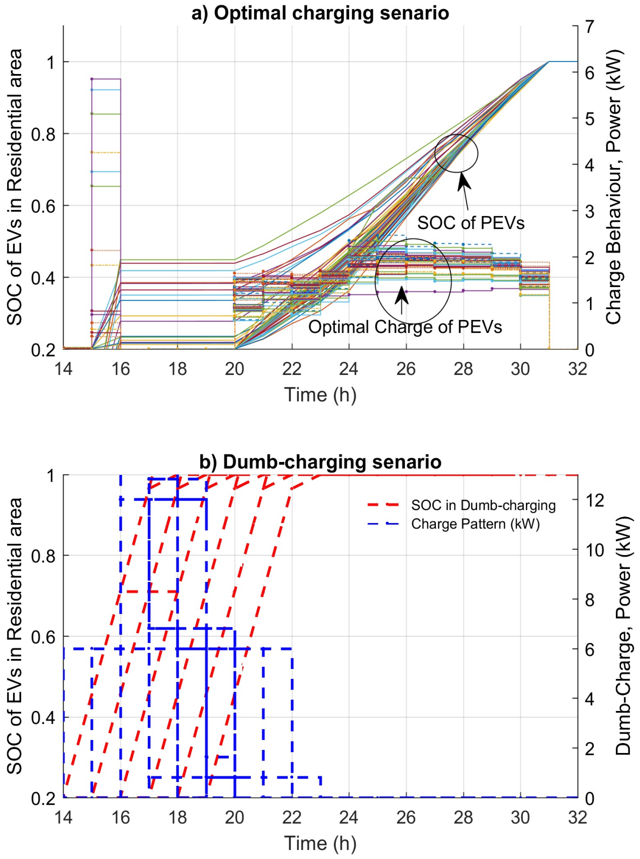

Figure 2.2: 70% EV and 100% PV penetration in the distribution grid. Charge behaviour and SOC of the EVs located at the residential area: a) with the proposed algorithm, and b) with dumb-charging method.

ratio of the summation of total EV energy consumption to the summation of total consumers' energy demand in one cycle. Note that consumers' energy demand is the standard energy demand excluding the EV energy demand. Table 2.4 shows the values of these ratios for different penetrations of EV-PV in the distribution grid. These values show that EV and PV have a smaller share compared to the actual consumer load demand in the distribution grid. One cycle is 24 hours from 0800 h of a day to 0800 h of the next day in the table.

$$R_1 = \frac{\sum_{t=1}^{t=24}\sum_{i=1}^{i=62} pv_{\{i,t\}}}{\sum_{t=1}^{t=24}\sum_{i=1}^{i=62} p^d_{\{i,t\}}}\ \% \tag{2.12}$$

$$R_2 = \frac{\sum_{t=1}^{t=24}\sum_{i=1}^{i=62} ev_{\{i,t\}}}{\sum_{t=1}^{t=24}\sum_{i=1}^{i=62} p^d_{\{i,t\}}}\ \% \tag{2.13}$$

where i is the number of prosumers, $pv_{i,t}$ is the active power generation of PV of prosumer i at time t, $ev_{i,t}$ is the active power demand of EV of prosumer i at time t, $p^d_{i,t}$ is the active load demand of prosumer i at time t, and total number of prosumers fed from a MV-LV transformer is 62.

Table 2.5 is the basis of this paper, see chapter V. The dumb-charging method and centralised charge scheduling method (MPOPF with operational grid constraints) are compared in detail with respect to the other two terms: R_3 and R_4. The maximum EV energy consumption in the considered time cycle is noted. Say this occurs at hour t_c, termed as a critical hour. The difference between the consumer energy demand and PV generation in this instance t_c is noted. The term R_3 is defined in Eq. (2.15).

$$ev_{max}\Big|_{t_c} = \max_t \sum_{i=1}^{i=62} ev_{\{i,t\}} \tag{2.14}$$

$$R_3 = \frac{ev_{max}\Big|_{t_c}}{\sum_{i=1}^{i=62} p^d_{\{i,t_c\}} - \sum_{i=1}^{i=62} pv_{\{i,t_c\}}}\ \% \tag{2.15}$$

R_3 is the criterion for how large the share of maximum EV load is on the net load of system, and R_4 is defined as Eq. (2.16).

$$R_4 = \sum_{i=1}^{i=62} p^d_{\{i,t_c\}} + ev_{max}\Big|_{t_c} - \sum_{i=1}^{i=62} pv_{\{i,t_c\}} \quad (kW) \tag{2.16}$$

Table 2.4: Variation of R_1 and R_2 for different EV-PV penetration levels for one-cycle 0800 - 0800

EV-PV(%)	0-0	10-10	20-20	30-30	40-40	50-50	60-60	70-70	80-80	90-90	100-100
R_1 %	0	0.84	2.89	4.03	6.19	7.32	9.77	11.20	12.81	13.40	17.74
R_2 %	0	2.58	5.16	7.748	10.33	12.91	15.49	18.07	20.66	23.56	26.15

Table 2.5: Variation of R_3, R_3, and minimised cost of power import for different EV-PV penetration levels

1		0-0	0-30	0-70	0-100	30-0	30-30	30-70	30-100	70-0	70-30	70-70	70-100	100-0	100-30	100-70	100-100
2	R_3 %	-	-	-	-	45.12	50.57	62.67	79.29	95.3	106.7	132	167	143	160	198	251
	R_4 (kWh/h)	-	-	-	-	348	321	277	239	480	451	406	367	603	573	527	486
	Cost (€)	6969	6391	5760	4994	6990	6453	5821	5055	7121	6543	5910	5144	7191	6611	5978	5211
3	R_3 %	-	-	-	-	53.4	53.4	53.4	53.4	54	54	54	54	Infeasible	Infeasible	78	106
	R_4 (kWh/h)	-	-	-	-	310	310	310	310	310	310	310	310			313	310
	Cost (€)	6969	6391	5760	4994	7031	6355	5664	4820	7025	6388	5697	4853			5895	5119

[1] EV-PV(%).

[2] Dumb-Charging method.

[3] Optimal Charging method.

R_4 is the criterion for how large the maximum EV load on the transformer can be with high penetration of EV, PV and in comparison with base load.

R_3 is almost constant for the optimal charging scenario for different levels of EV-PV penetration; it increases when EV penetration is 100%. For the optimal charging scenario, the total transformer load at hour t_c is almost 315 kW, whereas for the dumb-charging scenario it is 600 kW. Moreover, the total cost of power imported from the main grid for the optimal charging scenario is always less than that of the dumb-charging scenario. Key findings of the paper (chapter V) are:

I. An MPOPF problem is solved using FMINCON, which is an internal solver of MATLAB. The simulation results prove that FMINCON solution to the problem with 33 hours' horizon is computationally slow and inefficient. Each solution takes almost 4 hours (14400 sec.) to converge. Therefore, in this stage we decided to develop a high computational performance solver and incorporate a scalable and tractable solution method.

II. From Eqs. (2.12),(2.13), and Table 2.4: the maximum total share (100%) of EVs and PVs on the total consumers' demand power in one day cycle (from 08:00 until 08:00 the next day) is 17.74% and 26.15%, which shows that the total energy share of renewable energy on the distribution network is not comparable with total consumer demands.

III. On the other hand, the share of EV power (kWh/h) on the summation of total demand $i = 1...i = 62$ in a specific time t_c is considerable.

IV. From items II and III, it can be concluded that DER and RES have a small share of energy in one day cycle compared with the consumer base loads. However, the impact of RES and DER in terms of power (kWh/h) is considerable.

V. Centralised charge control of EVs takes into account the operational grid constraints. This lifts the impact of RES and DER in terms of high power (kWh/h) demand discussed in the previous item. However, this strategy requires the implementation of control apparatus in the distribution grid, both in terms of hardware and software, where the detailed investment cost could be investigated in the future studies.

VI. Centralised control of EVs culminates in lower operational costs than an uncoordinated charging strategy. A detailed long-term cost analysis (investment cost, grid reinforcement and operational costs) is suggested here as a future research direction in order to formulate a more realistic strategy to follow for policy makers and engineers.

2.6 Optimal Scheduling of Plug-in Electric Vehicles in Distribution Systems Including PV, Wind and Hydropower Generation

This work was developed: 1) to find responses for RQ 1., RQ 2., and RQ 3. in the section 1.6, and 2) also fulfill the Task 1., Task 3. and Task 5. in the section 1.7 of chapter 1.

A MPOPF formulation is developed during this PhD study to consider: 1) the intertemporal constraints of energy storage systems, and 2) operational constraints of medium sized distribution grid (147 buses, 146 lines, 2 generators, 62 consumers in the LV network and 32 MV-LV transformers). Figure 2.3 shows the LV side of the distribution network studied in this paper. Critical buses of the network are coloured in red, and are located at the end point of branches.

It is assumed that 50% of the households have PV systems with a rated capacity of 4 kW. Moreover, it is assumed that 50% of the households own EVs with 20 kWh capacity, and a charging rate of 6 kW. A wind generator is connected to the MV side with 600 kW capacity. Figure 2.4 shows the voltage fluctuations at the

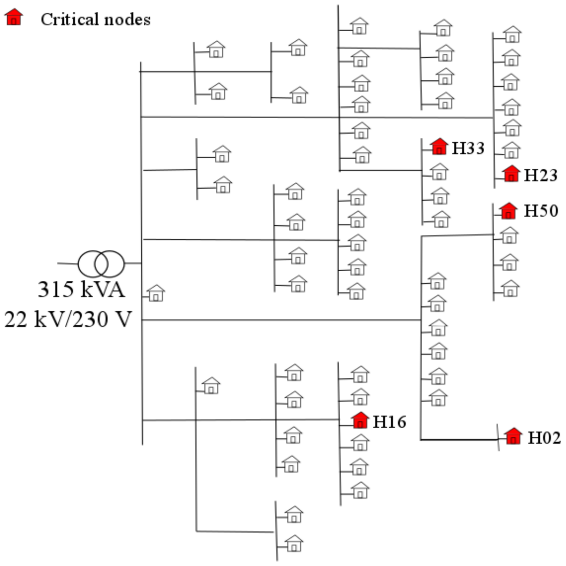

Figure 2.3: LV network (230 V) supplied by the transformer-DT1.

critical nodes for two cases: 1) optimal charge method using MPOPF, and 2) uncoordinated charge method.

It should be kept in mind that the voltage profiles shown in figure 2.4 are relative

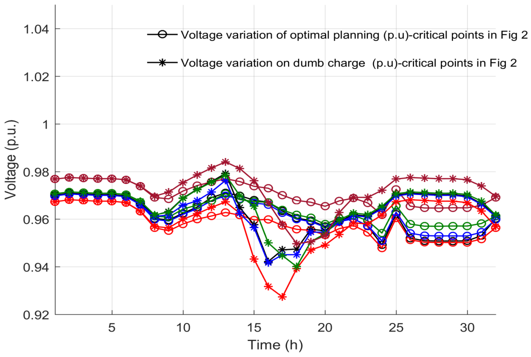

Figure 2.4: Voltage variation at the critical nodes of the network with optimal charging and dumb charging (Black: H50, Red: H23, Blue: H02, Green: H16 and Brown: H33). 50% EV and 50% PV in the network.

to the voltage of the reference bus (slack bus) of the distribution network, which is set to 1 (p.u.). Voltage profiles of critical node follow almost the same pattern. There is a peak of voltage during the time that PV production is high, and there is a

trough when EVs are charging. The difference between optimal charging and uncoordinated charging strategies is that the optimal charging strategy schedules the EVs to charge during midnight; therefore, a voltage trough occurs between 01:00 until 06:00 for optimal charge strategy, while a voltage trough occurs between the hours 14:00 until 19:00 for the dumb charging strategy.
Key findings of this paper can be summarised into:

I. A real local distribution grid, including EVs, PVs, wind energy, and hydropower generation, are taken as the simulation input in this paper.

II. A MPOPF algorithm is implemented in order to optimise the generation cost plus system loss. Simulation results indicated that the proposed algorithm saves 2.4% total cost in compare with that of dumb-charging strategy.

2.7 Agent Based Modelling and Simulation of Plug-in Electric Vehicles Adoption in Norway[2]

This work was developed: 1) to find response for RQ 2. in the section 1.6, and 2) also fulfill the Task 2. and Task 3. in the section 1.7 of chapter 1.
An Agent-Based Modelling (ABM) simulation of EVs is conducted in the seventh paper, see chapter VII of this thesis. The paper investigated the demand side of the power systems and the effects of utilising an increasingly larger fleet of EVs. Different charging strategies have been undertaken as the basis of the agents' decision making criteria, and tested in the simulations to determine the variability of the agents' charging profile. There are two key points in the ABM simulations, ABM is the key to 1) estimating the future power demand, and 2) understanding and determining the effect of different incentives and policies in terms of energy prices (€/MWh), tariffs, location of fast/public charging stations and time of charge on the distribution grid power system.
Simulations ran for the Trondheim city reinforces the notion that the rising adoption of EVs might not only pose a substantial challenge due to the relative size of the power demanded, but more critically also because of the variability that the charging profiles exhibit. On the other hand, the different behaviour of the EV agents, as modelled through different charging strategies, indicates that incentives such as price signals might affect how much the agents charge at different times. Hence it may even lead to the EVs' batteries as assets to help stabilise the power balance in the electric grid. The proposed charging strategies in this study are:

---

[2] The PhD candidate has partially contributed in this work, since the simulations have been conducted with the master's student Sondre Harbo. For more details, please see the co-authorship forms attached as a part of the submission package.

Strategy.1 Uncoordinated (Dumb) charging.

Strategy.2 Probabilistic charging based on SOC.

Strategy.3 Probabilistic charging strategy based on SOC and price.

In Figs. 2.5 and 2.6 we may observe the profiles of the simulations run for 40 days with 1500 agents. In the former the agents utilise the strategy 2, that i.e. charging based solely on SOC, whereas in the strategy 3 the agents are influenced by both their SOC and the energy price. A feature with these graphs is that they present the average, 5%, 25%, 75% and 95%, percentiles for the data in the same minute for the 40 days. Hence, we may better observe the variability within the data. From the Figures we can see it is clear that there is a considerable variability band, especially in figure 2.5 representing the SOC-scaled charging strategy.

Additionally, the same statistics were computed for the whole aggregated time series overall the 40 days. The results are presented along with the standard deviation (SD) in Table 2.6. From Table 2.6, we see that the maximal value of power demanded is around the same, although the average value seems to be higher in the Strategy.3 case. However, in contrast to what the graphs seem to display, we also see that the standard deviation, a measure of variability in a time series, is also slightly higher in the Strategy.3 case as well. However, the standard deviation on

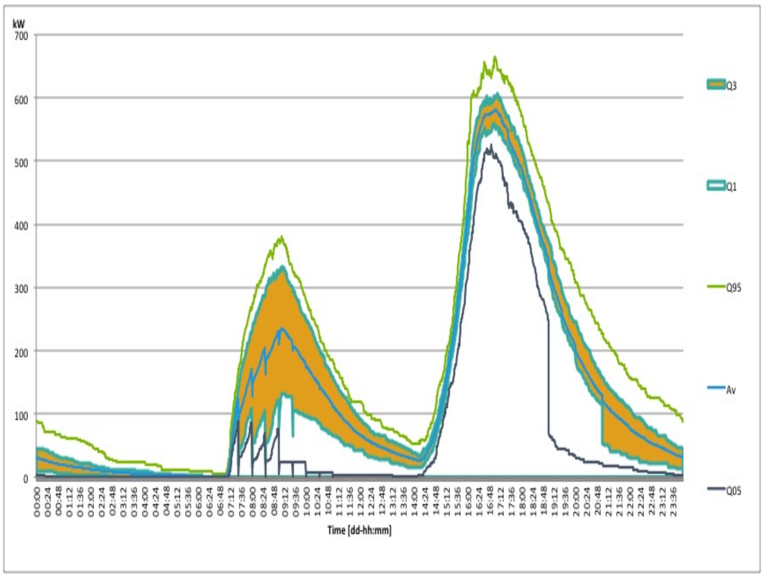

Figure 2.5: Total power demand from 1500 EVs during 40 days with charging based on SOC.

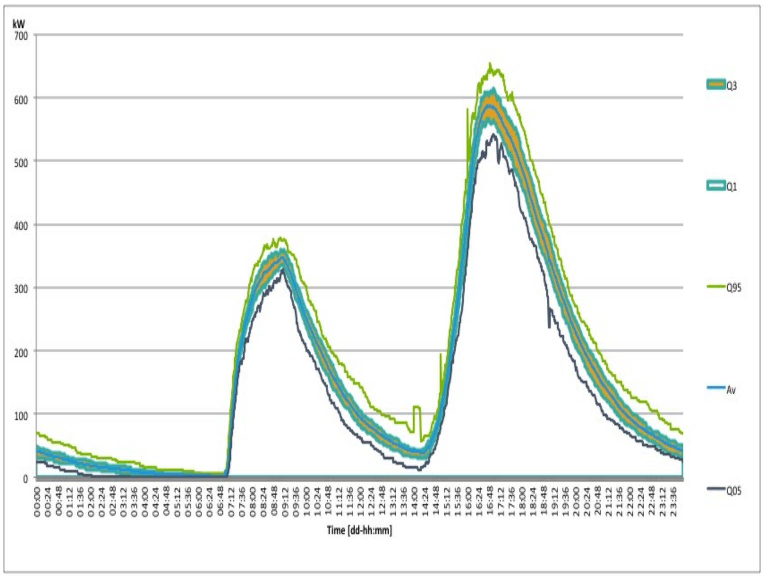

Figure 2.6: Total power demand from 1500 EVs during 40 days with charging strategy based on SOC and price.

relative changes is high in the Strategy.3, but remarkable in the Strategy.2.

Main findings of this paper can be concluded as:

Table 2.6: Statistics for 40-day simulation statistics with 1500 agents with different charging strategies

Stats [/kW]	Q95	Avg	Q05	SD	SD of prof.av.
Strategy.2:SOC	522	137	0	163	38,66
Strategy.3:SOC&Price	537	161	3	167	17,88

I. Since this model was simulated using real data for Trondheim, the analysis provides take-aways for policy makers in this city.

II. The maximal value of power demanded is about the same for both cases of Strategy.2 and Strategy.3.

III. The STD on relative changes is extremely high in the case of the Strategy.2. However, a measure of variability in a time series is slightly higher for the Strategy.3 than that of Strategy.2.

IV. The model Strategy.3 shows that price signals might work in order to incentivise PEV owners to charge at times more beneficial to the power system.

V. With the ABM developed here, the prognosis of the average and peak power demands of 2030 and 2050 is investigated (refer to chapter VII for more details).

2.8 Impact of large-scale EV integration and fast chargers in a Norwegian LV grid[3]

This work was developed: 1) to find response for RQ 2. in the section 1.6, and 2) also fulfill the Task 3. in the section 1.7 of chapter 1.

In this paper, chapter VIII of this thesis, by using real power measurements obtained from household advanced metering systems (AMS) in load flow analyses, the impact of increasing EV penetration levels in a Norwegian distribution grid is assessed. The possibility of installing fast EV chargers is investigated through two criteria: 1) voltage deviation, and 2) system power loss. The results show that the network can be operated safely, with respect to the voltage levels at all end-users, with the ultimate EV penetration of 50%. Moreover, it is shown that injecting reactive power at the location of an installed fast charger proved to significantly reduce the largest voltage deviations otherwise imposed by the charger.

2.8.1 Load Flow Analysis

In Figure 2.7, the load ratio for all buses in the network is shown. In this figure, it can be seen that the aggregated end-consumer load connected to the radial labelled "I" reaches the nominal power capacity at a low level of EV penetration.

Figure 2.8 displays the largest voltage drops below 1 p.u. for all buses, sorted by

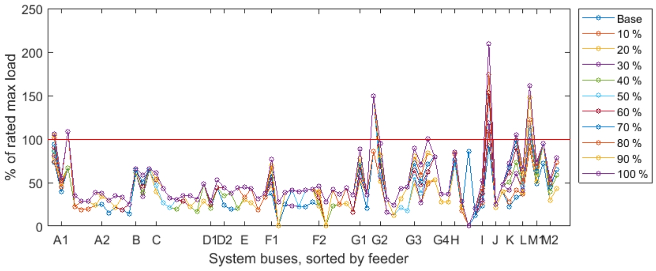

Figure 2.7: Largest load ratio value reached for all buses in the system, for all 10 EV penetration cases, sorted by which feeder to which they are connected.

---

[3] The PhD candidate has partially contributed in this work, since the simulations have been conducted with the master's student Martin Lillebo. For more details, please see the co-authorship forms attached as a part of the submission package.

the feeders to which they are connected.

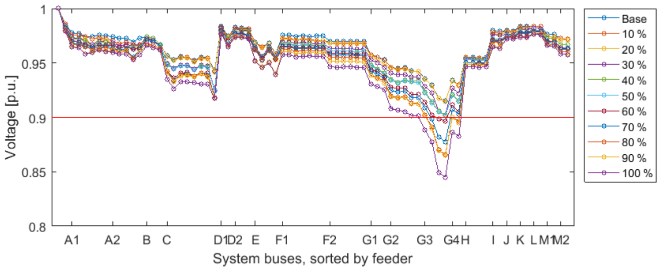

Figure 2.8: Lowest voltage magnitudes reached for all buses in the system, for all 10 EV penetration cases, sorted by which feeder to which they are connected.

2.8.2 Optimal Placement of Fast Charger and Reactive Power Provision

Once all necessary data on how a base EV penetration and a fast charger placement at the potential locations would affect the voltage stability and power flows throughout the system were found, we weighed the voltage deviation levels and total active power loss of the system using a weighed-loss-voltage-factor (WLFV) as shown in Eq.(2.17) . By doing this so, a location for the fast charger that minimises the overall voltage drops and system power losses can be chosen.

$$WLVF = w_1 \times V_{dev} + w_2 \times P_{loss} \tag{2.17a}$$

$$w_1 + w_2 = 1 \tag{2.17b}$$

where P_{loss_i} is the percentage-wise increase in total system power losses when the FC is placed at location i, compared to the base case, V_{dev_i} is the average voltage deviation observed at all 20 feeder connections when an FC is placed at location i, in comparison with the base case. w_1 weighing factor determines the importance of voltage deviation, and w_2 weighing factor determines the importance of the system power loss.

By calculating the WLVF-factor for all 20 investigated fast-charger locations, ‘G4’ returned the worst results. Figure 2.9 displays the voltage deviations in the system for three cases: The 30% EV-penetration case as the base case, a fast charger located at ‘G4’ with a power factor of 0.98 lagging, and the same case but with the charger having a power factor of 0.74 leading, thus effectively injecting reactive power. In the base case and the case with PF=0.74, the voltage levels in the system remained within bounds, while it was 0.03 p.u. below the base case when the power factor was 0.98. The main findings of this paper can be summarised as:

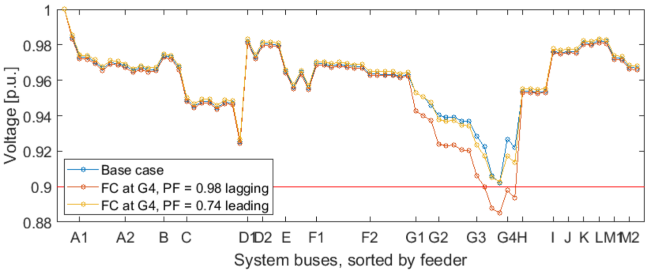

Figure 2.9: Locating the fast charger at G4 gave the most voltage deviations in the network.

I. This paper explored the effects of increasing EV penetration levels in a Norwegian distribution grid, relying on real power measurements obtained from household AMSs and realistic load flow analyses with increasing EV penetration levels.

II. The impact of a new fast charger in the grid has been assessed, and the optimal location for it has been proposed, minimising losses and voltage deviations.

III. By utilizing the voltage-stabilising properties of injecting reactive power, larger loads such as a fast charger or a large EV household charger might be installed in weaker parts of a power grid than would otherwise be possible.

2.9 Value Comparison of EV and House Batteries at End-user Level under Different Grid Tariffs[4]

Battery Energy Storage Systems (BESS) now play an important role for the transition towards the sustainable implementation and utilisation of renewable energy sources given that they reduce costs, and provide electricity power self-balance for the end-users in the distribution network. In this respect, EV and home batteries are compared to investigate the economic potential of utilising PV and batteries at an end-user level. A dynamic programming algorithm is used to minimise the electricity costs under four different grid tariff structures. The results show that, by utilising an EV battery together with rooftop PV, the cost is reduced by 12.0 - 19.2%, depending on the grid tariff structure, whereas a home battery installation together with PV reduces the cost by 8.9 - 14.4%.

---

[4] The PhD candidate has partially contributed in this work, since the simulations have been conducted with the master's student Sigurd Bjarghov. For more details, please see the co-authorship forms attached as a part of the submission package.

The results shown in Table 2.7 and figure 2.10 are the total annual customer costs. These include grid tariffs, taxes, fees and energy prices. In other words, the actual costs that the customer has to pay. Figure 2.10 shows the relative cost of each scenario, again compared to the base case. Note that all scenarios with an EV battery, the cost of energy spent driving the EV was subtracted from the original sum, to avoid the results including the cost of daily transport. The values used were the average driving distance of a Norwegian car, which is approximately 35 km/day. With an average efficiency of 0.2 kWh/km, this accumulates to 7.0 kWh/day.

Even though there are some variations in the annual cost, the overall clear tendency is that the EV and PV battery solution is the most cost-effective solution, with savings ranging from 4000 to 7000 NOK (12.0 - 19.2%) per year depending on tariff structure. The house battery and PV installations saved 8.9 - 14.4%, when PV is included. The same tendency is observed when PV is not included - the EV battery is capable of saving a considerable amount, whereas the house battery is only able to save a few percent.

Table 2.7: Total costs for customer for different scenarios and tariff structures. All numbers are given in NOK.

Structure	**Base case**	**Base case incl. PV**	**House battery**	**EV battery**	**House battery incl. PV**	**EV battery incl. PV**
Photo-voltaic	-	X	-	-	X	X
EV Battery	-	-	-	X	-	X
House Battery	-	-	X	-	X	-
Energy Based	35 775	31 813	35 624	33 915	31 735	30 352
Power Based	35 498	31 574	34 724	33 333	30 790	29 704
Time- of-use	35 427	31 285	34 599	32 487	30 531	28 632
Subscr. based	35 442	32 531	35 126	33 629	32 229	31 191

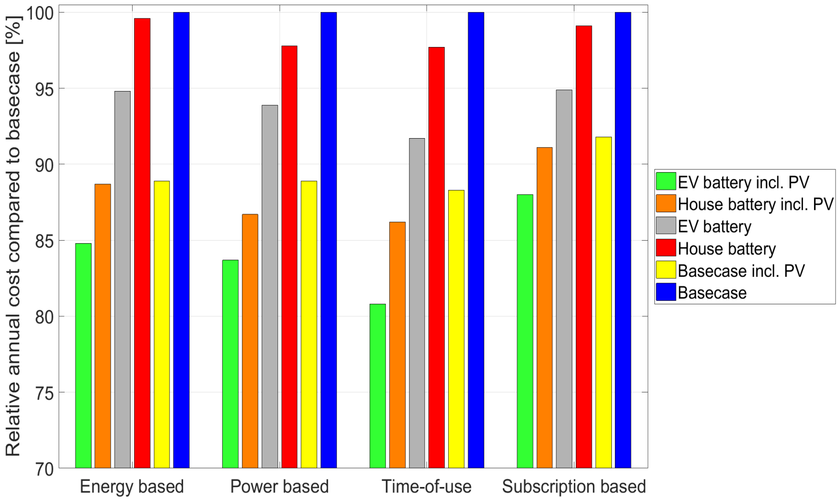

Figure 2.10: Relative annual cost for different scenarios, all compared to the base case cost.

Chapter 3

Response to Research Questions and Tasks

3.1 Answer to Research Questions

The thesis is concluded by the following brief answers to the posed research question in the introduction.

RQ 1. With only "passive charging", the deployment of EVs will be limited by grid constraints. Can "smart-charging" overcome this problem?
The answer is Yes. In paper III, chapter III we indicated that, with the centralised charging scheduling strategy, it is possible to accommodate and schedule 100% of the EVs. It should be kept in mind that the daily energy demand in this paper is estimated based on average drive distance. Thus, the EVs are not using all their stored energy capacities during one simulation cycle (24 hours).
However, the results in paper V, chapter V, show that the distribution grid might not be capable of providing sufficient energy for, cases of: 1) 100% EV-0% PV, and 2) 100% EV-30% PV penetration, due to the assumption that EVs need 20kWh charging energy every day, see the Table 2.5, where there are two infeasible cases. However, the same table indicates that the problem can be lifted in the case of penetration of EV-PV of either 1) 100 EV-70 PV or 2) 100 EV-100 PV.

RQ 2. How many additional EVs can be served by fast-charging points with a "smart-charging" regime compared to "passive charging"?

C 1. Without any reinforcements of the grid.

C 2. Without any reduction in driving range.

I. **Passive Charging:**

P 1. **Line/Transformer Capacity:** The results in paper III, chapter III, (see Table I), w.r.t C 1. and C 2., specify that with the growing penetration of EVs, the Norwegian distribution grid can only handle 20% with respect to line/transformer capacity violation. The results in paper VIII, chapter VIII, w.r.t C 1. and C 2., confirm the same number with real power measurements data of the distribution grid.

P 2. **Voltage violation:** The results in paper III, chapter III, (see Table I), w.r.t C 1. and C 2., indicate that with the growing penetration of EVs, the distribution grid can only handle a margin below 50%-70% with respect to voltage violation. The results in paper VIII, chapter VIII, w.r.t C 1. and C 2., suggest that the voltage violation can be reached at 50% EV penetration.

These points are a result of a combination of all charging stations, from slow to fast in the LV side (2.3 kW until 11 kW).

II. **Smart-Charging:** The results of papers III, V and VI indicate that smart-charging (centralised charging scheduling with respect to the grid operational constraints) can handle 100% EV charging in the LV distribution grid.

RQ 3. How much grid reinforcement is required with smart vs passive-charging to fulfill increasing targets for an EV fleet (as a replacement for gas and diesel cars)?

(a) With the proposed smart-charging strategy, there is no need to reinforce the grid, see paper III, V, and VI, chapter III, V, and VI respectively; however, the control and ICT infrastructure must be installed to apply the idea of centralised charging scheduling (MPOPF considering operational grid constraints).

(b) With an uncoordinated charge strategy, the grid's lines and transformers must be replaced with ones that have a higher capacity.

RQ 4. Could integration of PV mitigate the impact of increasing EV penetration on the distribution grid?
Yes, according to the results obtained in paper V, chapter V, it can be concluded that:

(a) The PV integration could potentially be a production source to be used to charge EVs. Table 2.5, chapter 2 shows different penetration of EV-PV and the subsequent simulation results. The results for two cases of EV-PV penetration of 100%-0% and 100%-30% show “infeasible” outcomes, which means that there is insufficient energy to satisfy 100% EV demand with respect to the operational grid constraints. However, it is possible to operate the system when there is enough PV production as can be seen with two cases of 100%-70% and 100%-100%.

(b) Table 2.5 in chapter 2 indicates that, with growing PV penetration, the system cost declines.

(c) Increasing penetration of PV could help to cancel out the low voltage problem made by the growing integration of EV in the distribution network.

3.2 Description of Tasks

Task 1. Develop a smart-charging algorithm/scheme with the objective to compare and analyse how many additional EVs can be served by a smart-charging method.
A high-performance memory-efficient multi-period AC optimal power flow solver is developed in paper I, chapter I, and further tested and examined in paper II, chapter II. A centralised charging strategy with consideration of operational grid constraint is proposed in paper III, chapter III using the previously developed solver. Thus, the question of “how many additional EVs can be served by a smart-charging method” is answered in RQ 2..

Task 2. Develop a simulator for the combined power-and-transport system that can measure the consequences of conditions C 1. and C 2. in RQ 2. on smart and passive-charging for a realistic case study.
Some efforts have been made in paper III, chapter III, and especially in paper VII, chapter VII, to fulfill Task 2..

I. An agent-based modelling simulation is conducted in paper VII, chapter VII of this thesis, to simulate the transport system, and to investigate the consumption side of the power system with respect to different incentives: 1) No incentive, when they arrive, they connect to charge, 2) Probabilistic charging based on state of charge, and 3) Probabilistic charging based on SOC and price of electricity. However, the power system side is not considered in this paper.

II. Paper III, chapter III, investigates the power system and considers smart-charging and passive-charging. Although the transport simulation is not performed, the estimation of demand is carried out according to the reports [116–119], in order to capture realistic input data, such as average driving distance and energy consumption per day.

Task 3. Simulate the combined system with an increasing number of charging points (and cars), and measure "saturation point" with respect to the requirements in RQ 2..
The saturation point is measured in papers III, V, and VIII, chapters III, V and VIII respectively. All the research conducted in this thesis confirmed the occurrence of overloading of lines/transformers when EV penetration is above 20% in the case of the uncoordinated charging method.

Task 4. Develop a power flow solver that takes into account grid constraints, losses and local generation.
A high-performance and memory-efficient multi-period AC optimal power flow solver is developed in this thesis, presented in papers I and II, chapters I and II respectively. The contributions of the proposed solver are:

I. Incorporating the analytical first and second partial derivatives of constraints and objective functions with respect to all optimisation variables.

II. Exploring the sparsity structures of partial derivatives.

III. Reordering the Jacobian matrix of the KKT structure.

IV. Designing a sparse Schur-Complement algorithm for the multi-period structure of the KKT matrix.

Task 5. Investigate the impact of growing penetration of EVs and PVs together in the distribution grid.
Paper V, chapter V, investigates the impact of increasing levels of EVs and PVs together in the distribution grid. Key points of the study are:

I. In the case of overlapping the PV production and EV charge, they could potentially cancel each other out and end up with a smooth voltage profile, as suggested by the research in the paper V, chapter V.

II. The growing penetration of PV contributes to the lower system cost. System loss declines if the demand from feeders decreases, which occurs with the higher local generation from PVs.

Fig. 3.1 provides an overview of the topic discussed in this chapter, where research questions are located in the left column and tasks are placed in the right column.

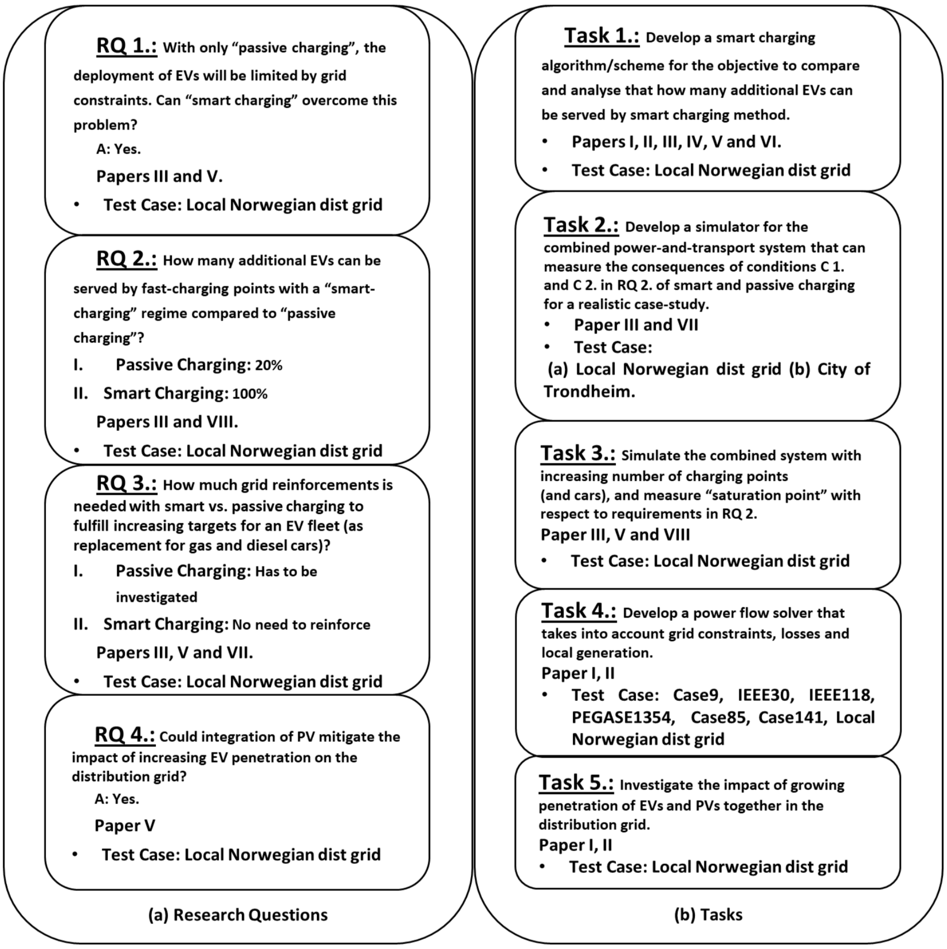

RQ 1.: With only "passive charging", the deployment of EVs will be limited by grid constraints. Can "smart charging" overcome this problem?

A: Yes.

Papers III and V.

- Test Case: Local Norwegian dist grid

RQ 2.: How many additional EVs can be served by fast-charging points with a "smart-charging" regime compared to "passive charging"?

I. Passive Charging: 20%

II. Smart Charging: 100%

Papers III and VIII.

- Test Case: Local Norwegian dist grid

RQ 3.: How much grid reinforcements is needed with smart vs. passive charging to fulfill increasing targets for an EV fleet (as replacement for gas and diesel cars)?

I. Passive Charging: Has to be investigated

II. Smart Charging: No need to reinforce

Papers III, V and VII.

- Test Case: Local Norwegian dist grid

RQ 4.: Could integration of PV mitigate the impact of increasing EV penetration on the distribution grid?

A: Yes.

Paper V

- Test Case: Local Norwegian dist grid

(a) Research Questions

Task 1.: Develop a smart charging algorithm/scheme for the objective to compare and analyse that how many additional EVs can be served by smart charging method.

- Papers I, II, III, IV, V and VI.
- Test Case: Local Norwegian dist grid

Task 2.: Develop a simulator for the combined power-and-transport system that can measure the consequences of conditions C 1. and C 2. in RQ 2. of smart and passive charging for a realistic case-study.

- Paper III and VII
- Test Case:

(a) Local Norwegian dist grid (b) City of Trondheim.

Task 3.: Simulate the combined system with increasing number of charging points (and cars), and measure "saturation point" with respect to requirements in RQ 2.

Paper III, V and VIII

- Test Case: Local Norwegian dist grid

Task 4.: Develop a power flow solver that takes into account grid constraints, losses and local generation.

Paper I, II

- Test Case: Case9, IEEE30, IEEE118, PEGASE1354, Case85, Case141, Local Norwegian dist grid

Task 5.: Investigate the impact of growing penetration of EVs and PVs together in the distribution grid.

Paper I, II

- Test Case: Local Norwegian dist grid

(b) Tasks

Figure 3.1: Overview of: (a) research questions, and (b) tasks

3.3 Relationships Between Papers

The relationships between papers in this thesis, and their associations to tasks and research questions explored in Fig. 3.2.

Relation 1. The papers located on the left side of the figure show the main contribution of the PhD thesis. The top left, paper III, includes the application of

"BATTPOWER" in large-scale integration of EVs into an active distribution grid. The idea of paper III was conceived from papers I and II. In turn, the idea for papers I and II originated from papers IV, V and VI.

Relation 2. Although the concept of paper VIII is similar to papers V and VI, it incorporates both the real grid data and the real AMS measurements. The output of paper VIII partially confirms the outcome of paper III.

Relation 3. Paper VII has some similarity to paper III. The input data of paper III are derived from standard published reports and surveys investigating the average and standard deviation of driving distance. The paper VII simulates the city of Trondheim and a number EV agents in order to obtain the driving distance of agents, and consequently their charging demand. Otherwise paper VII does not incorporate the grid side of the simulation.

Relation 4. Finally, paper IX has a link to the others, since it deals with EV flexibility, but differs in the methods (Dynamic programming) and scope (home EV instead of a fleet of EVs).

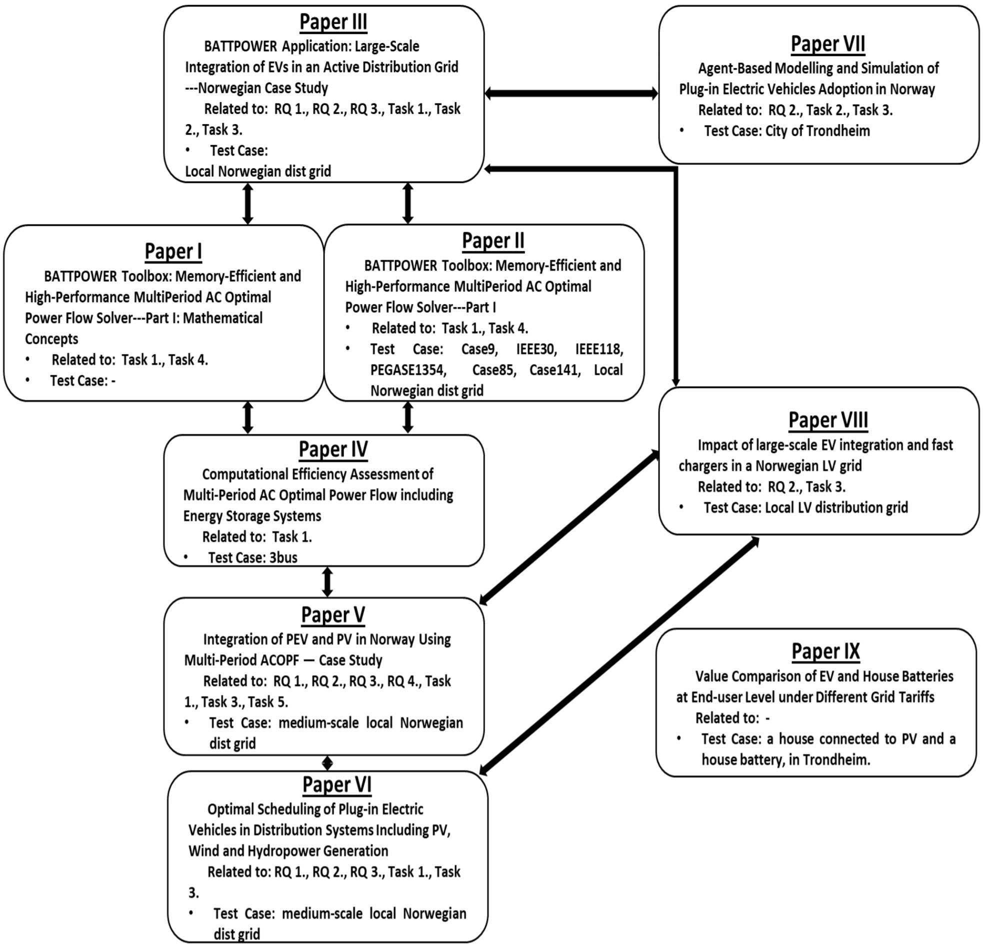
Paper III
BATTPOWER Application: Large-Scale Integration of EVs in an Active Distribution Grid ---Norwegian Case Study
Related to: RQ 1., RQ 2., RQ 3., Task 1., Task 2., Task 3.
• Test Case:
Local Norwegian dist grid
Paper VII
Agent-Based Modelling and Simulation of Plug-in Electric Vehicles Adoption in Norway
Related to: RQ 2., Task 2., Task 3.
• Test Case: City of Trondheim
Paper I
BATTPOWER Toolbox: Memory-Efficient and High-Performance MultiPeriod AC Optimal Power Flow Solver---Part I: Mathematical Concepts
• Related to: Task 1., Task 4.
• Test Case: -
Paper II
BATTPOWER Toolbox: Memory-Efficient and High-Performance MultiPeriod AC Optimal Power Flow Solver---Part I
• Related to: Task 1., Task 4.
• Test Case: Case9, IEEE30, IEEE118, PEGASE1354, Case85, Case141, Local Norwegian dist grid
Paper VIII
Impact of large-scale EV integration and fast chargers in a Norwegian LV grid
Related to: RQ 2., Task 3.
• Test Case: Local LV distribution grid
Paper IV
Computational Efficiency Assessment of Multi-Period AC Optimal Power Flow including Energy Storage Systems
Related to: Task 1.
• Test Case: 3bus
Paper V
Integration of PEV and PV in Norway Using Multi-Period ACOPF — Case Study
Related to: RQ 1., RQ 2., RQ 3., RQ 4., Task 1., Task 3., Task 5.
• Test Case: medium-scale local Norwegian dist grid
Paper IX
Value Comparison of EV and House Batteries at End-user Level under Different Grid Tariffs
Related to: -
• Test Case: a house connected to PV and a house battery, in Trondheim.
Paper VI
Optimal Scheduling of Plug-in Electric Vehicles in Distribution Systems Including PV, Wind and Hydropower Generation
Related to: RQ 1., RQ 2., RQ 3., Task 1., Task 3.
• Test Case: medium-scale local Norwegian dist grid

Figure 3.2: The relationships between the papers in this thesis.

Chapter 4

Conclusion

This thesis primarily evaluates the integration and scheduling of large-scale EVs with the distribution network while aiming to consider reliability, cost-effectiveness, tractability, and scalability of the operational strategy to deliver power for end-users.

In this respect, a high-performance memory-efficient multi-period AC optimal power flow solver incorporating Stationary Energy Storage System (SESS) and Electric Vehicle (EV) as intertemporal constraints, was developed and examined. Papers I and II in chapters I and II of this thesis details the solver. In order to speed-up the solution, the analytical derivatives of the cost-associated objective function and operational grid constraints were explored, and their sparse structures were exploited. Moreover, a new reordering permutation matrix is proposed and a Schur-Complement algorithm is developed. Finally, the proposed method is tested and examined with several benchmarks.

In paper III, chapter III, the BATTPOWER solver is applied on a real local and large-scale case with 974 buses, 1023 lines and 2 generators. Input data, regarding the power demand, EV arrival and departure, EV demand and initial state of charge of EVs were estimated using data from local DSO and previously published reports. It is found that with an uncoordinated charging method, the distribution grid can accommodate only 20% EV penetration. However, using the proposed method, centralised charging scheduling with consideration of grid operational constraints, the distribution grid can handle 100% EV penetration.

In paper IV, chapter IV, analytical derivatives were investigated. The proposed method is tested on a 3 bus case study, and the computational performance is compared with that of commercial solvers. The result indicates that the proposed method provides an almost 10 times faster solution. This was the first step in developing the BATTPOWER solver.

A MPOPF mathematical formulation was developed in papers V and VI, chapters V and VI respectively, and solved using the FMINCON solver of MATLAB. It was tested on a real local medium sized distribution grid with a large integration of EV and PV. The simulation results indicated that with the smart-charging strategy, a 100% integration of EVs is feasible to be performed. However, the solution time of the proposed method was noticeably slow.

An agent-base modelling (ABM) of EVs was developed and tested on the city of Trondheim, to investigate the demand side of the power system, and specifically on the consequences of the deployment of a large fleet of EVs. Different charging strategies were defined and implemented as the utility function of the agents: 1) dumb charging, when the EV arrives, it charges to reach 100% state of charge, 2) probabilistic charging strategy based on the state of charge, and 3) probabilistic charge strategy based on price of energy and state of charge. The simulation results reinforce the notion that the rising adoption of EVs might not only pose a considerable challenge due to the relative size of the power demanded, but more critically also because of the variability that the charging profiles exhibit. In addition, ABM simulations can provide insight for policymakers in order to predict and assess the spatial and temporal future power demand enforced through agents' behaviour.

Real hourly active power measurements in a Norwegian distribution grid feeding 54 consumers were used as input simulation data for power flow analysis in paper VIII, chapter VIII of this thesis. The purpose of this study was to investigate the impact of increasing EV penetration using real input data. EV charging profiles were generated using some active power measurements from some households equipped with smart meters and confirmation that they own an EV. Power flow analysis reveals that the EV hosting capacity of the grid is suitable for a majority of the end-users; however, the weakest power cable in the system will be overloaded at a 20% EV penetration level. The network tolerated an EV penetration of 50% with regard to the voltage levels at all end-users.

EV batteries and home batteries were used in optimisation simulations integrated with PV solar panels in order to investigate the economic potential of utilising PV and batteries at an end-user level. The simulation results show reduced annual electricity costs for both utilisation of EV battery and home battery. Through utilising an EV battery together with PV the cost is thus reduced by 12.0-19.2%, depending on the grid tariff structure, whereas a home battery installation together with PV reduces the cost by 8.9-14.4%.

4.1 Recommendations for Future Research

Possible future research directions could be summarised into the following approaches/categories:

I. **Planning problem:** In paper VIII of this thesis, a method is proposed to find the optimal location of a fast charger on the LV side of the distribution grid. A future project could be to set up an optimisation problem to locate the fast charger(s) with an objective function to minimise the system loss and minimise voltage fluctuations.

II. **Include future value of energy stored at the departure time into an objective function as a soft constraint:** A possible approach for future research could be to consider the future value of energy stored at the departure time as a soft constraint. With this method, it is possible to allocate a price for energy stored at the departure time.

III. **Mathematical programming:** A research direction might be to extend the mathematical background of the currently implemented "BATTPOWER"; specially, it could involve developing libraries of sparse operations for power flow matrices, and their subsequent derivatives. Another mathematical approach could be to search for the global optimum while the local generation is available.

IV. **Including shiftable loads:** In addition to the current research, one might include other technologies in the model such as other shiftable loads (e.g. electric heating) and other storage technologies (e.g. hydrogen).

Bibliography

[1] IEA, *Global ev outlook 2019*, 2019. [Online]. Available: https://www.iea.org/reports/global-ev-outlook-2019 (visited on 02/27/2020).

[2] Elbilforeningen, *Elbilstatistikk*, 2020. [Online]. Available: https://elbil.no/elbilstatistikk/ (visited on 02/27/2020).

[3] NVE, Pöyry, and DNV-GL, *Kostnader i strømnettet - gevinster ved koordinert lading av elbiler*, 2019. [Online]. Available: http://publikasjoner.nve.no/eksternrapport/2019/eksternrapport2019_51.pdf (visited on 02/27/2020).

[4] P. Maille and B. Tuffin, "Pricing the Internet With Multibid Auctions," *IEEE/ACM Transactions on Networking*, vol. 14, no. 5, pp. 992–1004, Oct. 2006, ISSN: 1558-2566. DOI: 10.1109/TNET.2006.882861.

[5] S. Bhattacharya, K. Kar, J. H. Chow, and A. Gupta, "Extended second price auctions for Plug-in Electric Vehicle (PEV) charging in smart distribution grids," in *2014 American Control Conference*, ISSN: 2378-5861, Jun. 2014, pp. 908–913. DOI: 10.1109/ACC.2014.6859300.

[6] A. Aveklouris, Y. Nakahira, M. Vlasiou, and B. Zwart, "Electric vehicle charging: A queueing approach," *ACM SIGMETRICS Performance Evaluation Review*, vol. 45, no. 2, pp. 33–35, Oct. 2017, ISSN: 0163-5999. DOI: 10.1145/3152042.3152054. [Online]. Available: https://doi.org/10.1145/3152042.3152054 (visited on 05/18/2020).

[7] *Nasjonal varedeklarasjon 2018 - NVE*. [Online]. Available: https://www.nve.no/energiforsyning/varedeklarasjon/nasjonal-varedeklarasjon-2018/ (visited on 05/24/2020).

[8] *Nord Pool*. [Online]. Available: https://www.nordpoolgroup.com/ (visited on 02/04/2020).

[9] O. Flataker and H. H. Nielsen, *rapport2018_74.pdf*. Norges vassdrags- og energidirektorat, ISBN: 978-82-410-1732-2. [Online]. Available: http://publikasjoner.nve.no/rapport/2018/rapport2018_74.pdf (visited on 05/24/2020).

[10] G. H. KjØlle, K. Samdal, B. Singh, and O. A. Kvitastein, "Customer Costs Related to Interruptions and Voltage Problems: Methodology and Results," *IEEE Transactions on Power Systems*, vol. 23, no. 3, pp. 1030–1038, Aug. 2008, ISSN: 1558-0679. DOI: 10.1109/TPWRS.2008.922227.

[11] K. Samdal, G. H. Kjolle, B. Singh, and O. Kvitastein, "Interruption Costs and Consumer Valuation of Reliability of Service in a Liberalised Power Market," in *2006 International Conference on Probabilistic Methods Applied to Power Systems*, ISSN: null, Jun. 2006, pp. 1–7. DOI: 10.1109/PMAPS.2006.360322.

[12] J. A. P. Lopes, F. J. Soares, and P. M. R. Almeida, "Identifying management procedures to deal with connection of Electric Vehicles in the grid," in *2009 IEEE Bucharest PowerTech*, ISSN: null, Jun. 2009, pp. 1–8. DOI: 10.1109/PTC.2009.5282155.

[13] K. Clement-Nyns, E. Haesen, and J. Driesen, "The Impact of Charging Plug-In Hybrid Electric Vehicles on a Residential Distribution Grid," *IEEE Transactions on Power Systems*, vol. 25, no. 1, pp. 371–380, Feb. 2010, ISSN: 1558-0679. DOI: 10.1109/TPWRS.2009.2036481.

[14] S. Deilami, A. S. Masoum, P. S. Moses, and M. A. S. Masoum, "Real-Time Coordination of Plug-In Electric Vehicle Charging in Smart Grids to Minimize Power Losses and Improve Voltage Profile," *IEEE Transactions on Smart Grid*, vol. 2, no. 3, pp. 456–467, Sep. 2011, ISSN: 1949-3061. DOI: 10.1109/TSG.2011.2159816.

[15] S. Sojoudi and S. H. Low, "Optimal charging of plug-in hybrid electric vehicles in smart grids," in *2011 IEEE Power and Energy Society General Meeting*, ISSN: 1944-9925, Jul. 2011, pp. 1–6. DOI: 10.1109/PES.2011.6039236.

[16] A. Masoum, S. Deilami, P. Moses, M. Masoum, and A. Abu-Siada, "Smart load management of plug-in electric vehicles in distribution and residential networks with charging stations for peak shaving and loss minimisation considering voltage regulation," *Transmission Distribution IET Generation*, vol. 5, no. 8, pp. 877–888, Aug. 2011, ISSN: 1751-8695. DOI: 10.1049/iet-gtd.2010.0574.

[17] L. Pieltain Fernández, T. Gomez San Roman, R. Cossent, C. Mateo Domingo, and P. Frías, “Assessment of the Impact of Plug-in Electric Vehicles on Distribution Networks,” *IEEE Transactions on Power Systems*, vol. 26, no. 1, pp. 206–213, Feb. 2011, ISSN: 1558-0679. DOI: 10.1109/TPWRS.2010.2049133.

[18] P. Richardson, D. Flynn, and A. Keane, “Local Versus Centralized Charging Strategies for Electric Vehicles in Low Voltage Distribution Systems,” *IEEE Transactions on Smart Grid*, vol. 3, no. 2, pp. 1020–1028, Jun. 2012, ISSN: 1949-3061. DOI: 10.1109/TSG.2012.2185523.

[19] ——, “Optimal Charging of Electric Vehicles in Low-Voltage Distribution Systems,” *IEEE Transactions on Power Systems*, vol. 27, no. 1, pp. 268–279, Feb. 2012, ISSN: 1558-0679. DOI: 10.1109/TPWRS.2011.2158247.

[20] N. Chen, T. Q. Quek, and C. W. Tan, “Optimal charging of electric vehicles in smart grid: Characterization and valley-filling algorithms,” in *2012 IEEE Third International Conference on Smart Grid Communications (SmartGridComm)*, ISSN: null, Nov. 2012, pp. 13–18. DOI: 10.1109/SmartGridComm.2012.6485952.

[21] W. Yao, J. Zhao, F. Wen, Y. Xue, and G. Ledwich, “A Hierarchical Decomposition Approach for Coordinated Dispatch of Plug-in Electric Vehicles,” *IEEE Transactions on Power Systems*, vol. 28, no. 3, pp. 2768–2778, Aug. 2013, ISSN: 1558-0679. DOI: 10.1109/TPWRS.2013.2256937.

[22] R. Li, Q. Wu, and S. S. Oren, “Distribution Locational Marginal Pricing for Optimal Electric Vehicle Charging Management,” *IEEE Transactions on Power Systems*, vol. 29, no. 1, pp. 203–211, Jan. 2014, ISSN: 1558-0679. DOI: 10.1109/TPWRS.2013.2278952.

[23] R.-C. Leou, C.-L. Su, and C.-N. Lu, “Stochastic Analyses of Electric Vehicle Charging Impacts on Distribution Network,” *IEEE Transactions on Power Systems*, vol. 29, no. 3, pp. 1055–1063, May 2014, ISSN: 1558-0679. DOI: 10.1109/TPWRS.2013.2291556.

[24] K. Zhou and L. Cai, “Randomized PHEV Charging Under Distribution Grid Constraints,” *IEEE Transactions on Smart Grid*, vol. 5, no. 2, pp. 879–887, Mar. 2014, ISSN: 1949-3061. DOI: 10.1109/TSG.2013.2293733.

[25] A. O’Connell, D. Flynn, and A. Keane, “Rolling Multi-Period Optimization to Control Electric Vehicle Charging in Distribution Networks,” *IEEE Transactions on Power Systems*, vol. 29, no. 1, pp. 340–348, Jan. 2014, ISSN: 1558-0679. DOI: 10.1109/TPWRS.2013.2279276.

[26] M. F. Shaaban and E. F. El-Saadany, "Accommodating High Penetrations of PEVs and Renewable DG Considering Uncertainties in Distribution Systems," *IEEE Transactions on Power Systems*, vol. 29, no. 1, pp. 259–270, Jan. 2014, ISSN: 1558-0679. DOI: 10.1109/TPWRS.2013.2278847.

[27] J. F. Franco, M. J. Rider, and R. Romero, "A Mixed-Integer Linear Programming Model for the Electric Vehicle Charging Coordination Problem in Unbalanced Electrical Distribution Systems," *IEEE Transactions on Smart Grid*, vol. 6, no. 5, pp. 2200–2210, Sep. 2015, ISSN: 1949-3061. DOI: 10.1109/TSG.2015.2394489.

[28] G. Benetti, M. Delfanti, T. Facchinetti, D. Falabretti, and M. Merlo, "Real-Time Modeling and Control of Electric Vehicles Charging Processes," *IEEE Transactions on Smart Grid*, vol. 6, no. 3, pp. 1375–1385, May 2015, ISSN: 1949-3061. DOI: 10.1109/TSG.2014.2376573.

[29] J. de Hoog, T. Alpcan, M. Brazil, D. A. Thomas, and I. Mareels, "Optimal Charging of Electric Vehicles Taking Distribution Network Constraints Into Account," *IEEE Transactions on Power Systems*, vol. 30, no. 1, pp. 365–375, Jan. 2015, ISSN: 1558-0679. DOI: 10.1109/TPWRS.2014.2318293.

[30] D. Wang, X. Guan, J. Wu, P. Li, P. Zan, and H. Xu, "Integrated Energy Exchange Scheduling for Multimicrogrid System With Electric Vehicles," *IEEE Transactions on Smart Grid*, vol. 7, no. 4, pp. 1762–1774, Jul. 2016, ISSN: 1949-3061. DOI: 10.1109/TSG.2015.2438852.

[31] J. Quirós-Tortós, L. F. Ochoa, S. W. Alnaser, and T. Butler, "Control of EV Charging Points for Thermal and Voltage Management of LV Networks," *IEEE Transactions on Power Systems*, vol. 31, no. 4, pp. 3028–3039, Jul. 2016, ISSN: 1558-0679. DOI: 10.1109/TPWRS.2015.2468062.

[32] M. Rahmani-andebili, "Optimal power factor for optimally located and sized solar parking lots applying quantum annealing," *Transmission Distribution IET Generation*, vol. 10, no. 10, pp. 2538–2547, 2016, ISSN: 1751-8695. DOI: 10.1049/iet-gtd.2015.1553.

[33] X. Su, M. A. S. Masoum, and P. J. Wolfs, "Multi-Objective Hierarchical Control of Unbalanced Distribution Networks to Accommodate More Renewable Connections in the Smart Grid Era," *IEEE Transactions on Power Systems*, vol. 31, no. 5, pp. 3924–3936, Sep. 2016, ISSN: 1558-0679. DOI: 10.1109/TPWRS.2015.2501845.

[34] C. Luo, Y.-F. Huang, and V. Gupta, “Placement of EV Charging Stations—Balancing Benefits Among Multiple Entities,” *IEEE Transactions on Smart Grid*, vol. 8, no. 2, pp. 759–768, Mar. 2017, ISSN: 1949-3061. DOI: 10.1109/TSG.2015.2508740.

[35] C. Shao, X. Wang, M. Shahidehpour, X. Wang, and B. Wang, “Partial Decomposition for Distributed Electric Vehicle Charging Control Considering Electric Power Grid Congestion,” *IEEE Transactions on Smart Grid*, vol. 8, no. 1, pp. 75–83, Jan. 2017, ISSN: 1949-3061. DOI: 10.1109/TSG.2016.2595494.

[36] L. Zhang, V. Kekatos, and G. B. Giannakis, “Scalable Electric Vehicle Charging Protocols,” *IEEE Transactions on Power Systems*, vol. 32, no. 2, pp. 1451–1462, Mar. 2017, ISSN: 1558-0679. DOI: 10.1109/TPWRS.2016.2582903.

[37] R. Mehta, D. Srinivasan, A. M. Khambadkone, J. Yang, and A. Trivedi, “Smart Charging Strategies for Optimal Integration of Plug-In Electric Vehicles Within Existing Distribution System Infrastructure,” *IEEE Transactions on Smart Grid*, vol. 9, no. 1, pp. 299–312, Jan. 2018, ISSN: 1949-3061. DOI: 10.1109/TSG.2016.2550559.

[38] O. Hafez and K. Bhattacharya, “Queuing Analysis Based PEV Load Modeling Considering Battery Charging Behavior and Their Impact on Distribution System Operation,” *IEEE Transactions on Smart Grid*, vol. 9, no. 1, pp. 261–273, Jan. 2018, ISSN: 1949-3061. DOI: 10.1109/TSG.2016.2550219.

[39] ——, “Integrating EV Charging Stations as Smart Loads for Demand Response Provisions in Distribution Systems,” *IEEE Transactions on Smart Grid*, vol. 9, no. 2, pp. 1096–1106, Mar. 2018, ISSN: 1949-3061. DOI: 10.1109/TSG.2016.2576902.

[40] J. Zhang, M. Cui, B. Li, H. Fang, and Y. He, “Fast Solving Method Based on Linearized Equations of Branch Power Flow for Coordinated Charging of EVs (EVCC),” *IEEE Transactions on Vehicular Technology*, vol. 68, no. 5, pp. 4404–4418, May 2019, ISSN: 1939-9359. DOI: 10.1109/TVT.2019.2904464.

[41] J. Chen, X. Huang, S. Tian, Y. Cao, B. Huang, X. Luo, and W. Yu, “Electric vehicle charging schedule considering user’s charging selection from economics,” *Transmission Distribution IET Generation*, vol. 13, no. 15, pp. 3388–3396, 2019, ISSN: 1751-8695. DOI: 10.1049/iet-gtd.2019.0154.

[42] Y. Shi, H. D. Tuan, A. V. Savkin, T. Q. Duong, and H. V. Poor, "Model Predictive Control for Smart Grids With Multiple Electric-Vehicle Charging Stations," *IEEE Transactions on Smart Grid*, vol. 10, no. 2, pp. 2127–2136, Mar. 2019, ISSN: 1949-3061. DOI: 10.1109/TSG.2017.2789333.

[43] K. Kotsalos, I. Miranda, N. Silva, and H. Leite, "A Horizon Optimization Control Framework for the Coordinated Operation of Multiple Distributed Energy Resources in Low Voltage Distribution Networks," en, *Energies*, vol. 12, no. 6, p. 1182, Jan. 2019. DOI: 10.3390/en12061182. [Online]. Available: https://www.mdpi.com/1996-1073/12/6/1182 (visited on 03/08/2020).

[44] X. Gong, A. De Paola, D. Angeli, and G. Strbac, "Distributed Coordination of Flexible Loads Using Locational Marginal Prices," *IEEE Transactions on Control of Network Systems*, vol. 6, no. 3, pp. 1097–1110, Sep. 2019, ISSN: 2372-2533. DOI: 10.1109/TCNS.2019.2920587.

[45] M. R. Islam, H. Lu, J. Hossain, M. R. Islam, and L. Li, "Multiobjective Optimization Technique for Mitigating Unbalance and Improving Voltage Considering Higher Penetration of Electric Vehicles and Distributed Generation," *IEEE Systems Journal*, pp. 1–11, 2020, ISSN: 2373-7816. DOI: 10.1109/JSYST.2020.2967752.

[46] R. Allan, R. Billinton, I. Sjarief, L. Goel, and K. So, "A reliability test system for educational purposes-basic distribution system data and results," *IEEE Transactions on Power Systems*, vol. 6, no. 2, pp. 813–820, May 1991, ISSN: 1558-0679. DOI: 10.1109/59.76730.

[47] M. Caramanis and J. M. Foster, "Management of electric vehicle charging to mitigate renewable generation intermittency and distribution network congestion," in *Proceedings of the 48h IEEE Conference on Decision and Control (CDC) held jointly with 2009 28th Chinese Control Conference*, ISSN: 0191-2216, Dec. 2009, pp. 4717–4722. DOI: 10.1109/CDC.2009.5399955.

[48] E. Sortomme and M. A. El-Sharkawi, "Optimal Charging Strategies for Unidirectional Vehicle-to-Grid," *IEEE Transactions on Smart Grid*, vol. 2, no. 1, pp. 131–138, Mar. 2011, ISSN: 1949-3061. DOI: 10.1109/TSG.2010.2090910.

[49] E. Sortomme, M. M. Hindi, S. D. J. MacPherson, and S. S. Venkata, "Coordinated Charging of Plug-In Hybrid Electric Vehicles to Minimize Distribution System Losses," *IEEE Transactions on Smart Grid*, vol. 2, no. 1, pp. 198–205, Mar. 2011, ISSN: 1949-3061. DOI: 10.1109/TSG.2010.2090913.

[50] Q. Gong, S. Midlam-Mohler, V. Marano, and G. Rizzoni, "Study of PEV Charging on Residential Distribution Transformer Life," *IEEE Transactions on Smart Grid*, vol. 3, no. 1, pp. 404–412, Mar. 2012, ISSN: 1949-3061. DOI: 10.1109/TSG.2011.2163650.

[51] P. Zhang, K. Qian, C. Zhou, B. G. Stewart, and D. M. Hepburn, "A Methodology for Optimization of Power Systems Demand Due to Electric Vehicle Charging Load," *IEEE Transactions on Power Systems*, vol. 27, no. 3, pp. 1628–1636, Aug. 2012, ISSN: 1558-0679. DOI: 10.1109/TPWRS.2012.2186595.

[52] B. Geng, J. K. Mills, and D. Sun, "Two-Stage Charging Strategy for Plug-In Electric Vehicles at the Residential Transformer Level," *IEEE Transactions on Smart Grid*, vol. 4, no. 3, pp. 1442–1452, Sep. 2013, ISSN: 1949-3061. DOI: 10.1109/TSG.2013.2246198.

[53] Y. He, B. Venkatesh, and L. Guan, "Optimal Scheduling for Charging and Discharging of Electric Vehicles," *IEEE Transactions on Smart Grid*, vol. 3, no. 3, pp. 1095–1105, Sep. 2012, ISSN: 1949-3061. DOI: 10.1109/TSG.2011.2173507.

[54] M. A. Ortega-Vazquez, F. Bouffard, and V. Silva, "Electric Vehicle Aggregator/System Operator Coordination for Charging Scheduling and Services Procurement," *IEEE Transactions on Power Systems*, vol. 28, no. 2, pp. 1806–1815, May 2013, ISSN: 1558-0679. DOI: 10.1109/TPWRS.2012.2221750.

[55] L. Gan, U. Topcu, and S. H. Low, "Optimal decentralized protocol for electric vehicle charging," *IEEE Transactions on Power Systems*, vol. 28, no. 2, pp. 940–951, May 2013, ISSN: 1558-0679. DOI: 10.1109/TPWRS.2012.2210288.

[56] Z. Luo, Z. Hu, Y. Song, Z. Xu, and H. Lu, "Optimal Coordination of Plug-In Electric Vehicles in Power Grids With Cost-Benefit Analysis—Part I: Enabling Techniques," *IEEE Transactions on Power Systems*, vol. 28, no. 4, pp. 3546–3555, Nov. 2013, ISSN: 1558-0679. DOI: 10.1109/TPWRS.2013.2262318.

[57] ——, "Optimal Coordination of Plug-in Electric Vehicles in Power Grids With Cost-Benefit Analysis—Part II: A Case Study in China," *IEEE Transactions on Power Systems*, vol. 28, no. 4, pp. 3556–3565, Nov. 2013, ISSN: 1558-0679. DOI: 10.1109/TPWRS.2013.2252028.

[58] M. Alizadeh, A. Scaglione, J. Davies, and K. S. Kurani, "A Scalable Stochastic Model for the Electricity Demand of Electric and Plug-In Hybrid Vehicles," *IEEE Transactions on Smart Grid*, vol. 5, no. 2, pp. 848–860, Mar. 2014, ISSN: 1949-3061. DOI: 10.1109/TSG.2013.2275988.

[59] P. Grahn, K. Alvehag, and L. Söder, "PHEV Utilization Model Considering Type-of-Trip and Recharging Flexibility," *IEEE Transactions on Smart Grid*, vol. 5, no. 1, pp. 139–148, Jan. 2014, ISSN: 1949-3061. DOI: 10.1109/TSG.2013.2279022.

[60] P. Rezaei, J. Frolik, and P. D. H. Hines, "Packetized Plug-In Electric Vehicle Charge Management," *IEEE Transactions on Smart Grid*, vol. 5, no. 2, pp. 642–650, Mar. 2014, ISSN: 1949-3061. DOI: 10.1109/TSG.2013.2291384.

[61] K. N. Kumar, B. Sivaneasan, P. H. Cheah, P. L. So, and D. Z. W. Wang, "V2G Capacity Estimation Using Dynamic EV Scheduling," *IEEE Transactions on Smart Grid*, vol. 5, no. 2, pp. 1051–1060, Mar. 2014, ISSN: 1949-3061. DOI: 10.1109/TSG.2013.2279681.

[62] J. Donadee and M. D. Ilić, "Stochastic Optimization of Grid to Vehicle Frequency Regulation Capacity Bids," *IEEE Transactions on Smart Grid*, vol. 5, no. 2, pp. 1061–1069, Mar. 2014, ISSN: 1949-3061. DOI: 10.1109/TSG.2013.2290971.

[63] W. Tang, S. Bi, and Y. J. Zhang, "Online coordinated charging decision algorithm for electric vehicles without future information," *IEEE Transactions on Smart Grid*, vol. 5, no. 6, pp. 2810–2824, Nov. 2014, ISSN: 1949-3061. DOI: 10.1109/TSG.2014.2346925.

[64] M. Majidpour, C. Qiu, P. Chu, R. Gadh, and H. R. Pota, "Fast Prediction for Sparse Time Series: Demand Forecast of EV Charging Stations for Cell Phone Applications," *IEEE Transactions on Industrial Informatics*, vol. 11, no. 1, pp. 242–250, Feb. 2015, ISSN: 1941-0050. DOI: 10.1109/TII.2014.2374993.

[65] C. Shao, X. Wang, X. Wang, and C. Du, "Layered and Distributed Charge Load Dispatch of Considerable Electric Vehicles," *IEEE Transactions on Power Systems*, vol. 30, no. 4, pp. 1858–1867, Jul. 2015, ISSN: 1558-0679. DOI: 10.1109/TPWRS.2014.2359234.

[66] W. Tang, S. Bi, and Y. J. Zhang, "Online Charging Scheduling Algorithms of Electric Vehicles in Smart Grid: An Overview," *IEEE Communications Magazine*, vol. 54, no. 12, pp. 76–83, Dec. 2016, ISSN: 1558-1896. DOI: 10.1109/MCOM.2016.1600346CM.

[67] E. Xydas, C. Marmaras, L. M. Cipcigan, N. Jenkins, S. Carroll, and M. Barker, "A data-driven approach for characterising the charging demand of electric vehicles: A UK case study," en, *Applied Energy*, vol. 162, pp. 763–771, Jan. 2016, ISSN: 0306-2619. DOI: 10.1016/j.apenergy.2015.10.151. [Online]. Available: http://www.sciencedirect.com/science/article/pii/S0306261915013938 (visited on 03/23/2020).

[68] W. Tang and Y. J. Zhang, "A Model Predictive Control Approach for Low-Complexity Electric Vehicle Charging Scheduling: Optimality and Scalability," *IEEE Transactions on Power Systems*, vol. 32, no. 2, pp. 1050–1063, Mar. 2017, ISSN: 1558-0679. DOI: 10.1109/TPWRS.2016.2585202.

[69] V. Monteiro, B. Exposto, J. C. Ferreira, and J. L. Afonso, "Improved Vehicle-to-Home (iV2H) Operation Mode: Experimental Analysis of the Electric Vehicle as Off-Line UPS," *IEEE Transactions on Smart Grid*, vol. 8, no. 6, pp. 2702–2711, Nov. 2017, ISSN: 1949-3061. DOI: 10.1109/TSG.2016.2535337.

[70] L. Zhang and Y. Li, "Optimal Management for Parking-Lot Electric Vehicle Charging by Two-Stage Approximate Dynamic Programming," *IEEE Transactions on Smart Grid*, vol. 8, no. 4, pp. 1722–1730, Jul. 2017, ISSN: 1949-3061. DOI: 10.1109/TSG.2015.2505298.

[71] T. Chen, B. Zhang, H. Pourbabak, A. Kavousi-Fard, and W. Su, "Optimal Routing and Charging of an Electric Vehicle Fleet for High-Efficiency Dynamic Transit Systems," *IEEE Transactions on Smart Grid*, vol. 9, no. 4, pp. 3563–3572, Jul. 2018, ISSN: 1949-3061. DOI: 10.1109/TSG.2016.2635025.

[72] S. Liu and A. H. Etemadi, "A Dynamic Stochastic Optimization for Recharging Plug-In Electric Vehicles," *IEEE Transactions on Smart Grid*, vol. 9, no. 5, pp. 4154–4161, Sep. 2018, ISSN: 1949-3061. DOI: 10.1109/TSG.2017.2652329.

[73] M. Razmara, G. R. Bharati, M. Shahbakhti, S. Paudyal, and R. D. Robinett, "Bilevel Optimization Framework for Smart Building-to-Grid Systems," *IEEE Transactions on Smart Grid*, vol. 9, no. 2, pp. 582–593, Mar. 2018, ISSN: 1949-3061. DOI: 10.1109/TSG.2016.2557334.

[74] C. Le Floch, E. C. Kara, and S. Moura, "PDE Modeling and Control of Electric Vehicle Fleets for Ancillary Services: A Discrete Charging Case," *IEEE Transactions on Smart Grid*, vol. 9, no. 2, pp. 573–581, Mar. 2018, ISSN: 1949-3061. DOI: 10.1109/TSG.2016.2556643.

[75] H.-M. Chung, W.-T. Li, C. Yuen, C.-K. Wen, and N. Crespi, "Electric Vehicle Charge Scheduling Mechanism to Maximize Cost Efficiency and User Convenience," *IEEE Transactions on Smart Grid*, vol. 10, no. 3, pp. 3020–3030, May 2019, ISSN: 1949-3061. DOI: 10.1109/TSG.2018.2817067.

[76] C. Grigg, P. Wong, P. Albrecht, R. Allan, M. Bhavaraju, R. Billinton, Q. Chen, C. Fong, S. Haddad, S. Kuruganty, W. Li, R. Mukerji, D. Patton, N. Rau, D. Reppen, A. Schneider, M. Shahidehpour, and C. Singh, "The IEEE Reliability Test System-1996. A report prepared by the Reliability Test System Task Force of the Application of Probability Methods Subcommittee," *IEEE Transactions on Power Systems*, vol. 14, no. 3, pp. 1010–1020, Aug. 1999, ISSN: 1558-0679. DOI: 10.1109/59.780914.

[77] P. M. Subcommittee, "IEEE Reliability Test System," *IEEE Transactions on Power Apparatus and Systems*, vol. PAS-98, no. 6, pp. 2047–2054, Nov. 1979, ISSN: 0018-9510. DOI: 10.1109/TPAS.1979.319398.

[78] M. D. Galus, R. A. Waraich, F. Noembrini, K. Steurs, G. Georges, K. Boulouchos, K. W. Axhausen, and G. Andersson, "Integrating Power Systems, Transport Systems and Vehicle Technology for Electric Mobility Impact Assessment and Efficient Control," *IEEE Transactions on Smart Grid*, vol. 3, no. 2, pp. 934–949, Jun. 2012, ISSN: 1949-3061. DOI: 10.1109/TSG.2012.2190628.

[79] E. L. Karfopoulos and N. D. Hatziargyriou, "A Multi-Agent System for Controlled Charging of a Large Population of Electric Vehicles," *IEEE Transactions on Power Systems*, vol. 28, no. 2, pp. 1196–1204, May 2013, ISSN: 1558-0679. DOI: 10.1109/TPWRS.2012.2211624.

[80] S. Bhattacharya, K. Kar, J. H. Chow, and A. Gupta, "Extended Second Price Auctions With Elastic Supply for PEV Charging in the Smart Grid," *IEEE Transactions on Smart Grid*, vol. 7, no. 4, pp. 2082–2093, Jul. 2016, ISSN: 1949-3061. DOI: 10.1109/TSG.2016.2546281.

[81] J. Tan and L. Wang, "A Game-Theoretic Framework for Vehicle-to-Grid Frequency Regulation Considering Smart Charging Mechanism," *IEEE Transactions on Smart Grid*, vol. 8, no. 5, pp. 2358–2369, Sep. 2017, ISSN: 1949-3061. DOI: 10.1109/TSG.2016.2524020.

[82] ——, "Real-Time Charging Navigation of Electric Vehicles to Fast Charging Stations: A Hierarchical Game Approach," *IEEE Transactions on Smart Grid*, vol. 8, no. 2, pp. 846–856, Mar. 2017, ISSN: 1949-3061. DOI: 10.1109/TSG.2015.2458863.

[83] N. Sadeghianpourhamami, J. Deleu, and C. Develder, “Definition and Evaluation of Model-Free Coordination of Electrical Vehicle Charging With Reinforcement Learning,” *IEEE Transactions on Smart Grid*, vol. 11, no. 1, pp. 203–214, Jan. 2020, ISSN: 1949-3061. DOI: 10.1109/TSG.2019.2920320.

[84] M. Shin, D.-H. Choi, and J. Kim, “Cooperative Management for PV/ESS-Enabled Electric Vehicle Charging Stations: A Multiagent Deep Reinforcement Learning Approach,” *IEEE Transactions on Industrial Informatics*, vol. 16, no. 5, pp. 3493–3503, May 2020, ISSN: 1941-0050. DOI: 10.1109/TII.2019.2944183.

[85] P. Papadopoulos, N. Jenkins, L. M. Cipcigan, I. Grau, and E. Zabala, “Coordination of the Charging of Electric Vehicles Using a Multi-Agent System,” *IEEE Transactions on Smart Grid*, vol. 4, no. 4, pp. 1802–1809, Dec. 2013, ISSN: 1949-3061. DOI: 10.1109/TSG.2013.2274391.

[86] J. Carpentier, “Contribution a l’etude du dispatching economique,” *Bulletin de la Societe Francaise des Electriciens*, vol. 3, no. 1, pp. 431–447, 1962.

[87] K. M. Chandy, S. H. Low, U. Topcu, and H. Xu, “A simple optimal power flow model with energy storage,” in *49th IEEE Conference on Decision and Control (CDC)*, ISSN: 0743-1546, Dec. 2010, pp. 1051–1057. DOI: 10.1109/CDC.2010.5718193.

[88] I. B. Sperstad and H. Marthinsen, “Optimal power flow methods and their application to distribution systems with energy storage: A survey of available tools and methods,” *report no. TR A7604, SINTEF Energy Research, Trondheim.*, 2016.

[89] F. Capitanescu, “Critical review of recent advances and further developments needed in ac optimal power flow,” *Electric Power Systems Research*, vol. 136, pp. 57–68, 2016, ISSN: 0378-7796. DOI: http://dx.doi.org/10.1016/j.epsr.2016.02.008.

[90] G. Carpinelli, G. Celli, S. Mocci, F. Mottola, F. Pilo, and D. Proto, “Optimal Integration of Distributed Energy Storage Devices in Smart Grids,” *IEEE Transactions on Smart Grid*, vol. 4, no. 2, pp. 985–995, Jun. 2013, ISSN: 1949-3061. DOI: 10.1109/TSG.2012.2231100.

[91] P. Fortenbacher, M. Zellner, and G. Andersson, “Optimal sizing and placement of distributed storage in low voltage networks,” in *2016 Power Systems Computation Conference (PSCC)*, Jun. 2016, pp. 1–7. DOI: 10.1109/PSCC.2016.7540850.

[92] P. Fortenbacher, J. L. Mathieu, and G. Andersson, “Modeling and Optimal Operation of Distributed Battery Storage in Low Voltage Grids,” *IEEE Transactions on Power Systems*, vol. 32, no. 6, pp. 4340–4350, Nov. 2017, ISSN: 1558-0679. DOI: 10.1109/TPWRS.2017.2682339.

[93] F. Geth, S. Leyder, C. Del Marmol, and S. Rapoport, “The PlanGridEV distribution grid simulation tool with EV models,” in *CIRED Workshop 2016*, Jun. 2016, pp. 1–4. DOI: 10.1049/cp.2016.0724.

[94] J. Warrington, P. Goulart, S. Mariéthoz, and M. Morari, “A market mechanism for solving multi-period optimal power flow exactly on AC networks with mixed participants,” in *2012 American Control Conference (ACC)*, ISSN: 0743-1619, Jun. 2012, pp. 3101–3107. DOI: 10.1109/ACC.2012.6315477.

[95] A. Gopalakrishnan, A. U. Raghunathan, D. Nikovski, and L. T. Biegler, “Global optimization of multi-period optimal power flow,” in *2013 American Control Conference*, ISSN: 2378-5861, Jun. 2013, pp. 1157–1164. DOI: 10.1109/ACC.2013.6579992.

[96] S. Moghadasi and S. Kamalasadan, “Real-time optimal scheduling of smart power distribution systems using integrated receding horizon control and convex conic programming,” in *2014 IEEE Industry Application Society Annual Meeting*, ISSN: 0197-2618, Oct. 2014, pp. 1–7. DOI: 10.1109/IAS.2014.6978408.

[97] ——, “Optimal Fast Control and Scheduling of Power Distribution System Using Integrated Receding Horizon Control and Convex Conic Programming,” *IEEE Transactions on Industry Applications*, vol. 52, no. 3, pp. 2596–2606, May 2016, ISSN: 1939-9367. DOI: 10.1109/TIA.2016.2531623.

[98] H. Wang, C. E. Murillo-Sanchez, R. D. Zimmerman, and R. J. Thomas, “On Computational Issues of Market-Based Optimal Power Flow,” *IEEE Transactions on Power Systems*, vol. 22, no. 3, pp. 1185–1193, Aug. 2007, ISSN: 0885-8950. DOI: 10.1109/TPWRS.2007.901301.

[99] A. Wächter and L. T. Biegler, “On the implementation of an interior-point filter line-search algorithm for large-scale nonlinear programming,” en, *Mathematical Programming*, vol. 106, no. 1, pp. 25–57, Mar. 2006, ISSN: 1436-4646. DOI: 10.1007/s10107-004-0559-y. (visited on 01/31/2020).

[100] R. H. Byrd, J. Nocedal, and R. A. Waltz, “Knitro: An Integrated Package for Nonlinear Optimization,” en, in *Large-Scale Nonlinear Optimization*, ser. Nonconvex Optimization and Its Applications, G. Di Pillo and

M. Roma, Eds., Boston, MA: Springer US, 2006, pp. 35–59, ISBN: 978-0-387-30065-8. DOI: 10.1007/0-387-30065-1_4. (visited on 01/31/2020).

[101] D. Kourounis, A. Fuchs, and O. Schenk, “Towards the Next Generation of Multiperiod Optimal Power Flow Solvers,” *IEEE Transactions on Power Systems*, vol. PP, no. 99, pp. 1–1, 2018, ISSN: 0885-8950. DOI: 10.1109/TPWRS.2017.2789187.

[102] I. B. Sperstad and M. Korpås, “Energy Storage Scheduling in Distribution Systems Considering Wind and Photovoltaic Generation Uncertainties,” en, *Energies*, vol. 12, no. 7, p. 1231, Jan. 2019. DOI: 10.3390/en12071231. (visited on 01/30/2020).

[103] F. Capitanescu and L. Wehenkel, “Experiments with the interior-point method for solving large scale Optimal Power Flow problems,” *Electric Power Systems Research*, vol. 95, pp. 276–283, Feb. 2013, ISSN: 0378-7796. DOI: 10.1016/j.epsr.2012.10.001. (visited on 10/09/2019).

[104] A. Castillo and R. P. O’Neill, “Computational performance of solution techniques applied to the acopf,” *Federal Energy Regulatory Commission, Optimal Power Flow Paper*, vol. 5, 2013.

[105] S. Zaferanlouei, H. Farahmand, V. Vadlamudi, and M. Korpås, “BATTPOWER Toolbox: Memory Efficient and High-Performance Multi-Period AC Optimal Power Flow Solver—Part I: Mathematical Concepts,” *submitted for review, 2020*,

[106] ——, “BATTPOWER Toolbox: Memory Efficient and High-Performance MultiPeriod AC Optimal Power Flow Solver—Part II: Case Study,” *submitted for review, 2020*,

[107] S. Zaferanlouei, V. Lakshmanan, S. Bjarghov, H. Farahmand, and M. Korpås, “BATTPOWER Application: Large Scale Integration of EVs in a Local Distribution Grid —Norwegian Case Study,” *submitted for review, 2020*,

[108] S. Zaferanlouei, M. Korpås, J. Aghaei, H. Farahmand, and N. Hashemipour, “Computational Efficiency Assessment of Multi-Period AC Optimal Power Flow including Energy Storage Systems,” in *2018 International Conference on Smart Energy Systems and Technologies (SEST)*, Sep. 2018, pp. 1–6. DOI: 10.1109/SEST.2018.8495683.

[109] S. Zaferanlouei, M. Korpås, H. Farahmand, and V. V. Vadlamudi, “Integration of PEV and PV in Norway using multi-period ACOPF — Case study,” in *2017 IEEE Manchester PowerTech*, ISSN: null, Jun. 2017, pp. 1–6. DOI: 10.1109/PTC.2017.7981042.

[110] S. Zaferanlouei, I. Ranaweera, M. Korpås, and H. Farahmand, *Optimal Scheduling of Plug-in Electric Vehicles in Distribution Systems Including PV, Wind and Hydropower Generation*, eng. Energynautics GMBH, 2016, ISBN: 978-3-9816549-3-6. [Online]. Available: https://ntnuopen.ntnu.no/ntnu-xmlui/handle/11250/2456183 (visited on 04/30/2020).

[111] S. Flinstad Harbo, S. Zaferanlouei, and M. Korpås, "Agent Based Modelling and Simulation of Plug-In Electric Vehicles Adoption in Norway," in *2018 Power Systems Computation Conference (PSCC)*, Jun. 2018, pp. 1–7. DOI: 10.23919/PSCC.2018.8442514.

[112] M. Lillebo, S. Zaferanlouei, A. Zecchino, and H. Farahmand, "Impact of large-scale EV integration and fast chargers in a Norwegian LV grid," *The Journal of Engineering*, vol. 2019, no. 18, pp. 5104–5108, 2019, ISSN: 2051-3305. DOI: 10.1049/joe.2018.9318.

[113] S. Bjarghov, M. Korpås, and S. Zaferanlouei, "Value comparison of EV and house batteries at end-user level under different grid tariffs," in *2018 IEEE International Energy Conference (ENERGYCON)*, Jun. 2018, pp. 1–6. DOI: 10.1109/ENERGYCON.2018.8398742.

[114] F. Berglund, S. Zaferanlouei, M. Korpås, and K. Uhlen, "Optimal Operation of Battery Storage for a Subscribed Capacity-Based Power Tariff Prosumer—A Norwegian Case Study," en, *Energies*, vol. 12, no. 23, p. 4450, Jan. 2019. DOI: 10.3390/en12234450. [Online]. Available: https://www.mdpi.com/1996-1073/12/23/4450 (visited on 05/03/2020).

[115] G. Sæther, P. Crespo del Granadob, and S. Zaferanlouei, "Peer-to-Peer Electricity Trading in an Industrial Site: Value of Buildings Flexibility on Peak Load Reduction," *Working paper, NTNU, 2020*,

[116] T. Bretteville-Jensen, "The Norwegian electric car controversy: The arguments and some empirical illustrations," eng, *60*, 2016. [Online]. Available: https://ntnuopen.ntnu.no/ntnu-xmlui/handle/11250/2406034 (visited on 03/25/2020).

[117] T. Report, E. Figenbaum, and M. Kolbenstvedt, "Learning from Norwegian Battery Electric and Plug-in Hybrid Vehicle users – Results from a survey of vehicle owners," en, p. 8, 2016.

[118] *Elbilbestand*, nb-NO. [Online]. Available: https://elbil.no/elbilstatistikk/elbilbestand/ (visited on 04/22/2020).

[119] T. Sterud, *Working time in the European Union: Norway*, en. [Online]. Available: https://www.eurofound.europa.eu/publications/report/2009/working-time-in-the-european-union-norway (visited on 02/22/2020).

[120] S. P. Boyd and L. Vandenberghe, *Convex optimization*, en. Cambridge, UK ; New York: Cambridge University Press, 2004, ISBN: 978-0-521-83378-3.

Papers

Paper I

BATTPOWER Toolbox: Memory-Efficient and High-Performance MultiPeriod AC Optimal Power Flow Solver—Part I: Mathematical Concepts

Submitted for review, 2020

This paper is awaiting publication and is not included in NTNU Open

Paper II

BATTPOWER Toolbox: Memory-Efficient and High-Performance MultiPeriod AC Optimal Power Flow Solver—Part II: Case Study

Submitted for review, 2020

This paper is awaiting publication and is not included in NTNU Open

Paper III

BATTPOWER Application: Large Scale Integration of EVs in a Local Distribution Grid —Norwegian Case Study

Submitted for review, 2020

This paper is awaiting publication and is not included in NTNU Open

Paper IV

Computational Efficiency Assessment of Multi-Period AC Optimal Power Flow including Energy Storage Systems

SEST2018

© 2018 IEEE. Personal use of this material is permitted. Permission from IEEE must be obtained for all other uses, in any current or future media, including reprinting/republishing this material for advertising or promotional purposes, creating new collective works, for resale or redistribution to servers or lists, or reuse of any copyrighted component of this work in other works.

Computational Efficiency Assessment of Multi-Period AC Optimal Power Flow including Energy Storage Systems

Salman Zaferanlouei
Magnus Korpås
Jamshid Aghaei
Hossein Farahmand
Department of Electric Power Engineering
Norwegian University of Science and Technology
Trondheim, Norway

Naser Hashemipour
Department of Electrical and electronics engineering
Shiraz University of Technology
Shiraz, Iran

***Abstract*—In this paper, firstly, a formulation for Multi-Period AC Optimal Power Flow is developed to incorporate inter-temporal constraints and, specifically, equations representing energy storage systems. Secondly, a solution method for the resulting optimisation model is proposed based on the primal-dual interior point method and the mathematical details underlying the solution approach are explicitly and extensively elaborated. The developed solver is tested on a simple 3 bus system. Finally, the computationally efficiency is compared with similar GAMS- and MATLAB-based non-linear commercial solvers. The main contributions of our proposed method can be summarised as follows: a) Shorter computational time is observed in the test due to the merit of using analytical differentiation in the solution method rather than numerical, which is typically used by commercial solvers. b) The formulation and solution method provides the basis of an open-box flexible solver that can be extended to include other components of power systems.**

Keywords*—*Multi-Period ACOPF, Interior Point Method, Energy Storage Systems

NOMENCLATURE

General

f, F	Objective function of one time-step and the next horizon
g, G	Vectors of equality constraint in one time-step and over future horizon
h, H	Vectors of inequality constraints in one time-step and over future horizon
$S_{bus,t}$	$n_b \times 1$ Vector of complex bus power injections for one time-step
$[\mathrm{A}]$	Diagonal matrix of vector A located on the diagonal
$V_{di,t}$, $V_{qi,t}$	Real and imaginary part of voltage at bus i and time t
I_{bus}	$n_b \times 1$ Vector of complex bus current injections
S^{fr}, S^{to}	$n_l \times 1$vectors of complex branch power flows, $from$ and to ends
S_g, S_d	$(n_g \times 1)$, $(n_b \times 1)$ Vectors of generator and load complex power injection
$Egrid$, $Igrid$	Equality and Inequality constraints related to grid
$Estorage$, $Istorage$	Equality and Inequality constraints related to storage
$A^{\top}$	(non-conjugate) transpose of matrix A
A_b	Derivative of vector A w.r.t variable b
A^*	Complex conjugate of A
$[\mathrm{A}]$	Diagonal matrix of vector A located on the diagonal

Parameters

$\eta_i^{ch}, \eta_i^{dch}$	Charging and discharging efficiency of the battery at i^{th} bus
Δt	time-step
$E_i^{ST,max}$	Rated energy of the battery at bus i
$P_{i,t}^{LD}, Q_{i,t}^{LD}$	Active and reactive power demand at i^{th} bus at time t
$Q_i^{gen,min}, Q_i^{gen,max}$	Minimum and maximum limit of the reactive power capability of the generator at i^{th} bus
Y_{bus}	Admittance matrix of the grid
SOC_i^{min}, SOC_i^{max}	Minimum and maximum limit of the SOC at i^{th} bus
$P_i^{ch,max}, P_i^{dch,max}$	Rated charging and discharging capacity of the battery at i^{th} bus
$\mathcal{V}_i^{min}, \mathcal{V}_i^{max}$	Minimum and maximum limit of the voltage amplitude at i^{th} bus
$C_g, C_b, C_{g,b}$	$n_b \times n_g$ generator, battery, and generator/battery connection matrix

Variables

λ, μ	Lagrange multipliers regarding to equality and inequality constraints
X, x	Set of all variables on the next horizon, set of variables at one time-step
$P_{i,t}^{ch}, P_{i,t}^{dch}$	Charging and discharging power at i^{th} bus at time t
$SOC_{i,t}$	State-of-charge of the battery at i^{th} bus at time t
$V_{i,t}, \mathcal{V}_{i,t}, \delta_{i,t}$	$n_b \times$ 1vectors of complex bus voltages,bus voltage magnitudes and angles at i^{th} bus at time t
$P_{i,t}^{gen}, Q_{i,t}^{gen}$	Active and reactive power production

978-1-5386-5326-5/18/$31.00 2018 IEEE

	from the distributed generator at i^{th} bus at time t

Indices

n_b, n_g, n_l, T	Number of buses, generators, branches, and steps in the next time horizon
i, t	Index of Bus and time
k, l	Number of equality and inequality equations
fr, to	from bus i to j, to bus i from j
v	Number of variables in one time
$-$, $\sim$	Signs for linear and non-linear equations

I. INTRODUCTION

The continuing introduction of renewable energy resources into the power system has already challenged the classical concept of generation, transmission and distribution of electrical power. The optimal operating point of the system changes over time due to the variable generation of intermittent renewable resources. Energy Storage Systems (ESS) can mitigate this variability, but this implies that optimal operating points for the system over an an extended planning horizon are estimated based on forecasted generation. Therefore, development and extension of tools and methods to evaluate and determine possible optimal operating points over multiple time steps is an increasingly important research objective.

One of the most extensively developed and studied methods to estimate the optimal operation point is AC Optimal Power Flow (ACOPF). ACOPF is a nonlinear and non-convex optimization problem, and many different solution proposals have been introduced so far to conditionally handle it, see for instance [1–3] for reviews of historical and recent development. Notable and easily accessible contributions include the OPF functionalities of the open-source MATLAB toolbox MATPOWER[4], including the MATPOWER Interior Point Solver (MIPS)[5]. Interior point methods is one of the most extensively applied methods to solve nonlinear optimisation problems, especially ACOPF problems[6], and briefly put typically involve solving the Karush-Kuhn-Tucker (KKT) conditions using the Newton-Raphson method.

Classical ACOPF gives the optimal operating point only for one time-step. Further extension of ACOPF has led to Multi-period ACOPF (MPOPF), also referred to as Dynamic OPF (DOPF) [7], [8]. In other words, the optimisation problem is extended over time, which in turn incorporates inter-temporal constraints such as storage equations and ramp generator limits. Particularly the recent prospect of large-scale integration of ESSs in power systems has attracted immense interest to research on MPOPF, and we refer to [6] for a review and to e.g. [9] for some more recent developments. Introduction of inter-temporal constraints into the ACOPF problem is a step towards the next generation of ACOPF tool necessitated by the ongoing transformation of the power system. However, the inclusion of inter-temporal constraints also gives rise to new computational challenges. For instance, [10] discusses how the presence of inter-temporal constraints makes the Jacobian of the Newton-Raphson method to become singular and to further lead to the divergence of the solution method. Discussions of the implication of the inter-temporal constraints on the structure of the KKT matrix is discussed in [11] and [9]. Furthermore, most of the DOPF models in the literature are presented relatively compactly and lack a explicit and complete description of the mathematical details of the formulation and the solution method. A few notable examples for single-period OPF are [12] and [13].

Here in this paper, we aim to expand the mathematical formulations of a MPOPF problem explicitly to firstly show that analytical differentiation of the Lagrangian with respect to different variable will reduce the computational cost of the solution method in compare with numerical methods, and secondly to explore the possibility of extension of the method for future research plans. Here, the first and second derivatives of equality and inequality constraints with respect to variables are analytically calculated over the future horizon. The proposed MPOPF solver is compared with MATLAB non-linear solver FMINCON and CONOPT through implementation of a three bus test system in MATLAB and GAMS. The results are presented and discussed to interpret the efficiency of the proposed method.

This paper is organised as follows: section II presents the general formulation of the problem. In section III, we show how to solve the problem though KKT conditions and Newton-Raphson method and finally propose how to calculate the analytical differentiation of the solution proposal. Section IV presents the case study and the interpretation of the numerical results. Finally, we conclude the main results and discuss future work enabled by the development of the proposed solution approach in section V.

II. FORMULATION OF MPOPF

A. General Structure and Formulation

The general formulation of MPOPT consists of an objective function over future horizon and bunch of equality and inequality constraints as it can be seen here:

$$\begin{aligned} &\min_X F(X) \\ &\text{s.t. } G(X) = 0, \\ &\qquad H(X) \leq 0 \end{aligned} \tag{1}$$

where

$$X = \begin{bmatrix} x_1 & x_2 & ... & x_t & ... & x_T \end{bmatrix}^\top \tag{2}$$

and also:

$$x_t = \begin{bmatrix} \delta_t \; \mathcal{V}_t \; P_t \; Q_t \; SOC_t \; P_t^{ch} \; P_t^{dch} \end{bmatrix}^\top_{1\times v} \tag{3}$$

$g(x)$ is the vector of equality and $h(x)$ is the vector of inequality constraints and both of them include linear and non-linear equations shown with $-$ and $\sim$ in the following equation respectively:

$$G(X) = \begin{bmatrix} \widetilde{g}(x_{t=1}) \\ \widetilde{g}(x_{t=2}) \\ \vdots \\ \widetilde{g}(x_{t=T}) \\ \overline{g}(x_{t=1}) \\ \overline{g}(x_{t=2}) \\ \vdots \\ \overline{g}(x_{t=T}) \end{bmatrix}_{k\times 1} \qquad H(X) = \begin{bmatrix} \widetilde{h}(x_{t=1}) \\ \widetilde{h}(x_{t=2}) \\ \vdots \\ \widetilde{h}(x_{t=T}) \\ \overline{h}(x_{t=1}) \\ \overline{h}(x_{t=2}) \\ \vdots \\ \overline{h}(x_{t=T}) \end{bmatrix}_{l\times 1} \tag{4}$$

B. Detail of Objective Function and Constraints:

1) Objective Function:
Objective function is simply minimization of costs for all generators over time horizon of T.

$$F(X) = \sum_{t=1}^{T} \sum_{i=1}^{n_g} f(P_{t,i}^{gen}) \tag{5}$$

If we assume all generators are modeled by a quadratic function, then objective function can be written as:

$$\min_X \sum_{t=1}^{T} \left(\sum_{i=1}^{n_g} a_i P^{gen2}{}_{i,t} + b_i P_{i,t}^{gen} + c_i \right) \tag{6}$$

2) Power Flow:
Using rectangular coordinates, voltage and power injection matrices V, S_{bus} (rectangular coordinate is used to ease the process of taking differentiation) can be written as:

$$V_{i,t} = V_{di,t} + jV_{qi,t} \tag{7}$$

$$I_{bus,t} = Y_{bus} V_t \tag{8}$$

$$S_{bus,t} = V_t . I_{bus,t}^{*} = V_t . Y_{bus} . V_t^{*} \tag{9}$$

Consider the power balance equation:

$$\widetilde{g}(x_t) = S_{bus,t} + S_{d,t} - C_{g,b} S_{g,t} = 0 \tag{10}$$

C. Voltage magnitude and angle Constraints

Upper and lower bounds of voltages magnitude and angles are defined with constraints 13 and 14. The voltage angle for slack bus is set to be zero.

$$\mathcal{V}_i^{min} \leq \mathcal{V}_{i,t} \leq \mathcal{V}_i^{max} \tag{13}$$

$$\delta_i^{min} \leq \delta_{i,t} \leq \delta_i^{max} \quad \forall i \neq slack \quad \& \quad \delta_{slack} = 0 \tag{14}$$

D. Line Constraints

If we take $(S^{max})^2$ as the squared vector of apparent power flow limits, then flow constraints, the non-linear part of H(X) for one time-step, can be written as:

$$[\widetilde{h}_t] = \begin{bmatrix} h_t^{fr} \\ h_t^{to} \end{bmatrix} = \begin{bmatrix} [S^{fr^*}] S^{fr} - (S^{max})^2 \\ [S^{to^*}] S^{to} - (S^{max})^2 \end{bmatrix} \leq 0 \tag{15}$$

where $S^{fr} = P^{fr} + jQ^{fr}$.

E. Storage Constraints

The storage model used here is a linear storage model including charge, discharge and SOC variables. We neglect the self-discharge and battery degradation over the next optimisation horizon.

$$\begin{aligned} 0 \leq P_{i,t}^{ch} \leq P_i^{ch,max} \\ 0 \leq P_{i,t}^{dch} \leq P_i^{dch,max} \end{aligned} \tag{16}$$

$$SOC_i^{min} \leq SOC_i(t) \leq SOC_i^{max} \tag{17}$$

$$SOC_{i,t} = \frac{E_{i,t}^{ST}}{E_i^{ST,max}} \tag{18}$$

$$\begin{aligned} E_{i,t}^{ST} &= \\ & E_{i,t-1}^{ST} + \eta_i^{ch} P_{i,t}^{ch} \Delta t - \frac{P_{i,t}^{ch} \Delta t}{\eta_i^{dch}} \end{aligned} \tag{19}$$

III. SOLUTION PROPOSAL

A. Primal-Dual Interior Point

The problem formulated in the last section can be solved using primal-dual interior method mainly inspired from [5]. Converting the inequality equations to equality in (1) then we get:

$$\begin{aligned} \min_X & \left[F(X) - \gamma \sum_{n=1}^{l} ln(Z_n) \right] \\ & \text{s.t. } G(X) = 0, \\ & H(X) + Z = 0 \end{aligned} \tag{20}$$

and Lagrangian of the formulated problem (1) becomes:

$$\begin{aligned} \mathcal{L}^{\gamma}(X, Z, \lambda, \mu) &= f(X) + \lambda^{\top} G(X) \\ &+ \mu^{\top} (H(X) + Z) - \gamma \sum_{n=1}^{l} ln(Z_n) \end{aligned} \tag{21}$$

To write Karush-Kuhn-Tucker (KKT) conditions, partial differentials of (21) can be extracted with respect to the all the variables:

$$\begin{aligned} \mathcal{L}_X^{\gamma}(X, Z, \lambda, \mu) &= f_X + \lambda^{\top} G_X + \mu^{\top} H_X \\ \mathcal{L}_Z^{\gamma}(X, Z, \lambda, \mu) &= \mu^{\top} - \gamma e^{\top} [Z]^{-1} \\ \mathcal{L}_{\lambda}^{\gamma}(X, Z, \lambda, \mu) &= G^{\top}(X) \\ \mathcal{L}_{\mu}^{\gamma}(X, Z, \lambda, \mu) &= H^{\top}(X) + Z^{\top} \end{aligned} \tag{22}$$

and the Hessian of the Lagrangian with respect to X can be written as:

$$\mathcal{L}_{XX}^{\gamma}(X, Z, \lambda, \mu) = f_{XX} + G_{XX}(\lambda) + H_{XX}(\mu) \tag{23}$$

$$\begin{aligned} F(X, Z, \lambda, \mu) &= \begin{bmatrix} f_X + \lambda^{\top} G_X + \mu^{\top} H_X \\ \mu^{\top} - \gamma e^{\top} [Z]^{-1} \\ G^{\top}(X) \\ H^{\top}(X) + Z^{\top} \end{bmatrix} = 0 \\ Z &> 0 \\ \mu &> 0 \end{aligned} \tag{24}$$

Using Newton-Raphson's method to solve equation (24) and some simplification, it can finally be written:

$$\begin{bmatrix} M & G_X^{\top} \\ G_X & 0 \end{bmatrix} = \begin{bmatrix} \Delta X \\ \Delta \lambda \end{bmatrix} = \begin{bmatrix} -N \\ -G_X \end{bmatrix} \tag{25}$$

In (25) M and N are defined as:

$$\begin{aligned} M &= f_{XX} + G_{XX}(\lambda) + H_{XX}(\mu) + H_X^{\top} [Z]^{-1} [\mu] H_X \\ N &= f_X^{\top} + G_X^{\top} \lambda + H_X^{\top} \mu + H_X^{\top} [Z]^{-1} (\gamma e + [\mu] H(X)) \end{aligned} \tag{26}$$

$$\overbrace{\left[P_{i,t}^{gen}+P_{i,t}^{SDch}-P_{i,t}^{SCh}\right]}^{\Re[C_{g,b}S_{g,t}]}-\overbrace{\left[P_{i,t}^{LD}\right]}^{\Re[S_{d,t}]}=\overbrace{\sum_{i=1}^{N}\left[V_{di,t}(G_{ik}V_{dk,t}-B_{ik}V_{qk,t})\qquad+V_{qi,t}(B_{ik}V_{dk,t}+G_{ik}V_{qk,t})\right]}^{\Re[S_{bus,t}]} \tag{11}$$

$$\overbrace{Q_{i,t}^{gen}}^{\Im[C_gS_{g,t}]}-\overbrace{Q_{i,t}^{LD,t}}^{\Im[S_{d,t}]}=\overbrace{-\sum_{i=1}^{N}\left[-V_{di,t}(B_{ik}V_{dk,t}-G_{ik}V_{qk,t})\qquad+V_{qi,t}(G_{ik}V_{dk,t}-B_{ik}V_{qk,t})\right]}^{\Im[S_{bus,t}]} \tag{12}$$

Solving (25) numerically results to the locally optimum point X^*. The detail of numerical solution in Newton's method can be seen in [5].

B. Analytical Derivatives

In this section the first and second derivatives of $H(X)$, $G(X)$ and $F(X)$ will be extracted. In general, if we assume a complex scalar function $f : \mathbb{R}^n \to \mathbb{C}$ of a real vector such as (2), the first derivative can be calculated as:

$$\begin{gathered} f_X=\frac{\partial f}{\partial X}=\begin{bmatrix}\frac{\partial f}{\partial x_1} & \frac{\partial f}{\partial x_2} & \cdots & \underbrace{\frac{\partial f}{\partial x_t}}_{\Downarrow} & \cdots & \frac{\partial f}{\partial x_T}\end{bmatrix} \\ \left[\frac{\partial f}{\partial \delta_t}\;\frac{\partial f}{\partial V_t}\;\frac{\partial f}{\partial P_t}\;\frac{\partial f}{\partial Q_t}\;\frac{\partial f}{\partial (SOC_t)}\;\frac{\partial f}{\partial P_t^{ch}}\;\frac{\partial f}{\partial P_t^{dch}}\right] \end{gathered} \tag{27}$$

$$f_{XX}=\frac{\partial^2 f}{\partial X^2}=\frac{\partial}{\partial X}\left(\frac{\partial f}{\partial X}\right)^{\top}=\begin{bmatrix}\frac{\partial^2 f}{\partial x_1^2} & \cdots & \frac{\partial^2 f}{\partial x_1 x_n} \\ \vdots & \ddots & \vdots \\ \frac{\partial^2 f}{\partial x_n x_1} & \cdots & \frac{\partial^2 f}{\partial x_n^2}\end{bmatrix} \tag{28}$$

Eqs. (27) and (28) are the basic forms of first and second derivatives of objective function which is $f : \mathbb{R}^n \to \mathbb{C}$. However, constraints G(X) and H(X) are complex vector functions $f : \mathbb{R}^n \to \mathbb{C}^m$ and therefore:

$$G(X)=\begin{bmatrix}g_1(X) & g_2(X) & \ldots & g_k(X)\end{bmatrix}^{\top}_{1\times k} \tag{29}$$

First derivative of this complex vector function can be written as:

$$G_X=\frac{\partial G}{\partial X}=\begin{bmatrix}\frac{\partial g_1}{\partial x_1} & \cdots & \frac{\partial g_1}{\partial x_t} & \cdots & \frac{\partial g_1}{\partial x_T} \\ \vdots & \ddots & \vdots & \ddots & \vdots \\ \frac{\partial g_k}{\partial x_1} & \cdots & \frac{\partial g_k}{\partial x_t} & \cdots & \frac{\partial g_k}{\partial x_T}\end{bmatrix}_{k\times(T.v)} \tag{30}$$

$$H_X=\frac{\partial H}{\partial X}=\begin{bmatrix}\frac{\partial h_1}{\partial x_1} & \cdots & \frac{\partial h_1}{\partial x_t} & \cdots & \frac{\partial h_1}{\partial x_T} \\ \vdots & \ddots & \vdots & \ddots & \vdots \\ \frac{\partial h_l}{\partial x_1} & \cdots & \frac{\partial h_l}{\partial x_t} & \cdots & \frac{\partial h_l}{\partial x_T}\end{bmatrix}_{l\times(T.v)} \tag{31}$$

Second derivative of G(X) and H(X) is only required to calculate the Hessian of the Lagrangian, Eq. (23). Calculation of second derivatives might be a bit confusing since 3D set of partial derivatives will not be calculated here [12]. The reason fairly simple and straightforward. In this context, we are using a Newton-Raphson method to find where the partials of a Lagrangian are equal to zero. It is the Hessian of the Lagrangian function in (21) that we need to compute and we always compute it with a known lambda vector. Therefore, its only the partial with respect to X of the vector resulting from multiplying the transpose of the Jacobian by lambda that is needed in this context, which means:

$$G_{XX}=\frac{\partial}{\partial X}(G_X^{\top}\lambda) \tag{32}$$

$$G_{XY}=\frac{\partial}{\partial Y}(G_X^{\top}\lambda) \tag{33}$$

The same types of derivatives can be written for $H(X)$ too. More details regarding the first and second partial differentials of $F(X)$, $G(X)$ and $H(X)$, and their matrices will be discussed in the future work.

C. Jacobian of the Newton-Raphson Method

Fig. 1 shows the non-zero part of Jacobian of Newton-Raphson's Method on Eq.(25) where $T = 2$. As it can be seen, M is constructed from two large squares which specifically comes from summation of $G_{XX}(\lambda)$, $H_{XX}(\mu)$ and $H_X^{\top}H_X$ and the diagonal line is summation of F_{XX} and a part that comes from interaction of $[Z]^{-1}[\mu]$ (inverse diagonal of slack variables times diagonal of Lagrangian of inequality constraints) in the following mathematical operations: $H_X^{\top}[Z]^{-1}[\mu]H_X$. G_X is formed from two large squares too, which are first derivatives of power flow equations w.r.t variables. Block A represents the equality equations regarding the grid constraints, and B stands for the Inter-temporal constraints that are related to storage equations.

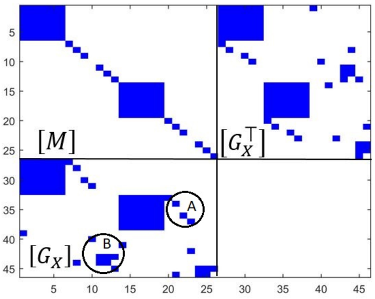

Fig. 1. Structure of Jacobian of the Newton-Raphson's algorithm for two timesteps, refer to Eq. (25)

IV. CASE STUDY AND NUMERICAL RESULTS

For the purpose of efficiency evaluation of the proposed MPOPF, we used a very simple 3 bus case study shown in

Fig. 2 which consists of a generator on bus 1, a battery on bus 2 and load on bus 3. The simulation time horizon is selected two for the sake of simplicity. Fig. 3 shows the variation of base load within two time-steps. With the assumption that the generator has a quadratic cost function and no costs over battery operation; therefore, optimal dispatch of generator, P_g, is to charge the battery at the first time and discharge the saved energy on the second time as it can be observed in Fig. 3. Fig. 4 shows the charge, discharge and stored energy of the battery within the same time horizon. As expected and discussed, since the battery operation cost is zero; therefore, battery charges at the first time-step and discharges on the second one to flatten the overall generation unit profile within two time-step.

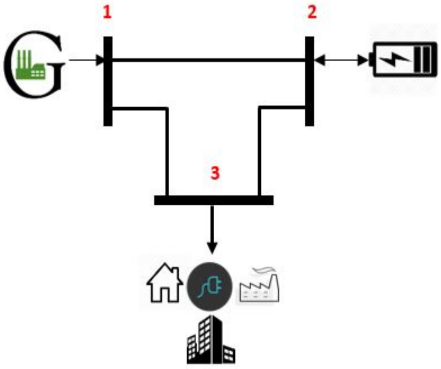

Fig. 2. Three bus case study simulated here in this study

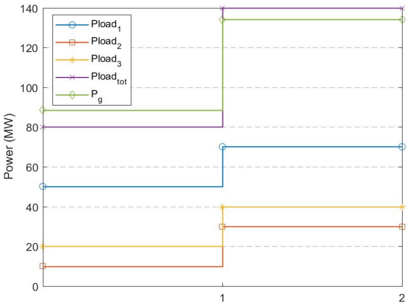

Fig. 3. Base loads and optimal generating power in the 3 bus case study

The case study is also formulated in GAMS and solved with NLP solvers, as listed in II, to compare the computational time and convergence speed. All convergence criteria for commercial solvers are selected to be the default value of each solver in the list. For the sake of comparison, the termination tolerances for the proposed algorithm can be seen in Table I. Definition and formulation of feasibility, complementary, gradient and cost conditions can be found in [5]. and These codes ran on the same PC with Intel 2.7 GHz Core i7 CPU. Table II represents the computational time comparison

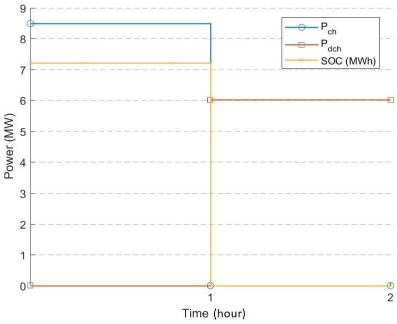

Fig. 4. Charge, discharge and SOC of battery with two time-steps, charging at the first time and discharging on the second one.

between all used solvers with exactly the same implemented formulations. All the numerical parameters are the same for each simulation on table II and consequently optimal solutions converged to the same objective value (the same optimal point).

As it is shown, the computational convergence time for the proposed solution method is almost 10 times less than the commercial solvers. The main reason here is to use the analytical derivatives of f_X,G_X, H_X, f_{XX}, G_{XX} and H_{XX} when Eq. 26 is calculated. However, commercial solvers use numerical methods to calculate derivatives regarding the NLP problem.

TABLE I. TERMINATION TOLERANCES FOR THE PROPOSED MPOPF

Criterion	Value ($\times E-10$)
feasibility condition	1.0
complementarity condition	1.0
gradient condition	1.0
cost condition	1.0

TABLE II. COMPUTATIONAL TIME FOR DIFFERENT SOLVERS AND WITH THE SAME CONVERGENCE CRITERIA

Implemented environment	Solver	Computational time (sec)
MATLAB	FMINCON	0.411
GAMS	CONOPT	0.408
GAMS	CONOPT4	0.592
GAMS	COUENNE	0.637
GAMS	IPOPT	0.538
GAMS	IPOPTH	0.517
GAMS	KNITRO	0.461
GAMS	MINOS	0.413
GAMS	PATHNLP	0.472
GAMS	SNOPT	0.385
MATLAB	The Proposed Method	0.056

V. CONCLUSION AND FUTURE WORK

A solution method of multi-period ACOPF based on primal-dual interior point method is proposed in this paper. Firstly, the method has been introduced and partial derivatives of linear and non-linear constraints, objective function, and KKT condition have been explored analytically. Secondly, a simple three bus case study has been solved through the proposed solution method. Finally, the same formulation has been implemented in GAMS and solved with different solvers to compare the convergence time. The computational cost of the proposed method is compared with different commercial solvers to assess the computational efficiency of the proposed method.

In future work, the Authors are planning to a) expand the analytical differentiation for new constraints and objective function into the current formulations, b) explore Jacobian singularities in Newton-Raphson's method and try to avoid it c) use the automatic differentiation instead of analytical to explore the possibility of computational efficiency improvements.

ACKNOWLEDGMENT

The authors acknowledge Iver Bakken Sperstad for his comments and discussions on this work.

REFERENCES

[1] S. Frank, I. Steponavice, and S. Rebennack, "Optimal power flow: A bibliographic survey i formulations and deterministic methods," *Energy Systems*, vol. 3, no. 3, p. 221258, 2012.

[2] ——, "Optimal power flow: A bibliographic survey ii non-deterministic and hybrid methods," *Energy Systems*, vol. 3, no. 3, p. 259289, 2012.

[3] F. Capitanescu, "Critical review of recent advances and further developments needed in ac optimal power flow," *Electric Power Systems Research*, vol. 136, p. 5768, 2016.

[4] R. D. Zimmerman, C. E. Murillo-Sanchez, and R. J. Thomas, "MATPOWER: Steady-State Operations, Planning, and Analysis Tools for Power Systems Research and Education," *IEEE Transactions on Power Systems*, vol. 26, no. 1, pp. 12–19, Feb. 2011.

[5] H. Wang, C. E. Murillo-Sanchez, R. D. Zimmerman, and R. J. Thomas, "On Computational Issues of Market-Based Optimal Power Flow," *IEEE Transactions on Power Systems*, vol. 22, no. 3, pp. 1185–1193, Aug. 2007.

[6] I. B. Sperstad and H. Marthinsen, "Optimal power flow methods and their application to distribution systems with energy storage - a survey of available tools and methods," SINTEF Energy Research, Report TR A7604, 2016. [Online]. Available: hdl.handle.net/11250/2432401

[7] M. E. El-Hawary and D. H. Tsang, "The Hydrothermal Optimal Load Flow, A Practical Formulation and Solution Techniques Using Newton's Approach," *IEEE Transactions on Power Systems*, vol. 1, no. 3, pp. 157–166, Aug. 1986.

[8] H. Wei, H. Sasaki, J. Kubokawa, and R. Yokoyama, "Large scale hydrothermal optimal power flow problems based on interior point nonlinear programming," *IEEE Transactions on Power Systems*, vol. 15, no. 1, pp. 396–403, Feb. 2000.

[9] D. Kourounis, A. Fuchs, and O. Schenk, "Towards the Next Generation of Multiperiod Optimal Power Flow Solvers," *IEEE Transactions on Power Systems*, vol. PP, no. 99, pp. 1–1, 2018.

[10] K. Baker, G. Hug, and X. Li, "Inclusion of inter-temporal constraints into a distributed Newton-Raphson method," in *2012 North American Power Symposium (NAPS)*, Sep. 2012, pp. 1–6.

[11] N. Meyer-Huebner, M. Suriyah, and T. Leibfried, "On efficient computation of time constrained optimal power flow in rectangular form," in *2015 IEEE Eindhoven PowerTech*, Jun. 2015, pp. 1–6.

[12] R. D. Zimmerman, "Ac power flows, generalized opf costs and their derivatives using complex matrix notation," 2010.

[13] S. Frank and S. Rebennack, "An introduction to optimal power flow: Theory, formulation, and examples," *IIE Transactions*, vol. 48, no. 12, pp. 1172–1197, 2016. [Online]. Available: https://doi.org/10.1080/0740817X.2016.1189626

VI. APPENDIX

Details regarding the case study are listed in tables V-III
Some simulation parameters:
$SOC_0 = 0.00$
$\eta_{chrg,i} = 0.85$
$\eta_{dischrg,i} = 1.2$

TABLE III. UPPER BOUND AND LOWER BOUND OF ALL VARIABLES IN ONE TIME STEP

-	δ_1	δ_2	δ_3	
LB	0.00	-3.14	-3.14	
UB	0.00	3.14	3.14	
-	V_3	V_3	V_3	
LB	0.90	0.90	0.90	
UB	1.10	1.10	1.10	
	P_1	P_{bat}	Q_1	Q_{bat}
LB	0.00	-0.50	-1.00	0.00
UB	3.00	0.50	1.00	0.00
	$P_{SCh,t}$	$P_{SDch,t}$	SOC	
LB	0.00	0.00	0.00	
UB	0.50	0.50	3.00	

TABLE IV. BRANCH DATA

From Bus	To Bus	r	x	b
1	2	0.01008	0.0504	0.1025
1	3	0.00744	0.0372	0.0775
3	2	0.00744	0.0372	0.0775

TABLE V. GENERATORS COEFFICIENTS

time	a	b	c
t_1	0.11	5	550
t_2	0.11	5	550

TABLE VI. BASE LOAD IN DIFFERENT TIME STEPS

Bus number	P_{d1}	P_{d2}
1	50	70
2	10	30
3	20	40

TABLE VII. BASE LOAD IN DIFFERENT TIME STEPS

Bus number	Q_{d1}	Q_{d2}
1	50	50
2	10	10
3	20	20

Paper V

Integration of PEV and PV in Norway Using Multi-Period ACOPF — Case Study

POWERTECH2017

© 2017 IEEE. Personal use of this material is permitted. Permission from IEEE must be obtained for all other uses, in any current or future media, including reprinting/republishing this material for advertising or promotional purposes, creating new collective works, for resale or redistribution to servers or lists, or reuse of any copyrighted component of this work in other works.

Integration of PEV and PV in Norway Using Multi-Period ACOPF — Case Study

Salman Zaferanlouei, Magnus Korpås, Hossien Farahmand, Vijay Venu Vadlamudi
Department of Electric Power Engineering
Norwegian University of Science and Technology
Trondheim, Norway

***Abstract*—Integration of Plug-in Electric Vehicles (PEVs) and renewables poses substantial challenges in electricity distribution networks. This paper investigates the impact of large-scale PEV penetration in distribution networks, when also considering the integration of other renewable energy resources, e.g., wind, hydropower and Photovoltaics (PVs). As such, analysis on an existing low voltage local power system is conducted through simulations. We propose an AC Optimal Power Flow (ACOPF) algorithm over a time horizon of several successive hours. The resulting optimisation framework considers the control of voltage fluctuations within safe bounds, and controlled charging of PEVs, taking into account the total energy consumption of users and the forecast generation of renewables. Simulation results show that the proposed algorithm saves the total cost when compared to an uncontrolled ('dumb') charging scenario.**

***Index Terms*—ACOPF, Multi-Period ACOPF, Plug-in Electric Vehicles, PV, Wind Power Plants, Optimal Charging.**

NOMENCLATURE

$\lvert Y_{ij}\rvert$	Magnitude of ij^{th} element in bus admittance matrix
Δt	Time step
$\eta_{chrg,i}, \eta_{dischrg,i}$	Charging and discharging efficiency of the PEV at i^{th} bus
$\lambda_{spot}(t)$	Electricity price in the wholesale market (spot price) at time t
θ_{ij}	Angle of ij^{th} element in bus admittance matrix
$E_{ST,i}(t)$	Energy stored in the PEV at i^{th} bus at time t
$E_{ST,i}^{max}$	Rated energy of the PEV at bus i
N	Total number of buses in the network.
$P_{DG,i}(t), Q_{DG,i}(t)$	Active and reactive power production from the distributed generator at i^{th} bus at time t
P_G	Active power flow from/to the upstream network.
$P_{LD,i}(t), Q_{LD,i}(t)$	Active and reactive power demand at i^{th} bus at time t
$P_{SCh,i}(t), P_{SDch,i}(t)$	Charging and discharging power of the PEV at i^{th} bus at time t
$P_{SCh,i}^{max}, P_{SDch,i}^{max}$	Rated charging and discharging capacity of the PEV at i^{th} bus
$Q_{DG,i}^{min}, Q_{DG,i}^{max}$	Minimum and maximum limit of the reactive power capability of the DG at i^{th} bus
$Q_{ST,i}(t)$	Reactive power supplied by the PEV at i^{th} bus at time t
S_{ij}	Apparent power flow from bus i to j
$SOC_i(t)$	State-of-charge of the PEV at i^{th} bus at time t
SOC_i^{min}, SOC_i^{max}	Minimum and maximum limit of the SOC at i^{th} bus
T	Total number of discrete intervals per planning horizon
$V_i(t), \delta_i(t)$	Voltage amplitude and the angle at i^{th} bus at time t
V_i^{min}, V_i^{max}	Minimum and maximum limit of the voltage amplitude at i^{th} bus

I. INTRODUCTION

In Norway, the introduction of incentive schemes for promoting electric vehicle users has accelerated the adoption of Plug-in Electric Vehicles (PEVs). All electric vehicles in Norway are exempt from taxation — value added tax and purchase tax. They are exempt from road tolls and parking fees in public parking spaces. Moreover, they have access to free battery charging at publicly funded charging stations, and are allowed to use collective transportation lanes [1]. As per 2017, Norway has the highest number of electric vehicles per capita in the world. PEVs are free of air pollutant emissions, and thus environmentally friendly, all the more so in Norway because 98% of the electricity production is from hydropower. Although PEVs help in the reduction of greenhouse gas emissions, high penetration of PEVs may result in significant technical issues in the distribution grids if charging is not properly coordinated. Uncoordinated charging of PEVs (also referred to as dumb charging) can overload the transformers, increase losses, cause under-voltage problems, and increase harmonic distortion [2], [3], [4]. Therefore, proper coordination of PEV charging with minimal negative effects on the distribution network is of utmost importance. Further, from an economic perspective, it is essential to have optimal scheduling of distributed generators in the distribution system, e.g., Photovoltaic (PV) systems and small-scale wind turbines, so that their energy production is maximally utilized.

Charging the PEVs during low electricity price period is economically attractive for the distribution system operator as well as the PEV owner. It is advantageous to shift the PEV load to periods when the grid is lightly loaded knowing that the electricity prices reflect the heavily loaded and lightly loaded times of the grid.

The Optimal Power Flow (OPF) solution is critical for the optimal operation of an electric power network over a specific time horizon, provided that both the load and the supply are deterministic. The application of AC Optimal Power Flow (ACOPF) for distribution systems is a recent development [5], [6], though several methods are in use and continue to be developed, for solving the general ACOPF problems efficiently [7], [8], [9], [10].

Optimisation of distribution networks with respect to wholesale market exchange including Distributed Energy Resources (DERs) has been explored in many papers. Some select-few literature survey highlights are as follows. Reference [11] pointed out the main aspects of DER, and the challenges and potential solutions in applying demand response in smart grids. Reference [12] proposed an algorithm for optimal coordination of DERs in active distribution networks. Reference [13] presented a mixed integer non-linear programming approach for determining optimal location and number of distributed generators in a hybrid electricity market.

In this paper, we present an optimal scheduling methodology for PEVs in a Norwegian distribution grid where significant amount of PVs and PEVs is accommodated. We use a multi-period ACOPF for finding the optimal charging schedule of the PEVs. Extensive simulations for different PEV-PV penetration scenarios are conducted to verify the flexibility introduced by PEVs and PVs, with respect to grid constraints. The rest of the paper is organised as follows. Section II explains the proposed multi-period ACOPF methodology. Section III presents the case study. Results from the simulations, and consequent discussion are provided in Section IV. Finally, conclusions are presented in Section V.

II. THE PROPOSED MULTI-PERIOD ACOPF METHODOLOGY

From the perspective of the distribution system operator, the charging of PEVs should be coordinated such that the cost of buying electricity from the upstream grid is minimised, while maintaining the quality of supply within the desired range, and ensuring that the loading on transformers and lines is well within their ratings. The overvoltage problem is a common problem that is experienced in residential areas with extensive distributed generators, especially PV[14]. The excess production from the PV system during the daytime when the network is usually lightly loaded causes reverse power flow. This can create overvoltage problems in some nodes in the network. On the other hand, PV generators do not produce power during nights. Usually peak load occurs in residential areas around 1800h - 2000h. During this period, network is prone to under-voltage problems. Charging the PEVs in this time slot can worsen the under-voltage problems. Therefore, due consideration must be given to the coordination of PEV charging. Moreover, it is advantageous if PEVs are charged using the production from the distributed generators within the system as much as possible. When there is not enough excess local production within the system, the required energy for PEV charging should be imported from the upstream grid. Hence, in order to minimise the cost of imported energy from the grid, batteries must be charged in time slots where electricity prices are the lowest.

A. Objective Function

The main objective of the distribution system operator is to minimise the cost of energy imported from the upstream grid over a certain time horizon.

$$Minimise \sum_{t=1}^{T} \lambda_{spot}(t).P_G(t) \tag{1}$$

B. AC Power Flow Equations

$$\begin{aligned} &P_{DG,i}(t) - P_{LD,i}(t) + P_{SDch,i}(t) - P_{SCh,i}(t) \\ &\quad = \sum_{j=1}^{N} |V_i(t)||V_j(t)||Y_{ij}| cos(\delta_j(t) - \delta_i(t) + \theta_{ij}) \end{aligned} \tag{2}$$

$$\begin{aligned} &Q_{DG,i}(t) - Q_{LD,i}(t) \\ &\quad = -\sum_{j=1}^{N} |V_i(t)||V_j(t)||Y_{ij}| sin(\delta_j(t) - \delta_i(t) + \theta_{ij}) \end{aligned} \tag{3}$$

C. Distributed Generator Constraints

$$Q_{DG,i}^{min} \leq Q_{DG,i}(t) \leq Q_{DG,i}^{max} \tag{4}$$

D. Voltage Constraints

$$V_i^{min} \leq V_i(t) \leq V_i^{max} \tag{5}$$

E. Line Constraints

The line constraints are apparent power flow limits in MVA:

$$|S_{ij}(\bar{\delta}, |\bar{V}|| - S_{ij}^{max} \leq 0 \tag{6}$$

$$|S_{ji}(\bar{\delta}, |\bar{V}|| - S_{ij}^{max} \leq 0 \tag{7}$$

F. PEV Constraints

$$\begin{aligned} 0 \leq P_{SCh,i}(t) \leq P_{SCh,i}^{max} \\ 0 \leq P_{SDch,i}(t) \leq P_{SDch,i}^{max} \end{aligned} \tag{8}$$

$$SOC_i^{min} \leq SOC_i(t) \leq SOC_i^{max} \tag{9}$$

$$SOC_i(t) = \frac{E_{ST,i}(t)}{E_{ST,i}^{max}} \tag{10}$$

$$\begin{aligned} &E_{ST,i}(t) = \\ &\quad E_{ST,i}(t-1) + \eta_{chrg,i} P_{Sch,i}(t)\Delta t - \frac{P_{SCch,i}(t)\Delta t}{\eta_{dischg,i}} \end{aligned} \tag{11}$$

The matrix solver also includes arrival and departure times of each PEV, which are not explicitly shown in the formulation above. Care has been taken in the implementation to ensure that the variables for charging and discharging do not conflict with each other. (A PEV can either be charging only or discharging only.)

III. CASE STUDY

The proposed method is applied for scheduling the charging of PEVs in the Norwegian distribution grid, at location Steinkjer, in the district of Nord Trøndelag. The distribution grid consists of 32 distribution transformers (22 kV / 230 V), a small scale hydro power plant with rated capacity 2.4 MW, and 856 customers. The distribution grid is supplied by a 25 MVA, 66 kV / 22 kV transformer at the grid substation. Fig. 1 illustrates the single line layout of the 22 kV network of the grid. In this study, only the LV network supplied by the distribution transformer, indicated as DT1 in Fig. 1, is modelled in detail to consider the voltage variation on the LV side (230 V) of the network. The single line diagram of this LV network is shown in Fig. 2. The number of customers supplied by this network is 62. The highlighted houses in red in Fig. 2 indicate the critical voltage nodes of the network, which have been identified through AC power flow simulations. The other LV networks are modelled as aggregated loads connected to the secondary side of the transformers. The total number of buses in the resulting network is 147.

It is assumed that the distribution grid accommodates significant amount of distributed generators. The distributed generation includes rooftop PV generators and one aggregated wind farm generation. The selected location for the wind farm and its connection to the grid is shown in Fig. 1. The rated capacity of the proposed wind generator is 500 kW. The wind generator is connected to the 22 kV network using a 500 kVA, 690 V / 22 kV transformer. The power production from the wind generator was estimated using the wind measurement data provided by the utility company Nord-Trøndelag Elektrisitetsverk (NTE).

Different scenarios of PV installation were considered: 30%, 70%, 100% of the households have PV systems with rated capacity of 4 kW. The location of households with PV systems are randomly assigned. In the other part of the distribution grid, PV production is added as an aggregated production at the LV side of all the other 22 kV / 230 V transformers in the distribution network. The hourly power production from PV systems were estimated using the solar irradiance data at Steinkjer, the selected location. Load profiles of the consumers over a period of one year (2012) were obtained from NTE. The day with the highest demand (2 February) was chosen for the simulation. The average number of vehicles per household in Norway is 1.3 [15]. Accordingly, the number of PEVs in the LV network with 62 households supplied by the transformer DT1 is selected as 40 for a penetration level of 50%. Note that the aggregated charging of PEVs connected to the LV network supplied only by transformer DT1 is taken into account in this study.

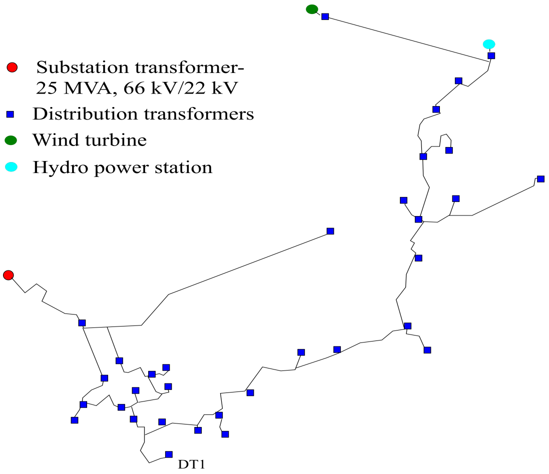

Fig. 1. Single-phase layout of the distribution network (22 kV).

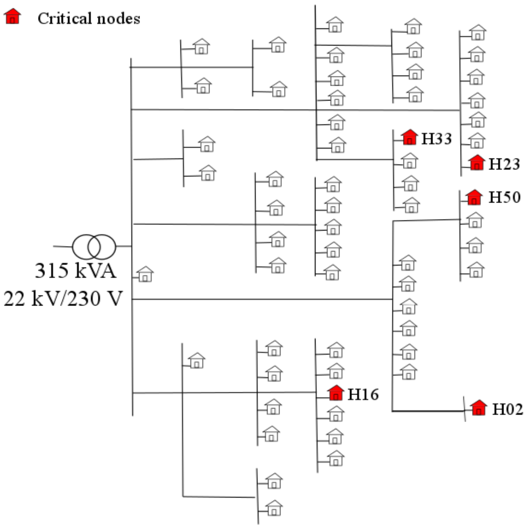

Fig. 2. LV network (230 V) supplied by the transformer- DT1.

The rated power and energy capacities of a single PEV are 6 kW and 20 kWh, respectively. Charging efficiency of all the PEVs is set at 85%. The maximum and minimum State-of-Charge (SOC) limits are set to 100% and 20%, respectively. Table I shows the arrival and departure times of PEVs in the residential area shown in Fig. 2 [15]. The arrivals begin at 1500 h and end at 2000 h. All departures take place the next day at 0800 h. For the case study, the optimisation problem was solved to obtain SOC, charging power and discharging power for each PEV at each hour.

TABLE I
ARIVAL AND DEPARTURE OF PEVS

Arrival		Departure	
Time(h)	Percentage (%)	Time(h)	Percentage(%)
1500	15	0800	100
1600	15	-	-
1700	40	-	-
1800	10	-	-
1900	10	-	-
2000	10	-	-

IV. RESULTS AND DISCUSSION

Fig. 3 illustrates the hourly power productions of hydropower, wind power plant and PVs for the configuration of the grid shown in Fig. 1. It also shows the hourly consumer load demand in the system on 2 Febuary, 2012. This a record peak demand for the year, and hence this worst-case scenario is chosen for the simulation.

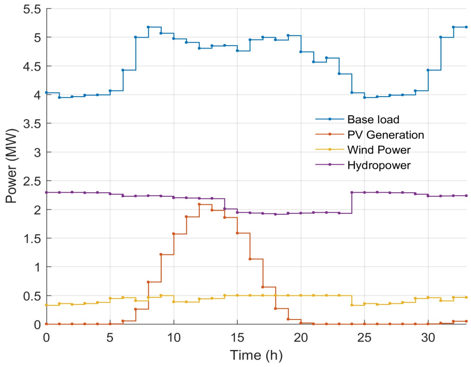

Fig. 3. Hourly average generation of wind, hydropower, aggregated PV and load data.

Fig. 4 shows the hourly power import into the distribution network; the corresponding electricity prices of the wholesale power market (Nord Pool) are also indicated. It can be clearly seen that the charging times are correlated with the lowest hourly electricity prices. However, charging power is only dependent on arrival time in the case of dumb-charging scenario.

Fig. 5 illustrates the charge behavior and SOC of individual PEVs located on the secondary side of transformer DT1. A comparison of the results of the proposed algorithm with those of the dumb-charging scenario are also shown in Fig. 5. From Fig. 5-a, it can be seen that charging occurs at the lowest marginal price around hours 25-31. However, for the dumb-charging scenario, the charging occurs at the arrival time. Fig. 5-b illustrates that the largest charge per hour can be 2.3 kW for the optimal charging scenario, whereas there is a constant profile for the dumb-charging scenario.

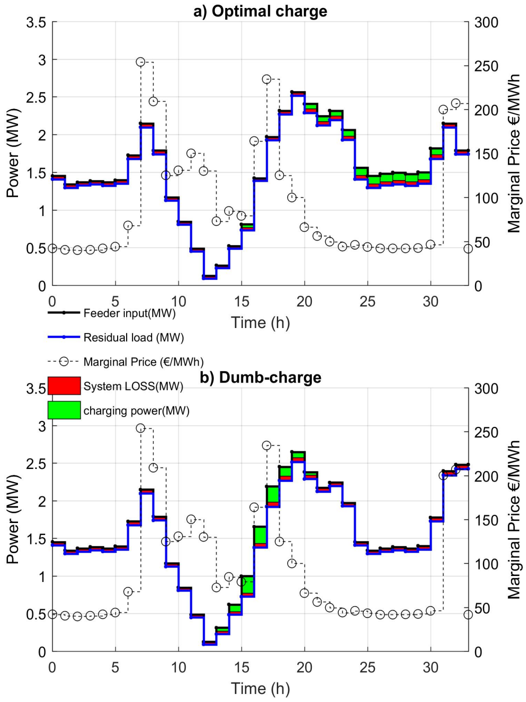

Fig. 4. 70% PEV and 100% PV penetration. Optimal charging profile with a) the proposed algorithm b) dumb-charging method.

Tables II and III present more detailed results of the simulations. Two ratio terms are defined: R_1 — ratio of the PV generation to the consumer energy demand in one cycle; R_2 — ratio of the PEV energy consumption to the consumer energy demand in one cycle. Note that consumer energy demand is the standard energy demand excluding the PEV energy demand. Table II shows the values of these ratios for different penetrations of PEV-PV in the distribution grid. These values show that PEV and PV have a smaller share compared to the actual consumer load demand in the distribution grid. One cycle is 24 hours from 0800 h of a day to 0800 h of the next day.

$$R_1 = \frac{PV \quad Generation \quad in \quad 1 \quad cycle}{Consumer \quad Energy \quad Demand \quad in \quad 1 \quad cycle} \tag{12}$$

$$R_2 = \frac{PEV \quad Energy \quad Consumption \quad in \quad 1 \quad cycle}{Consumer \quad Energy \quad Demand \quad in \quad 1 \quad cycle} \tag{13}$$

Table III is the gist of this study. Dumb- and optimal charging methods are compared in detail with respect to another two terms: R_3 and R_4. The maximum PEV energy consumption in the considered time cycle is noted. Say, this occurs at hour t_c, termed as critical hour. The difference between the consumer

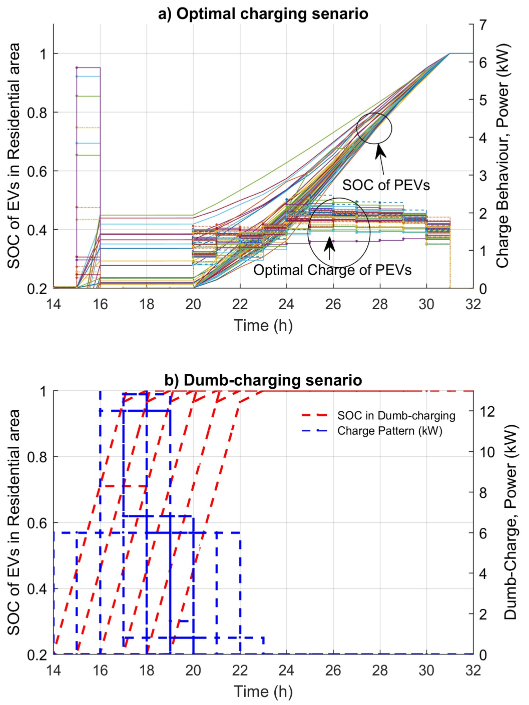

Fig. 5. 70% PEV and 100% PV penetration in the distribution grid. Charge behavior and SOC of the PEVs located at the residential area a) with the proposed algorithm b) with dumb-charging method

energy demand and PV generation in this instance t_c is noted. The term R_3 is defined as follows:

$$R_3 = \frac{Max \quad PEV \quad Energy \quad Consumption \quad at \quad t_c}{(Consumer \quad Energy \quad Demand- \quad PV \quad Generation) \quad at \quad t_c} \tag{14}$$

$$R_4 = A + B - C \quad (at \quad t_c) \tag{15}$$

Where A = Consumer Energy demand, B = PEV energy consumption and C = PV generation

R_3 is almost constant for the optimal charging scenario for different levels of PEV-PV penetration; it increases when PEV penetration is 100%.

For the optimal charging scenario, the total transformer load at hour t_c is almost 315 kW, whereas for the dumb-charging scenario it is 600 kW. Also, the total cost of power import from the main grid for the optimal charging scenario is always less than that for the dumb-charging scenario, as expected.

Fig. 6 clears the concept behind Table III. Green bars show the PEV load and red bars represent PV production. PV production during hours 15-19 could alleviate the PEV load on the system for the case of dumb-charging. Total share of

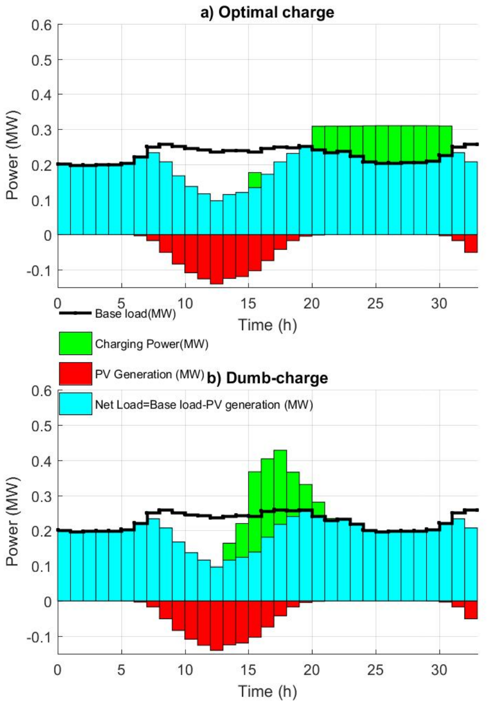

Fig. 6. Share of base load, 70% PEV load and 100% PV generation at the secondary of transformer DT1 shown in Fig. 2. a) Optimal charge behavior. Binding loading constraint on transformer DT1 makes a flat profile from hour 21 until 30. b) Dumb-charge behavior.

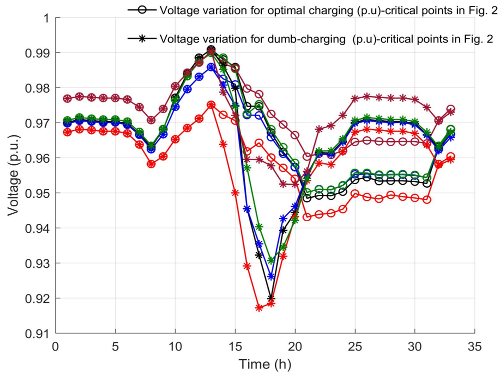

Fig. 7. Voltage variation at the critical nodes of the network with optimal charging and dumb-charging (Black: H50, Red: H23, Blue: H02, Green: H16 and Brown: H33). 70% PEV and 100% PV in the network.

TABLE II
VARIATION OF R_1 AND R_2 FOR DIFFERENT PEV-PV PENETRATION LEVELS FOR ONE-CYCLE 0800 - 0800

PEV-PV(%)	0-0	10-10	20-20	30-30	40-40	50-50	60-60	70-70	80-80	90-90	100-100
R_1	0	0.84	2.89	4.03	6.19	7.32	9.77	11.20	12.81	13.40	17.74
R_2	0	2.58	5.16	7.748	10.33	12.91	15.49	18.07	20.66	23.56	26.15

TABLE III
VARIATION OF R_3, R_3, AND MINIMISED COST OF POWER IMPORT FOR DIFFERENT PEV-PV PENETRATION LEVELS

PEV-PV(%)		0-0	0-30	0-70	0-100	30-0	30-30	30-70	30-100	70-0	70-30	70-70	70-100	100-0	100-30	100-70	100-100
Dumb-Charging method	R_3	-	-	-	-	45.12	50.57	62.67	79.29	95.3	106.7	132	167	143	160	198	251
	R_4	-	-	-	-	348	321	277	239	480	451	406	367	603	573	527	486
	Cost (€)	6969	6391	5760	4994	6990	6453	5821	5055	7121	6543	5910	5144	7191	6611	5978	5211
Optimal Charging method	R_3	-	-	-	-	53.4	53.4	53.4	53.4	54	54	54	54	Infeasible	Infeasible	78	106
	R_4	-	-	-	-	310	310	310	310	310	310	310	310			313	310
	Cost (€)	6969	6391	5760	4994	7031	6355	5664	4820	7025	6388	5697	4853			5895	5119

PEV in comparison with consumer load demand is noticeable as well.

Fig. 7 represents the voltage profile of critical nodes at the network as shown in Fig. 2 The result is for the case of 70% PEV and 100% PV in the network.

V. CONCLUSIONS

This paper presents a multi-period ACOPF including storage equations to simulate a large-scale PEV-PV penetration in a distribution grid also consisting of small wind generators and hydropower. The simulation results suggest that the proposed approach is advantageous over the traditional uncontrolled charging methodology. First, it minimises the total cost of power imported into the distribution system from the main grid. Further, it can be used to schedule charging optimally to satisfy the distribution grid constraints. The studies conducted demonstrate that flexibility can be introduced in the system through appropriate PEV integration.

REFERENCES

[1] S. Allard, P. C. See, M. Molinas, O. B. Fosso, and J. A. Foosns, "Electric vehicles charging in a smart microgrid supplied with wind energy," in *IEEE PowerTech Conference*, Jun. 2013, pp. 1–5.

[2] A. M. A. Haidar, K. M. Muttaqi, and D. Sutanto, "Technical challenges for electric power industries due to grid-integrated electric vehicles in low voltage distributions: A review," *Energy Conversion and Management*, vol. 86, pp. 689–700, Oct. 2014.

[3] M. Liu, P. McNamara, R. Shorten, and S. McLoone, "Residential electrical vehicle charging strategies: the good, the bad and the ugly," *Journal of Modern Power Systems and Clean Energy*, vol. 3, no. 2, pp. 190–202, Jun. 2015.

[4] S. Shao, M. Pipattanasomporn, and S. Rahman, "Challenges of PHEV penetration to the residential distribution network," in *IEEE Power Energy Society General Meeting*, Jul. 2009, pp. 1–8.

[5] M. Khanabadi, S. Moghadasi, and S. Kamalasadan, "Real-time optimization of distribution system considering interaction between markets," in *2013 IEEE Industry Applications Society Annual Meeting*, Oct. 2013, pp. 1–8.

[6] S. Moghadasi and S. Kamalasadan, "Real-time optimal scheduling of smart power distribution systems using integrated receding horizon control and convex conic programming," in *IEEE Industry Application Society Annual Meeting*, Oct. 2014, pp. 1–7.

[7] J. Carpentier, "Contribution to the economic dispatch problem," *Bulletin de la Socit Franaise des Electriciens*, vol. 8, pp. 431–447, 1962.

[8] M. Huneault and F. D. Galiana, "A survey of the optimal power flow literature," *IEEE Transactions on Power Systems*, vol. 6, no. 2, pp. 762–770, May 1991.

[9] J. A. Momoh, R. Adapa, and M. E. El-Hawary, "A review of selected optimal power flow literature to 1993. I. Nonlinear and quadratic programming approaches," *IEEE Transactions on Power Systems*, vol. 14, no. 1, pp. 96–104, Feb. 1999.

[10] S. Frank, I. Steponavice, and S. Rebennack, "Optimal power flow: a bibliographic survey I," *Energy Systems*, vol. 3, no. 3, pp. 221–258, 2012.

[11] F. Rahimi and A. Ipakchi, "Demand response as a market resource under the smart grid paradigm," *IEEE Transactions on Smart Grid*, vol. 1, no. 1, pp. 82–88, Jun. 2010.

[12] F. Pilo, G. Pisano, and G. G. Soma, "Optimal coordination of energy resources with a two-stage online active management," *IEEE Transactions on Industrial Electronics*, vol. 58, no. 10, pp. 4526–4537, Oct. 2011.

[13] A. Kumar and W. Gao, "Optimal distributed generation location using mixed integer non-linear programming in hybrid electricity markets," *IET Generation, Transmission and Distribution*, vol. 4, no. 2, pp. 281–298, Feb. 2010.

[14] R. Tonkoski, D. Turcotte, and T. H. M. EL-Fouly, "Impact of high PV penetration on voltage profiles in residential neighborhoods," *IEEE Transactions on Sustainable Energy*, vol. 3, no. 3, pp. 518–527, Jul. 2012.

[15] Ø. Sagosen, "Analysis of large scale integration of electric vehicles in Nord-Trøndelag," *Master Thesis, NTNU*, 2013. [Online]. Available: https://brage.bibsys.no/xmlui/handle/11250/257521

Paper VI

Optimal Scheduling of Plug-in Electric Vehicles in Distribution Systems Including PV, Wind and Hydropower Generation

International Workshop on Integration of Solar Power into Power System

This paper was presented at the 6th Solar Integration Workshop International Workshop on Integration of Solar Power into Power System. Energynautics GmbH 2016

Optimal Scheduling of Plug-in Electric Vehicles in Distribution Systems Including PV, Wind and Hydropower Generation

Salman Zaferanlouei , Iromi Ranaweera, Magnus Korpås, Hossein Farahmand
Department of Electric Power Engineering
Norwegian University of Science and Technology
Trondheim, Norway

***Abstract*— Integration of Plug-in Electric Vehicles (PEVs) and renewables pose substantial challenges on electricity distribution networks. The focus of this paper is to investigate the impact of large-scale PEVs penetration combined with the integrating of variable Renewable Energy Resources, e.g., wind, hydropower and PVs on distribution network. In this respect, simulation analysis on an existing low voltage local power system is conducted. We propose an ACOPF algorithm over a time horizon of several successive hours. Controlling voltage fluctuations in the safe bound, optimal charging of PEVs, covering the total energy consumption of users, and forecast generation of renewables are considered in an optimization framework. Simulation results show our proposed algorithm saves 2.4% total cost in compared with a dumb-charging scenario.**

Keywords- ACOPF, Plug-in Electric Vehicles, Voltage quality, PV, Wind Power Plants, Optimal Charging

I. NOMENCLATURE

i	Bus index
t	Time index
P_G	Active power flow from/to the upstream network.
N	Total number of buses in the network.
$T, \Delta t$	Total number of discrete intervals per planning horizon and the time step.
$\gamma_{spot}(t)$	Electricity price at the wholesale market (spot price)
$P_{LD,i}(t)$, $Q_{LD,i}(t)$	Active and reactive power demand
$P_{DG,i}(t)$, $Q_{DG,i}(t)$	Active and reactive power production from the distributed generator.
$P_{SCh,i}(t), P_{SDch,i}(t)$,	Charging and discharging power of a PEV.
$Q_{ST,i}(t)$	Reactive power supplied from the battery energy storage.
$V_i(t), \delta_i(t)$	Voltage amplitude and the angle.
$Y_{ij}(t), \theta_{i,j}(t)$	Network admittance amplitude and angle.
$I_{line,rated}$	Rated current capacity of the lines.
$Q_{DG,i}^{\min}$, $Q_{DG,i}^{\max}$	Minimum and maximum limit of the reactive power capability of the DG.
$V_{\min}$, $V_{\max}$	Minimum and maximum limit of the voltage amplitude.
$P_{SCh,i}^{\max}$, $P_{SDch,i}^{\max}$	Rated charging and discharging capacity of a PEV.
$SOC_i(t)$	State of charge of PEV.
$SOC_i^{\min}$, $SOC_i^{\max}$	Minimum and maximum limit of the SOC.
$E_{ST,i}(t)$	Energy stored in the PEV at time step t.
$E_{ST,i}^{\max}$	Rated energy capacity of the PEV.
$\eta_{chrg,i}$, $\eta_{dischrg,i}$	Charging and discharging capacity of the PEV.

II. INTRODUCTION

The introduction of incentive schemes for promoting electric vehicles users accelerated the plug-in electric vehicles (PEV) adoption in Norway. All electric vehicles in Norway are exempt from the value added tax and purchase tax. Moreover, they are exempt from road tolls and get free parking in public parking spaces, free battery charging at publicly funded charging stations, and are allowed to use bus and collective traffic lanes [1]. By 2016, Norway is the largest user of electric vehicles per capita in the world. PEVs are free of air pollutant emissions, hence environmentally friendly, particularly in Norway because 98% of the electricity production is from the hydropower. Although, PEVs help to reduce the greenhouse gas emissions, high penetration of PEVs may result in significant technical issues in distribution grids if charging is not properly coordinated. Uncoordinated charging of PEVs can overload the transformers, increase losses, cause under-voltage problems, and increase harmonic distortion [2], [3], [4]. Therefore, proper coordination of PEVs charging is required in order to utilize the existing infrastructure optimally for PEVs charging without adversely affecting the distribution network. Further, it is important to consider the cost of energy and the production from the distributed generators in the distribution grid for example photovoltaic (PV) systems and small-scale wind turbines. Charging the PEVs during low electricity price period is economically attractive for the distribution system operator as well as the PEV owner. Indirectly, that helps the grid to shift the PEV load to the period when the grid is lightly loaded, because the electricity price reflect the heavily loaded and lightly loaded times of the grid. Moreover, it is important to maximally utilize the energy production from the distributed generators in the network.

The optimal power flow has been applied to find an optimal operating of an electric power grid over a certain time horizon provided that both the load and the supply are deterministic. Several methods have been proposed for solving ACOPF problems efficiently [5], [6]. Therefore, this has been effectively applied for distribution system optimization recently. The conventional AC Optimal Power Flow (ACOPF) is a numerical analysis toolbox that can be used to consider system costs, grid limitations and charging coordination of storages. It formulated in 1962 [7] for a basic problem to find a local optimum operating point for power systems. Since that time, many efforts have been made for solution of optimization algorithm more efficiently [8], [9], [10]. They use nonlinear programming (NLP) based methods. The need for optimization of distribution system with wholesale market transactions including distributed energy resources (DER) have been discussed in the literature earlier. [11] indicates the main aspects of DER, and the challenges and potential solutions for implementing Demand Response in smart grid market. Ref. [12] suggests a new algorithm for distribution management system (DMS) that can be applied to active distribution networks and [13] proposes an algorithm for distribution system operation. Several forecasting methods have been proposed that integrates variability and changes in the resources. Reference [14] introduced a method for maximizing the profits for market participants. Reference [15] and [16] discusses a study with mixed integer non-linear programming (MINLP) approach for determining optimal location and number of distributed generators in hybrid electricity market.

In this paper, we present an optimal scheduling of PEVs in a Norwegian distribution grid accommodating significant amount of distributed generators and PEVs. We use ACOPF for finding the optimal charging schedule of the PEVs. The rest of the paper is organized as follows. Section III explains the method and Section IV presents the case study. Results from the simulations are provided in Section V along with discussions. Section VI presents conclusions.

III. METHOD – AC OPTIMAL POWER FLOW

From the perspective of the distribution system operator, the charging of the PEVs should be coordinated so that the cost of buying electricity from the upstream grid is minimized, while maintaining the quality of supply within the desired range, and loading on the transformers and lines below the ratings. The over-voltage problem is a common problem that has been experienced in residential areas with extensive distributed generators mainly PV [17]. The over-power production from PV system during the daytime when the network is usually lightly loaded causes reverse power flow. This can create over-voltage problems in some nodes in the network. On the other hand, PV generators do not produce power during nights. Usually peak load happen in residential areas around 1800h-2000h. During this period, network is prone to under-voltage problems. Charging the PEVs around this time slot can worsen the under-voltage problems. Therefore, both of these conditions should be taken into consideration when coordinating the charging of PEVs. Moreover, the PEVs should be charged using the production from the distributed generators within the system as much as possible. When there is not enough excess local production within the system, the required energy for charging of PEVs should be imported from the upstream grid. Hence, in order to minimize the cost of imported energy from the grid, we have to charge batteries at the time slots where electricity prices are lowest.

A. Objective Function

The main objective of the distribution system operator is to minimize the cost of energy taken from the upstream grid over a certain time horizon. Here, we assume that the total load on the grid substation transformer is always higher than the production from the distributed generators in the distribution grid. With this assumption, the distribution system operator always buys energy from the upstream grid for the wholesale market price (spot price). Then the objective function can be written as Eq. (1).

$$\text{Objective function} = \min \sum_{t=1}^{T} \gamma_{spot}(t)\ .\ P_G(t)\ .\ \Delta t \tag{1}$$

where $P_G(t)$ is always positive.

1) AC Power Flow Equations

The Kirchhoff's current low must be satisfied at every bus of the network. This results following AC power flow equations for active and reactive power in Eqs. (2) and (3).

$$\begin{aligned} &P_{DG,i}(t) - P_{LD,i}(t) + P_{SDch,i}(t) - P_{SCh,i}(t) \\ &= \sum_{j=1}^{N} |\mathbf{V}_i(t)||\mathbf{V_j}(t)||\mathbf{Y_{i,j}}(t)|\cos(\delta_j(t) - \delta_i(t) + \theta_{i,j}(t)) \end{aligned} \tag{2}$$

$$\begin{aligned} &Q_{DG,i}(t) - Q_{LD,i}(t) \\ &= -\sum_{j=1}^{N} |\mathbf{V}_i(t)||\mathbf{V_j}(t)||\mathbf{Y_{i,j}}(t)|\sin(\delta_j(t) - \delta_i(t) + \theta_{i,j}(t)) \end{aligned} \tag{3}$$

B. Distributed Generator Constraints

Distributed PV systems and a wind generator are considered as the available distributed generators in the system. The active power production from these units are un-controllable but deterministic. It is assumed that these units can provide reactive power support when required. The reactive power produced from these units should be within its reactive power capability limits represented by Eq. (4).

$$Q_{DG,i}^{\min} \le Q_{DG,i}(t) \le Q_{DG,i}^{\max} \tag{4}$$

C. Voltage Constraints

The voltage magnitude at all buses in the network should be maintained within the statutory limits illustrated in Eq. (5).

$$V_{\min} \le V_i(t) \le V_{\max} \tag{5}$$

D. Line Constraints

The current flow in the lines are limited to their rated currents. This limit is represented in Eq. (6).

$$\left|\mathbf{I}_{\mathbf{line,ij}}(t)\right| \le I_{line,rated}\ , \tag{6}$$

where the line current is given by Eq. (7).

$$\mathbf{I}_{\mathbf{line,ij}}(t) = \frac{\mathbf{V}_i - \mathbf{V}_j}{\mathbf{Y}_{ij}} \tag{7}$$

E. *Plug-in Electric Vehicles*

The battery energy storage in a PEV has a limited energy capacity and its state of charge (SOC) should be maintained within a certain safety limits in order to prolong the battery lifetime. Moreover, the charging and discharging rate should be kept below the rated charging and discharging capacities of the battery. This introduces the following constraints in to the optimization problem.

$$\begin{gathered} 0 \le P_{SCh,i}(t) \le P_{SCh,i}^{\max} \\ 0 \le P_{SDch,i}(t) \le P_{SDch,i}^{\max} \end{gathered} \tag{8}$$

$$SOC_i^{\min} \le SOC_i(t) \le SOC_i^{\max} \tag{9}$$

The SOC of the battery is given by Eq. (10).

$$SOC_i(t) = \frac{E_{ST,i}(t)}{E_{ST,i}^{\max}}\ , \tag{10}$$

where

$$E_{ST,i}(t) = E_{ST,i}(t-1) + \eta_{chrg,i}\ P_{Sch,i}(t)\ \Delta t - \frac{P_{SDch,i}(t)\ \Delta t}{\eta_{dischg}\ , i} \tag{11}$$

This problem is formulated with a matrix, which includes arrival and departure time of each PEV, to specify variables and equations regarding each PEV separately. The problem is solved using MATLAB, fmincon optimization solver, which uses the Interior point method.

IV. CASE STUDY

The presented method is applied for scheduling the charging of PEVs in the Norwegian distribution grid, which is located in Steinkjer, Nord Trøndelag. This distribution grid consists of 32 distribution transformers (22 kV/230 V), a small scale hydro power plant with rated capacity 2.4 MW, and 856 customers. This distribution grid is supplied by 25 MVA, 66 kV/22 kV transformer at the grid substation. Fig. 1 illustrates the single-phase layout of the 22 kV network of this grid. In this study, only the LV network supplied by the distribution transformer-DT1 indicated in the figure was modelled in detail to account the voltage variation in the LV side (230 V) of the network. The single phase diagram of this LV network is shown in Fig. 2. The number of customers supplied by this network is 62. The highlighted houses in red in Fig. 2 indicate the critical voltage nodes of the network, which have been identified through AC power flow simulations. The other LV networks were modelled as aggregated loads connected to the secondary side of the transformers. The total number of buses in the resulting network is 147.

We assumed that the distribution grid accommodates significant amount of distributed generators. These distributed generators include, rooftop PV generators and single wind generator. The selected location for the wind generator and its connection to the grid is shown in Fig. 1. The rated capacity of the proposed wind generator is 500 kW. The wind generator is connected to the 22 kV network using 500 kVA, 690 V/22 kV transformer. The power production from the wind generator was estimated using the wind measurement data provided by the utility company Nord-Trøndelag Elektrisitetsverk (NTE). We assumed that 50% of the households have PV systems with rated capacity of 4 kW. The locations of the households having PV systems are randomly chosen. In the other part of the distribution grid, PV production is added as an aggregated production at the LV side of the transformer. The hourly power production from PV systems were estimated using the solar irradiance data at the considered location. The load profiles of the consumers over a year (2012) were obtained from NTE. The day with highest demand (February, 2) was chosen for the simulation.

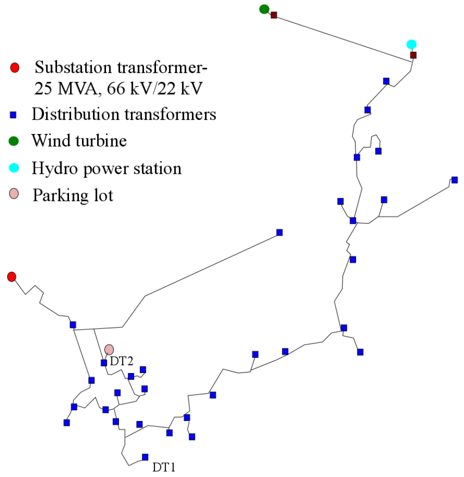

Figure 1. Single-phase layout of the distribution network (22 kV).

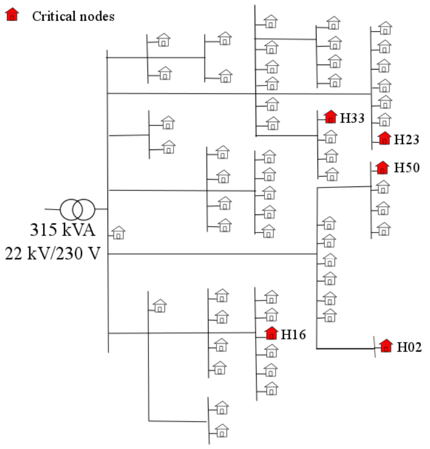

Figure 2. LV network (230 V) supplied by the transformer- DT1.

The average number of vehicles per household in Norway is 1.3 [18]. We assumed a scenario of 50% PEV adoption in Norway. Then the expected number of PEVs in the LV network with 62 households supplied by transformer DT1 is 40. However, the aggregated charging of PEVs connected to the LV networks supplied by the other transformers is not taken into account. We also considered a parking lot located by the transformer DT2 indicated in Fig. 1. The considered number of PEVs connected to the parking lot is 50. The rated power and energy capacities of one PEV are 6 kW and 20 kWh respectively. Then the aggregated power and energy capacities of the PEVs connected to the parking lot is 300 kW and 1000 kWh respectively. Charging efficiency of all the PEV is set to 85%. The maximum and minimum SOC limits are set to 100 % and 20 % respectively. Table 1 shows the arrival and departure times of the PEVs in the residential area shown in Fig. 2, and at the parking lot [18].

Time interval of 33 hours was chosen with 1 hour time step (Δt) for the simulations. This time interval was specifically chosen in order to cover one charging cycle of the PEVs. For the defined case, the optimization problem was solved with 11694 variables.

TABLE 1. ARRIVAL AND DEPARTURE TIMES OF THE PEVS.

Arrival				**Departure**			
Residential area		**Parking lot**		**Residential area**		**Parking lot**	
T (h)	%	T (h)	%	T (h)	%	T (h)	%
15	15	9	100	8	100	16	100
16	15						
17	40						
18	10						
19	10						
20	10						

V. RESULTS AND DISCUSSION

In order to verify the performance of our proposed algorithm, simulation results are dicussed to show firstly how the algorithm keep the voltage into the prefered bound, secondly how it sets proper charge times for fleet of vehicles either in residential area or parking lot with respect to wind, hydropower and PVs production and finally, how it minimizes the total cost.

Fig. 3 illustrates the hourly power productions of hydropower, wind power plant and PVs, which are injected into the grid at different buses shown in Fig. 1. It also includes hourly base load of system on Febuary 2nd , 2012. This a record peak demand for the year, and hence we simulate the worst case scnario and compare it with the results obtained from the case with PEV adoption.

Fig. 4 depicts the voltage fluctuations of critical points in the LV network (highlighted in Fig. 2). Dumb charging senario shows different pattern and voltage drops significantley. In this case, chargings start at arrival time accoring to Table I, without taking into account the critical situation of the system. It can be seen during hours 13-22, voltage magnitudes at nodes H50, H23, H02, H16 and H33 drop significatly. These abnormal voltage drops occur due to the fact that PEV charge and base load second peak happen at the same time. However, in optimal charging scenario, chargings are postponed around hours 26-30 and voltages are kept within normal operating range.

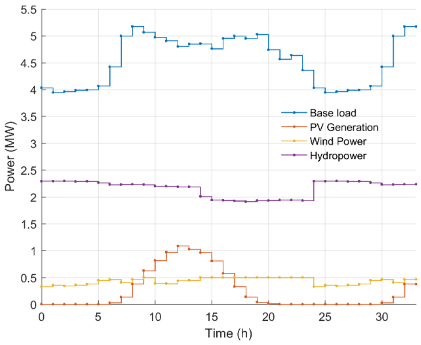

Figure 3. Hourly average generation of wind, hydropower, aggregated PV and load data.

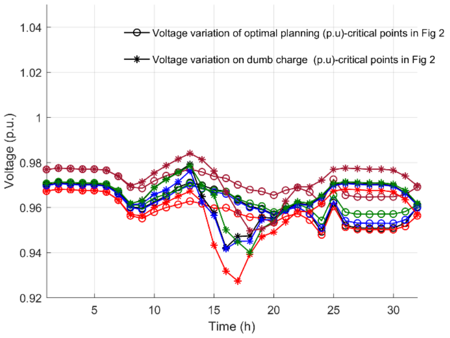

Figure 4. Voltage variation at the critical nodes of the network with time-horizon-ACOPF and dumb charging (Black: H50, Red: H23, Blue: H02, Green: H16 and Brown: H33).

Fig. 5 shows the hourly power exchange through feeder bus of the network with electricity prices specified by wholesale power market, which is Nord Pool, in the case of Norwegian system. It is clearly shown that charging in both parking lot and residential area are correlated with the lowest hourly electricity prices. However, charging power is only dependent on arrival time in the case of dumb charging scenario. Fig. 6 illustrates the charging pattern in the parking lot for both the optimal-charging scenario and dumb-charge scenario. Charging starts at low prices of wholesale market, which obviously minimizes total cost for DISCO to buy electricity from wholesale market. Fig. 7 illustrates the charge behavior and state of charge of PEVs located at residential area. It compares the results of the proposed algorithm with dumb-charging scenario. In Fig. 7-a, it is shown that charging occurs at the lowest marginal price around hours 25-31. However, it happens at arrival time for dumb charging scenario Fig. 7-b illustrates that the largest charge per hour can be 2.3 kW for optimal-charging and it is constant profile for dumb charging scenario.

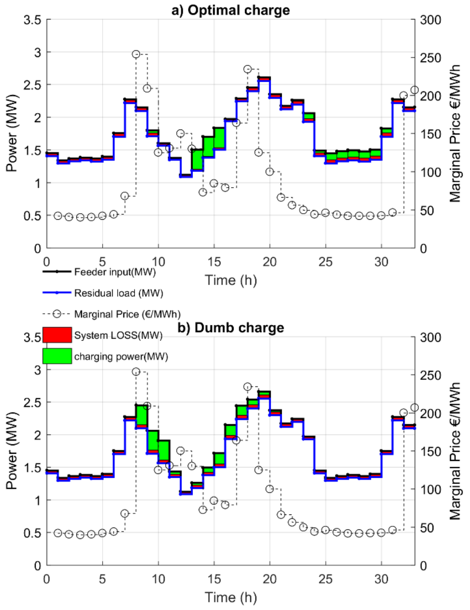

Figure 5. a) Optimal charging with the proposed algorithm, b) Dumb charging.

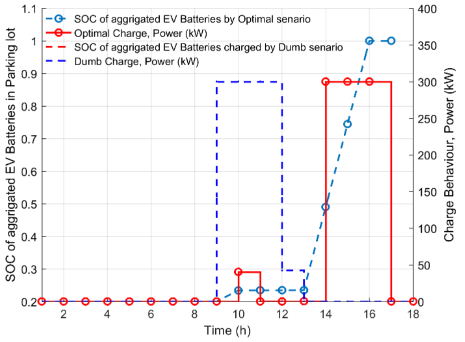

Figure 6. Charge behavior and the SOC of the EVs located at the parking lot with time-horizon-ACOPF and dumb charging.

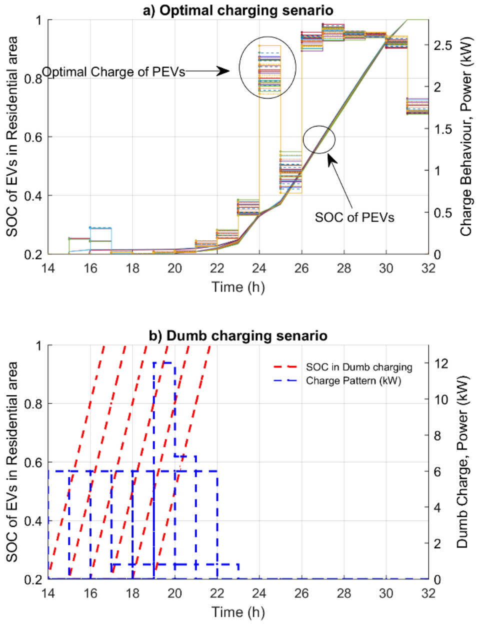

Figure 7. a) Charge behavior and the SOC of the PEVs located at the residential area with proposed algorithm, b) With dumb charging.

VI. CONCLUSIONS

The paper has presented the time-horizon-ACOPF algorithm including storage equations to simulate large-scale PEV penetration in a distribution grid including large number of distributed generators such as photovoltaics (PV), small wind generators and hydropower. The simulation results suggest proposed approach has some advantages over traditional dumb-charging scenario. First it minimizes the total cost of the system, and secondly it can be used to schedule charging to satisfy grid constraints such as voltage constrain, line and transformer overload constrains which are extremely important factors in LV network. Table 2 shows the total electricity cost bought from wholesale market in both simulation cases with our proposed method and dumb-charging scenario. This table indicates 2.4% of the total cost reduction in time-horizon-algorithm.

TABLE 2. TOTAL COST OF POWER IMPORTED FROM THE WHOLESALE MARKET.

Method	Total cost €
Dumb-charging	6096
Time-horizon-ACOPF	5949

REFERENCES

[1] S. Allard, P. C. See, M. Molinas, O. B. Fosso and J. A. Foosnæs, "Electric vehicles charging in a smart microgrid supplied with wind energy," in *PowerTech (POWERTECH)*, Grenoble, 2013.

[2] A. M. Haidar, K. M. Muttaqi and D. Sutanto, "Technical challenges for electric power industries due to grid-integrated electric vehicles in low voltage distributions: A review," *Energy Conversion and Management*, vol. 86, pp. 689-700, 2014.

[3] M. Liu, P. McNamara, R. Shorten and S. McLoone, "Residential electrical vehicle charging strategies: the good, the bad and the ugly," *Journal of Modern Power Systems and Clean Energy*, vol. 3, pp. 190-202, 2015.

[4] S. Shao, M. Pipattanasomporn and S. Rahman, "Challenges of PHEV penetration to the residential distribution network," in *IEEE power and energy society general meeting*, 2009.

[5] M. Khanabadi, S. Moghadasi and S. Kamalasadan, "Real-time optimization of distribution system considering interaction between markets," in *Industry Applications Society Annual Meeting, 2013 IEEE*, Lake Buena Vista, 2013.

[6] S. Moghadasi and S. Kamalasadan, "Real-Time Optimal Scheduling of Smart Power Distribution Systems Using Integrated Receding Horizon Control and Convex Conic Programming," in *IEEE Industry Application Society Annual Meeting*, Vancouver, 2014.

[7] J. Carpentier, "Contribution to the economic dispatch problem," *Bulletin de la Societe Francoise des Electriciens*, vol. 3, no. 2, p. 762–770, 1991.

[8] M. Huneault and F. Galiana, "A survey of the optimal power flow literature," *Power Systems, IEEE Transactions on*, vol. 6, no. 2, p. 762–770, 1991.

[9] J. A. Momoh, M. El-Hawary and R. Adapa, "A review of selected optimal power flow literature to 1993. part I: Nonlinear and quadratic programming approaches," *IEEE transactions on power systems*, vol. 14, no. 1, p. 96–104, 1999.

[10] K. Pandya and S. Joshi, "A survey of optimal power flow methods," *Journal of Theoretical & Applied Information Technology*, vol. 4, no. 5, 2008.

[11] F. Rahimi and A. lpakchi, "Demand response as a market resource under the smart grid paradigm," *Smart Grid, IEEE Transactions on*, vol. 1, no. 1, pp. 82 -88, 2010.

[12] F. Pilo, G. Pisano and G. Soma, "Optimal coordination of energy resources with a two-stage online active management," *Industrial Electronics, IEEE Transactions on*, vol. 58, no. 10, pp. 4526 -4537, 2011.

[13] A. Algarni and K. Bhattacharya, "Disco operation considering DG units and their goodness factors," *Power Systems, IEEE Transactions on*, vol. 24, no. 4, pp. 1831 -1840, 2009.

[14] L. Hu, G. Taylor, H.-B. Wan and M. Irving, "A review of shortterm electricity price forecasting techniques in deregulated electricity markets," in *Universities Power Engineering Conference (UPEC)*, 2009.

[15] E. Castronuovo and J. Lopes, "On the optimization of the daily operation of a wind-hydro power plant," *Power Systems, IEEE Transactions*, vol. 19, no. 3, pp. 1599 - 1606, 2004.

[16] A. Kumar and W. Gao, "Optimal distributed generation location using mixed integer non-linear programming in hybrid electricity markets," *Generation, Transmission Distribution, IET*, vol. 4, no. 2, pp. 281 -298, 2010.

[17] R. Tonkoski, D. Turcotte and T. H. M. EL-Fouly, "Impact of High PV Penetration on Voltage Profiles in Residential Neighborhoods," *IEEE Transactions on Sustainable Energy*, vol. 3, no. 3, pp. 518-527, 2012.

[18] Ø. Sagosen, "Analysis of Large Scale Integration of Electric Vehicles in Nord-Trøndelag," 2013.

Paper VII

Agent Based Modelling and Simulation of Plug-in Electric Vehicles Adoption in Norway

PSCC2018

© 2018 IEEE. Personal use of this material is permitted. Permission from IEEE must be obtained for all other uses, in any current or future media, including reprinting/republishing this material for advertising or promotional purposes, creating new collective works, for resale or redistribution to servers or lists, or reuse of any copyrighted component of this work in other works.

Agent Based Modelling and Simulation of Plug-in Electric Vehicles Adoption in Norway

Sondre Flinstad Harbo
Salman Zaferanlouei
Magnus Korpås
Department of Electric Power Engineering
Norwegian University of Science and Technology
Trondheim, Norway
{sondrefh, salman.zaf, magnus.korpas}@ntnu.no

Abstract—**This paper looks into the consumption side of the power balance, and more specifically on the effects of utilizing an increasingly larger fleet of Plug-in electric vehicles (PEVs) for personal transportation. To asses this, an Agent Based Model of PEVs has been extended and developed with different charging strategies. The model simulates power demand from a given number of PEVs in a given area, and may be useful for policymakers and researchers alike. Simulations ran for the city of Trondheim reinforce the notion that the rising adoption of PEVs might not only pose a substantial challenge due to the relative size of the power demanded, but more critically also because of the variability that the charging profiles exhibit. On the other hand, the different behaviour of the PEV agents, as modelled through different charging strategies, indicate that incentives such as price signals might effect how much the agent charge at different times. Hence it may even lend the PEVs batteries as assets to help stabilize the power balance in the electric grid.**

Index Terms—**Agent Based Modelling, Plug-in Electric Vehicles, Power Demand Variability**

I. INTRODUCTION

The transition to a more sustainable society and economy imposes a challenge for the power system due to raising variability in the system. It is induced by an increasing share of renewable energy sources on the supply side, and the growing adoption of Plug-in Electric Vehicles (PEVs) on the demand side. The focus of this paper is on the latter. The adoption of PEVs has seen a tremendous rise throughout the last decade, facilitated by batteries seeing a steady improvement for both cost and energy density [1]. As such, Norway poses an interesting case study, as the country is one of the greatest PEV adopters to date with PEVs at 3,7% of the total fleet and market share of new car sales above 15% [2]. Hence, it is increasingly crucial to understand how the rising adoption of PEVs will impact the energy system, especially from a Norwegian perspective. Publications from the Norwegian Water Resources and Energy Directorate (NVE), [3] and [4], shows how the PEV adoption will pose challenges especially for transformer stations, transmission lines and voltage quality in Norway. Yet, a challenge when analyzing the electricity consumption of PEVs is the complexity added by human decisions. However, one accredited method to analyze such complex, socio-technical systems[5] is that of Agent Based Modelling (ABM), from the field of Complexity Science.

There is abundant research done on understanding the challenges that arise as an increasing PEV fleet demand more energy, as well as modeling how flexible charging might aid the integration of PEVs to the power system. The reports of [1] and [6] gives a great overview and outlook on the adoption of PEVs. As for analyses based on real data and surveys, the paper of [7] is to recommend. It present information from the ”The EV Project” which gathered PEV driving and charging data in the US. In [8] it is discussed how the PEVs will impact the grid. For the Norwegian case, there are other studies to take note of, besides the two mentioned NVE reports.For instance, [9] discusses charging behaviour in Norway specifically, based on survey data from a few hundred PEV owners. There are also many papers who discusses how to smooth out PEV charging variability. Many of these presents optimization methods which may be used for peak shaving and valley filling. Examples of such are [10] who uses game theory and Nash equilibrium for decentralized charging, [11] who utilizes transition matrix for decentralized charging, [12] and [13] who are solving AC-OPF with Wind, Hydro Power and PEV scheduling, and [14] who gives an assessment of the need for flexibility for PEV integration in Norway.

As for work that has utilized the methodology of ABM in the context of Power Systems, the work of [15] offers a great introduction to the possibilities of AMBs for grid systems. Other important work is that of [16] and [17], which both utilizes the MATSim[18] ABM software to simulate PEV driving and charging behaviour. The former uses game theoretical perspectives to analyze competition for power and the benefits and possibilities with an aggregated PEV manager, the latter parking. Where these works are dependent on a much bigger model built for transport simulations in general, the work of [19] develops a custom-made ABM for PEVs driving and charging.

This paper looks into the effects of utilizing an increasingly larger fleet of Plug-in electric vehicles (PEVs) for personal transportation, by extending the fundamental ABM model of [19], analyzing different PEV behaviour and power system implications. None of the previous work has yet, in the authors opinion, fully utilized the most valuable feature of ABM - namely the possibility to analyze the uprising of extreme events from complex behaviour - to assess the key question of power demand variability. The charging behaviour of PEVs that we want to analyze, may due to human influence be characterized as Socio-technical systems. Hence the use of ABM is a well-suited method to cope with the complexities of our task. Through the implementation of an ABM mimicking the basic characteristics and interactions of the individual components of a PEV charging system, and the heterogeneous nature of an ABM, we should not only be able to simulate the PEV charging behaviour, but also observe the rise of seemingly unpredictable and complex patterns[20] in their power consumption. The paper is organized as follows; part II presents general information, assumptions and specific charging strategies, gathered information on how PEV charging behaviour, discusses how this may be utilized for an ABM, before defining rules for the agents to operate after based on the presented material. part III an overview of the model and the case of Trondheim, presents a brief overview of the implementation of the model, as well as the case study of Trondheim for which the model was further customized. part IV presents some of the main results from the simulation and analysis, of the Trondheim case study, and discusses the findings. part V discusses the findings, and part VI concludes the paper.

II. AGENT BASED MODELLING OF PEV BEHAVIOUR

A few empirical studies have been made that collects data from existing populations of eclectic vehicles, and analyze them to get a sense of their behaviour. In [7], they present the Fig. 1, showing that most EVs are charged once per day and start charging with 20-80% SOC.

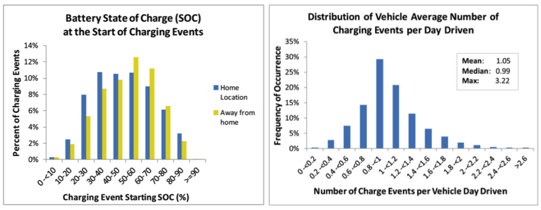

Fig. 1: Charging in terms of SOC and frequency. [7]

However, despite observable profile characteristics, the charging behaviour is still rather volatile, and can also change from different times of year and different locations [21]Contrasting the daily profiles presented in [4], with [21] and [8], it is clear that there are a lot of variation in the charging profiles across different regions.

Agent Based Models are generally bottom-up computational programs where the set of agents all have certain characteristics, and where one specifies certain interaction rules between them and also with the environment. To simulate the fundamental behaviour of the agents, we develop a few basic rules that allows the reproduction of the real observed phenomena and data. From this we may change the parameters, or add a new rule, to observe how it effects the system. It should be noted that by using an ABM one seeks insights on complex problems that is not possible to gain through explicit techniques. As a result, the mathematics here is by itself not very advanced.

To build an ABM of PEVs, we start by making similar assumptions as [19], namely that:

a) The charging of the agent vehicles happens either when they are at home, or at a charging station within a certain distance from their working place in the city.
b) For simplicity, we let the agents decide whether to start charging or not when they arrive either at home or at work. Thus, if they don't connect at first, they will wait until the next arrival at a charging station to charge.
c) Every agent has a home location and work location, which for the sake of simplicity is assigned randomly within some defined areas outside the city.
d) There is a chance that each agent has an errand after work.
e) Every agent has the possibility to charge its car at home.

With these ground rules we may begin building an ABM of PEV energy demand. It is of course possible to alter these assumptions, yet for instance assumption b) simplifies some of the details required to build a the model.

In addition, it is also important to define further the exact mechanism of how the agent decides to charge its car. We need to define a few charging strategies or charging behaviour that the agents should adhere to. The strategies are what will have the most impact on the results, and will give insights on how PEV agents may behave given certain conditions.

The charging strategies that are used in this work is presented below:

1. **"Dumb" charging:** The agents charge whenever they have the need and there is a free charging spot close by.
2. **Probabilistic charging based on SOC:** As seen in Fig. 1, most PEV owners charge when their battery has between 0,2-0,8 SOC. With this strategy the agents do not start charging as soon as they have the need. Instead they will charge according to a certain probability that becomes higher and higher the less power they have left on their battery. For the sake of simplicity, we hence assume a linear probability function, such that

$$Pr_{SOC}(SOC_t, SOC_{min}) = 1 - \frac{SOC_t - SOC_{min}}{SOC_{max} - SOC_{min}} \tag{1}$$

that is, the probability of charging, Pr_{SOC} at a given time instance with a corresponding SOC_t of agent n's battery is given by the difference to the desired minimum SOC_{min} scaled with the difference to the maximum $SOC_{max}(=1)$.
3. **Probabilistic charging strategy based on SOC and price:** Where the first two strategies allow for minimal interaction between the agents, the agents here take into account the price of electricity as well. The higher the price, the less likely they are to charge. This approach allows indirect communications through their response to the price, that here change according to power demanded.

The price in our model may for simplicity determined by how much of a specified maximal power capacity is used, in a linear fashion. More formally the price, $\pi(t)$ at time t is given as

$$\pi(t) = \pi_{min} + C \cdot \frac{\sum_{i=1}^{N(t)} P_i^{PEV}}{P_{max}} \tag{2}$$

where C is a scaling constant, N(t) is the number of connected vehicles at time step t, P_i^{EV} is the power charged by PEV i, and P_{max} is the maximum charging capacity of the power system. If $C = (\pi_{max} - \pi_{min})$, then π_{max} and π_{min} simply defines the range for the price.

We also add the assumption that all agents have available electricity at a given price at their homes, π_{home}, which is higher than π_{min}. This reflect that many home owners in Norway don't buy their electricity on spot at their homes, but with monthly contracts. To develop a probability model based on price and SOC, we may start out with price alone. To make the probability 0.5 for $\pi_t = \pi_{home}$, we may use a function of the form

$$Pr_{price}(\pi_t) = \frac{1 + f_1(\pi_t)}{2} \tag{3}$$

where $f_1(\pi_{home}) = 0$. Moreover, if we let

$$f_1(\pi_t) = \frac{(\pi_{home} - \pi_t)^3}{(\pi_{home})^n} \tag{4}$$

where

$$n = \frac{3 \cdot \ln(\pi_{home} - \pi_{min})}{\ln(\pi_{home})} \tag{5}$$

A function describing likelihood to charge based on price to be 0 at highest price and 1 at lowest, and fairly flat at the middle, refer to Fig. 2, it will need to be of a polynomial with a higher than 2. Hence cubic power in the numerator of Eq.(4) is the easiest. we have a third order polynomial function where $Pr_{price}(\pi_{min}) = 1$, and hence $Pr_{price}(\pi_t = 2(\pi_{home} - \pi_{min})) = 0$. However, we also want the function to be less curved when $\pi_t > \pi_{home}$, which for instance may be invoked by multiplying $f_1(\pi_t)$ with

$$f_2(\pi_t) = \left(\frac{\pi_{max}}{\pi_t}\right)^m \tag{6}$$

where π_{max} is some maximum desired price to pay for power. Choosing $m = 5$ and updating n to

$$n = \frac{3 \cdot \ln(\pi_{home} - \pi_{min}) + 5(\ln(\pi_{max}) - \pi_{min})}{\ln(\pi_{home})} \tag{7}$$

we express the probability of charging according to price as

$$Pr_{price}(\pi_t) = \frac{1 + f_1(\pi_t) f_2(\pi_t)}{2} = \frac{1 + \frac{(\pi_{home} - \pi_t)^3}{(\pi_{home})^n} \left(\frac{\pi_{max}}{\pi_t}\right)^m}{2} \tag{8}$$

We multiply f_1 by f_2 to make the curve less curved above $\pi_t = \pi_{home}$. It means it is less important how much the electricity price is over home price, than how cheaper it is. This is to reflect that many agents will be eager to be at the margin, than to loose extra money if they really have to charge, see Fig. 2. To calculate the probability affected by both price and SOC, we multiply these together and multiply them by 2,

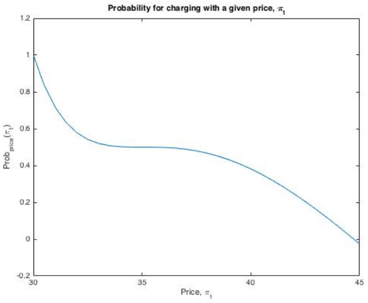

Fig. 2: Probability for charging based on price.

$$Pr_{SOC\&price}(\pi_t) = 2 \cdot Pr_{SOC}(\pi_t) \cdot Pr_{price}(\pi_t) \tag{9}$$

so that if they are both at their middle case (50% SOC and $\pi_t = \pi_{home}$), then the joint probability will still be 50% for charging.

III. CASE: IMPLEMENTING AN ABM OF PEVS FOR TRONDHEIM

The simulation of the Agent Based Model has been implemented in JAVA, as it is a widely used object-oriented programming language. It facilitates the use of classes of objects that intact, a native part of ABM. It is also fairly straight forward to get to interact with Internet APIs.

To get a general impression of how the ABM, it is here presented a UML class diagram. The Fig. 3 shows the model architecture used. To get more information about the details of this particular ABM, see [19] for the underlying model, and [22] for the specifics of the model implemented here.

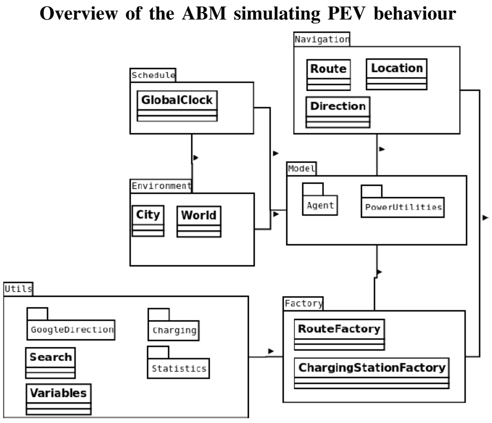

Fig. 3: Overview of high-level architecture of the agent based model[19].

The city of implementation in this model has been chosen to be Trondheim, the city of residence of the Norwegian University of Science and Technology (NTNU). The charging stations used in the model, as displayed in Fig. 4, are the ones actually excising in the city. An up-to-date list of stations and their characteristics may upon request be accessed from [23] and downloaded using their API. An API to Google Maps was also used to find the distance and time for all the agent's driving routes, laying the basis for all the energy consumption calculations.

At the heart of this model we have the PEV agents. To introduce some diversity to the electric vehicle agents, it is possible to include many types of cars, as well as different agent characteristics (eg. different working times) etc, to make the model more realistic or reach a desired level of detail. Therefore a few different types of cars implemented as specific types of electric vehicles for a certain agent, such as Tesla

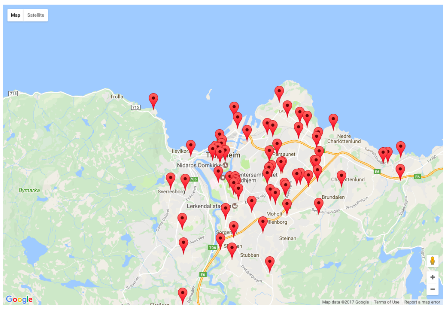

Fig. 4: Map of charging stations in Trondheim as of 12.06.2017.

Model S, Volkswagen eGolf and Nissan Leaf as can be seen in table I. For this simulation each agent has a probability of 1/3 to have each of the cars.

Brand Model	Nissan Leaf	Tesla Model S	Volkswagen E-Golf
Consumption Rate [kWh/km]	0,174	0,198	0,179
Charge Rate [kW]	6,6	10	7,2
Battery size [kWh]	30	100	24

TABLE I: Variety of cars implemented in simulation, data from [24] and [25]

IV. RESULTS FROM THE CASE

This section presents results from the simulations of the ABM for the city Trondheim. It also presents the observed variation in simulation data for two of the cases, and at the end prognosis for PEV power demand in the future based on this model.

A. *Daily profiles of total demand and SOC for the ABM with different charging strategies*

After implementing the ABM in Java with different strategies, a number of different simulation runs was conducted, from which to compare the four different strategies. The simulation runs were each done with 1500 agents over 10 days, with the maximum power of the grid set to 4500kW in most cases. One should also keep in mind that all simulations are based on several random realizations, and such one could run even more iterations to get better insights in the results.

1) Dumb charging: Fig. 5 depicts the total demanded power by both home and public chargers from the grid with the dumb charging strategy. The graph shows that the charging has a characteristic pattern, with larger amount of charging in the evening at the home stations, indicating there are too few chargers in the city. In Fig. 6 we see how the State of Charge (SOC) of the battery of 100 out of the 1500 agents during a 10-day period. We may observe that the agents, by design, charge as soon as they have the opportunity, maintaining their battery level close to maximum.

2) Probabilistic charging strategy based on SOC: Fig. 7 depicts the total demanded power from the grid. Again, it shows that the power used for charging is almost twice as much power from the home-stations compared to the city ones. However, we observe that the graph has a more gradual increase and decrease.Fig. 8 shows how 100 of the 1500 agents store energy in their batteries during the simulation. As can be observed from the graph, this strategy clearly makes it more probable that the agents wait a while before charging their batteries. However, it does not seem to generate a almost even distribution around 80%-20% of SOC, as in Fig. 1.

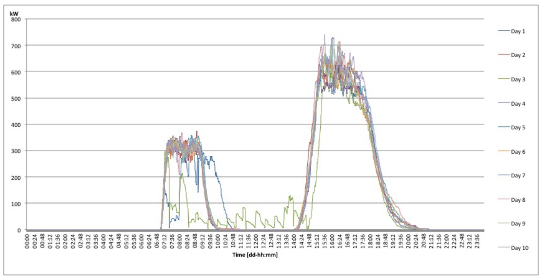

Fig. 5: Total power demand from 1500 EVs during 10 days with dumb charging

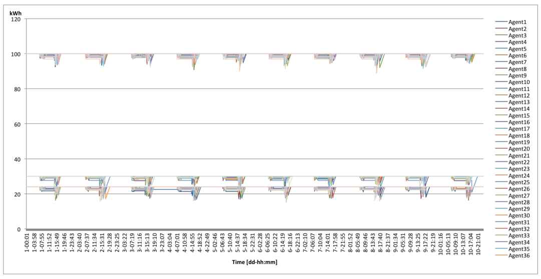

Fig. 6: SOC during 10 days for 100 to 1500 EVs with dumb charging

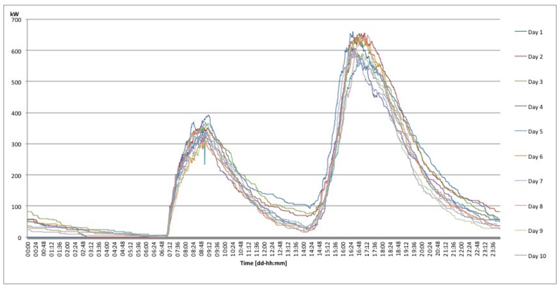

Fig. 7: Total power demand from 1500 EVs during 10 days with charging strategy based on SOC

Fig. 9 shows the power demand from the different charging stations. Notably, charging station with ID: 0 with the highest peak, corresponds to the agents charging at their homes. Two of the other stations with quite high peaks are the stations of ID: 1309 and ID: 66, corresponding to the largest charging stations at Sirkus Shopping Mall and IKEA in Trondheim with 10 and 12 charging spots respectively.

3) Probabilistic charging strategy based on SOC and price: The graph in Fig. 10 shows the total demanded power from the grid when the maximum desired power level is set to 4500 kW. We here observe that the graph shows some of the main characteristics of the previous cases, just more smoothed out,

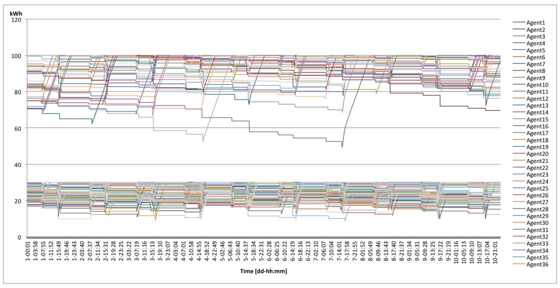

Fig. 8: SOC during 10 days for 100 ot 1500 EVs with charging strategy based on SOC

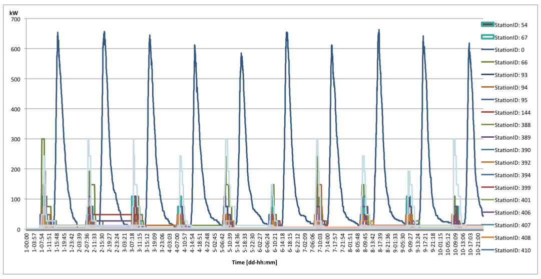

Fig. 9: Power demand per station during 10 days of 1500 EVs with charging strategy based on SOC

and with pikes in the first period due to more complex agent indirect interaction.

The results shown here, is not to emphasise that smoothing is possible through different charging strategies, but rather to assess the short-term variation and volatility that is present in scenarios with different charging strategies.

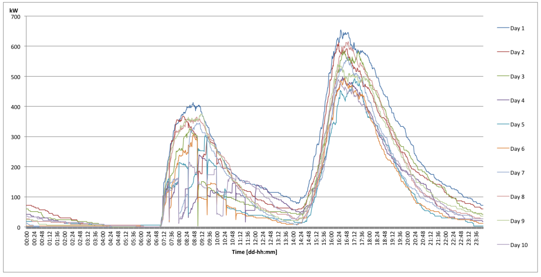

Fig. 10: Total power demand from 1500 EVs during 10 days with charging strategy based on SOC and price and P_{max}=4500 kW

B. *Variability in simulated scenarios*

In Figs. 11 and 12 we may observe the profiles of the runs simulation 40 days with 1500 agents. In the former the agents utilize the 2nd strategy, that is charging based solely on SOC, whereas in the latter the agents are influenced by both their SOC and the energy price with a P_{max} = 1500kW. A feature with these graphs is that they present the average, 5%, 25%, 75% and 95% percentiles for the data in the same minute for the 40 days. Hence, we may better observe the variability within the data. From the Figs. we can see it is clear that there is a considerable variability band especially in Fig. 11 representing the SOC scaled charging strategy.

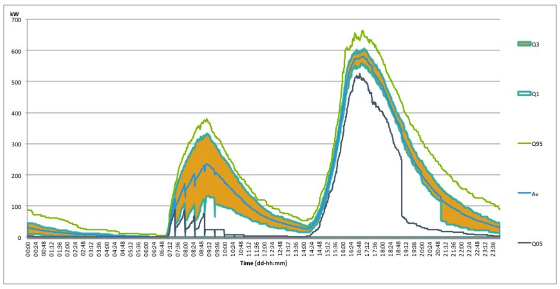

Fig. 11: Total power demand from 1500 EVs during 40 days with charging based on SOC

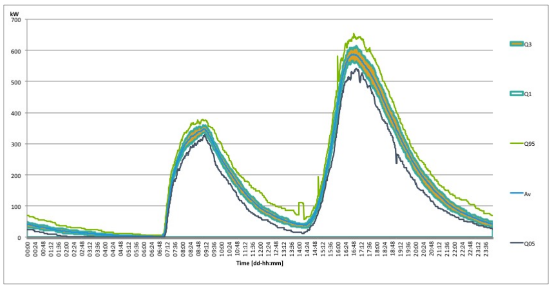

Fig. 12: Total power demand from 1500 EVs during 40 days with charging strategy based on SOC and price and P_{max}=1500 kW

Additionally, the same statistics was computed for the whole aggregated time series over all the 40 days. The results are presented, along with the standard deviation (SD) in table II. From table II, we see that the maximal value of power demanded is about the same, however the average value seems to be higher in the latter case. However, contrary to what the graphs seem to display, we also see that the standard deviation, a measure of variability in a time series, is slightly higher in the latter case as well. However, the standard deviation on relative changes is high in the second, but astonishing in the first.

TABLE II: Statistics for 40 day simulation statistics with 1500 agents with different charging strategies

Stats [/kW]	Q95	Avg	Q05	SD	SD of prof.av.
SOC	522	137	0	163	38,66
SOC&Price, 1500P_{max}	537	161	3	167	17,88

C. *Prognosis of power demand*

With the reports of [3] and [4] from NVE, and data from Statistics Norway (SSB), we surmise make a prognosis for PEV adoption, as presented in table III.

Data for Norway	2015	2030	2050
Inhabitants	5 100 000	5 900 000	6 300 000
Personal vehicles	2 600 000	2 900 000	3 300 000
Electric vehicles	73 000	1 500 000	3 300 000
Power to EVs [TWh]	0,2	4	7,9

TABLE III: Prognosis of Population, Cars and EVs in Norway, (NVE)

One thing that stands out from this table, is the amount of energy demanded from the electrical vehicles is expected

TABLE IV: Projections of vehicle fleet and power demand [kW]

Base case	**Vs in Nor.**	**PEVs Tr.hm.**	**Avg dmnd**	**Q95 dmnd**
2030	2 900 000	61 921	6 147	22 106
2050	3 300 000	131 481	13 052	46 939

Today's rate	**Vs in Nor.**	**PEVs Tr.hm.**	**Avg dmnd**	**Q95 dmnd**
2030	2 900 000	111 539	11 073	39 820
2050	3 300 000	131 999	13 104	47 124

Lower rate	**Vs in Nor.**	**PEVs Tr.hm.**	**Avg dmnd**	**Q95 dmnd**
2030	2 900 000	39 496	3 921	14 100
2050	3 300 000	98 204	9 749	35 059

only to be 4 TWh in 2030 and a maximum of 7,9 TWh in 2050. Compared to the total amount of energy of 43 TWh that went to transportation using personal vehicles in 2015 (see [26]), that reduction is quite substantial. The lowered energy consumption from transportation will be thanks to the efficiency gain of not having to convert energy to another energy carrier than electricity.

Another analysis conducted was to compare the results of the data insight from the last section IV-B, with the outlook presented in table III.To do this, we first had to make projections for the adaption of PEVs in Norway, and then make some scenarios based on this. One alternative here is to use a System dynamic approach. A simple System Dynamic model was implemented in VENSIM[27]. However, the tuning of the parameters in the model did not yield realistic enough results. Instead we use an S-curve, or logistic function,

constructing a base case based on the prognosis of NVE presented in Table III, a high case which uses the growth rate of the last couple of years as the starting point of its S-curve, and a low case where we assume full electrification will not happen.

To make the projected adoption cases relevant to our model, we assume that the PEV adoption in Trondheim scales similarly. Hence, based on the fact that in 2016 SSB accounts a total 4190 PEVs in Trondheim in 2016, and the NVE prognosis for vehicle adoption displayed in table III, we may scale the average statistical data from table II and make a prognosis for power demand in Trondheim due to PEV, presented in table IV

From table IV we see that there is quickly a high demanded power from the PEVs, reaching above 10 MW already in 2030 in all cases. However, if one compares these results with the energy consumption calculation of NVE from table III, we find that the number presented in the projections of table IV are a little low. Indeed, if one multiplies the number of PEVs in each scenario with an average driving distance of 12 300 km/year (assuming it will be the same as the 2015 statistics from SSB) and an average energy consumption of 0,2 kWh/km for the PEVs, we find that the base case in 2030 should have had an average power demand of 17 389 kW and similarly 36 923 kW for 2050.

The lower value of energy demand from out model may be well explained by the fact that we only simulate driving to and from work and errands on weekdays, and do not include transportation back and forth to cabins for instance in weekdays and holidays. However, our bottom-up model seems to do a fairly good job in predicting the power demand within a reasonable range of the top down calculation.

Comparing the figures of 17 389 kW and 36 923 kW to the total energy consumption of about 3,5 TWh in Trondheim yearly, see [28], corresponding to an average of 400 MW per hour, the power demand is about 4% and 9%, in 2030 and 2050 respectively, of average demanded power in Trondheim, or 6% and 13% of average electricity demand.

Hence, a substantial electrification of the car fleet will demand a significant amount of available power from the grid. If we take this trail of though further and scale the Q95 results also, it seems probable that the grid in Trondheim also has to supply a peak power demand that will be about 22% and 43% of average power demand from electricity.

V. DISCUSSION

The ABM built in this project allows for a few more in depth insights as well. Since this model was simulated using real data for Trondheim, the analysis provides take-aways for policy makers in this city.

Firstly, regarding the spatial distribution of charging demand. The amount of charging stations installed in the city center of Trondheim is somewhat limited forcing many of the agents to charge at home instead. Yet, this is not really a consumer problem, since most cars are more that capable of riding back and forth to job and charge at home. What might be a problem, is that the distribution grid of areas outside the city might not be dimensioned for having many PEVs charging simultaneously. Coupling this with the fact that the average chairing power for home charging is assumed to rise from an average of 3,1 kW today to 5,6 kW [3] with full electrification, we see that there might be even greater issues with the grid in home areas in the skirts of the city.

A key question from the introduction was the magnitude of power demand. Whereas the model and simulations here give an average demand of power of about 6 MW in 2030 and 13 in 2050, the revised numbers shows us a electric power demand of about 6% and 13% and peaks routinely be about 22% and 43%. If one is to take account for extreme charging event after holidays which again is not captured in these simulations, the maximum charging demand would be even greater. In any case this would be a challenge for the grid to handle if it happens uncontrollably, and some mechanisms will be needed to guide or incentivise when the PEVs should charge.

The other main inquiry we wanted to make was on the variability as the personal transportation system develops to an electrified one. From the general charging profiles, we see that there are not only considerable peak-to-trough variations intraday at in these simulations. Moreover, one specific charging profile may also vary considerable from the average profile, and the minute to minute variations are also substantial. However, due to the nature of the model with only weekdays in consideration, the coincidence of these simulations is at most about 20%. Again, with more extreme cases eg after weekends, the absolute variability may be even higher if more cars are charging at the same time.

Coupling the findings mentioned above, of substantial spatial and temporal variability and a rinsing magnitude of demand, it is clear that the power grid may face challenges when serving a ever growing number of PEVs. However, the models also show that price signals might work in order to incentivise PEV owners to charge at times more beneficial to the power system. Moreover, a even more connected system, both in terms of energy and information through the rise of Smart Grids, might enhance the possibly to achieve peak-shaving and valley-filling.

VI. CONCLUSION

To conclude, we have developed an PEV fleet model that captures the uncertainty and complexity of agents with different probability scenarios and then tested it on a real case-study which is city of Trondheim with existing public charging stations. it seems clear that the rising adoption of PEVs pose a challenge due to both the relative size of the power demanded but also the variability that the charging profiles exhibit. On the other hand, the different agent, or PEV owner, behaviour, as modelled through different charging strategies, indicate that incentives such as price signals might effect how much the agent charge at different times. As such, a development towards Smart Grid might even lend the PEVs as assets to help stabilize the power balance.

REFERENCES

[1] P. Cazzola, M. Gorner, J. Teter, and W. Yi, “Global ev outlook 2016 - beyond one million electric cars,” Paris, France, Tech. Rep., 2016.

[2] Norsk Elbilforening, “Elbilstatistikk - Bestand og markedsandel,” 2017. [Online]. Available: https://elbil.no/elbilstatistikk/

[3] D. Spilde and C. Skotland, “Hvordan vil en omfattende elektrifisering av transportsektoren pvirke kraftsystemet?” NVE, Oslo, Norway, Tech. Rep., 2015.

[4] C. H. Skotland, E. Eggum, and D. Spilde, “Hva betyr elbiler for strmnettet?” NVE, Oslo, Norway, Tech. Rep., 2016.

[5] J. D. Farmer and D. Foley, “The economy needs agent-based modelling,” *Nature*, vol. 460 (6), pp. 685–686, 2009.

[6] IEA, “Energy technology perspectives - harnessing electricitys potential,” Paris, France, Tech. Rep., 2014.

[7] J. Smart and S. Schey, “Battery electric vehicle driving and charging behavior observed early in the ev project,” *SAE Int. J. Alt. Power*, 2012.

[8] J. Smart, D. Scoffield, and S. Schey, “A first look at the impact of electric vehicle charging on the electric grid in the ev project,” *SAE Int. J. Alt. Power*, 2012.

[9] H. T. Tveter, “Large scale transition from conventional to electric vehicles and the consequences for the security of electricity supply - a demand side analysis of electricity consumption,” Master’s thesis, NHH, 2014.

[10] Z. Ma, D. Callaway, and I. Hiskens, “Decentralized charging control for large populations of plug-in electric vehicles,” *49th IEEE Conference on Decision and Control*, 2010.

[11] K. Zhana, Z. Hu, Y. Song, N. Lu, Z. Xu, and L. Jia, “A probability transition matrix based decentralized electric vehicle charging method for load valley filling,” *Electric Power Systems Research*, vol. 125, pp. 1–7, 2015.

[12] S. Zaferanlouei, I. Ranaweera, M. Korpås, and H. Farahmand, “Optimal scheduling of plug-in electric vehicles in distribution systems including pv, wind and hydropower generation.” Energynautics GMBH, 2016.

[13] S. Zaferanlouei, M. Korpås, H. Farahmand, and V. V. Vadlamudi, “Integration of pev and pv in norway using multi-period acopfcase study,” in *PowerTech, 2017 IEEE Manchester*. IEEE, 2017, pp. 1–6.

[14] . Vatne, M. Molinas, and J. A. Foosn s, “Analysis of a Scenario of Large Scale Adoption of Electrical Vehicles in Nord-Trndelag,” *Energy Procedia*, 2012.

[15] E. Kremers, “Modelling and Simulation of Electrical Energy Systems Through a Complex Systems Approach Using Agent-Based Models,” Ph.D. dissertation, UPV, Valencia, Spain, 2013.

[16] M. D. Galus, “Agent-based modelling and simulation of large scale electric mobility in power systems,” Ph.D. dissertation, ETH Zrich, Switzerland, 2012.

[17] R. A. Waraich, “Agent-based simulation of electric vehicles: Design and implementation of a framework,” Ph.D. dissertation, ETH Zrich, Switzerland, 2013.

[18] A. Horni, K. Nagel, and K. W. Axhausen, *The Multi-Agent Transport Simulation - MATSim*. London, UK: ubiquity press, 2016.

[19] D. A. Eilertsen, “Integration of plug-in electrical vehicles in the software ecosystem of smart grids,” Master’s thesis, NTNU Trondheim, Norway, 2013.

[20] J. H. Holland, “Complex adaptive systems,” *Daedalus, The MIT Press*, vol. 121 (1), pp. 17–30, 1992.

[21] M.J. Bradley & Associates LLC, “Electric Vehicle Grid Integration in the U.S., Europe, and China - Challenges and Choices for Electricity and Transportation Policy,” Concord MA, US, Tech. Rep., 2013.

[22] S. F. Harbo, “Agent based modelling and simulation of plug-in electric vehicles,” 2017, unpublished project report, Norwegian University of Science and Technology.

[23] nobil.no, “TA API-ET I BRUK,” 2017. [Online]. Available: http://info.nobil.no

[24] www.plugincars.com, “Compare Electric Cars and Plug-in Hybrids By Features, Price, Range,” 2017. [Online]. Available: http://www.plugincars.com/

[25] Norsk Elbilforening, “Elbiler i dag - Sammenlikn pris, rekkevidde og garanti p elbiler du kan kjpe i dag.” 2017. [Online]. Available: https://elbil.no/elbil-2/elbiler-idag/

[26] Statistics Norway, “Registered vehicles, 2016,” 2017. [Online]. Available: https://www.ssb.no/en/transport-og-reiseliv/statistikker/bilreg/aar/

[27] Vensim, 2017. [Online]. Available: https://vensim.com

[28] Trondheim kommune, “Lokal energiutredning 2013,” Trondheim, Norway, Tech. Rep., 2013.

Paper VIII

Impact of large-scale EV integration and fast chargers in a Norwegian LV grid

IET-RPG2018

The Journal of Engineering

The 7th International Conference on Renewable Power Generation (RPG 2018)

Impact of large-scale EV integration and fast chargers in a Norwegian LV grid

eISSN 2051-3305
Received on 29th October 2018
Accepted on 09th January 2019
E-First on 21st June 2019
doi: 10.1049/joe.2018.9318
www.ietdl.org

Martin Lillebo[1] ✉, Salman Zaferanlouei[1], Antonio Zecchino[2], Hossein Farahmand[1]

[1]Department of Electric Power Engineering, Norwegian University of Science and Technology, Norway

[2]Center for Electric Power and Energy, Technical University of Denmark, DTU Risø Campus Roskilde, Denmark

✉ *E-mail: lillebomartin@gmail.com*

Abstract: Norway has implemented economic incentives over several years to encourage a transition from conventional vehicles to electric vehicles (EVs), and now has the largest share of EVs per capita in the world. In this study, the authors explore the impacts of increasing EV penetration levels in a Norwegian distribution grid, by using real power measurements obtained from household smart meters in load flow analyses. The implications of installing a fast charger in the grid have been assessed, and an optimal location for it is proposed, aiming at minimising both grid losses and voltage deviations. Moreover, the potential for reactive power injection to reduce the voltage deviations caused by fast chargers has been investigated. Results show that the EV hosting capacity of the grid is good for a majority of the end-users, but the weakest power cable in the system will be overloaded at a 20% EV penetration level. The network tolerated an EV penetration of 50% with regard to the voltage levels at all end-users. Injecting reactive power at the location of an installed fast charger proved to significantly reduce the largest voltage deviations otherwise imposed by the charger.

1 Introduction

When driven on electricity with a low carbon footprint, most electric vehicles (EVs) cause less greenhouse gas emissions over the course of their life cycle than similar cars with internal combustion engine [1]. Viewed as an effective measure to reduce the climate impact of the transport sector, governments around the world have initiated policies to encourage consumers to drive electric. Norway's economic incentives have been particularly effective, and Norway has today the largest share of EVs per capita in the world [2].

The electrical energy required to fuel an increasingly more electrified transport sector in Norway is expected to constitute a tolerable addition to the existing consumption. The Norwegian Water Resource and Energy Directorate (NVE) estimated that Norway might host 1.5 million EVs by 2030, which will require 4 TWh of electricity annually [3]. This is less than the estimated 6.5 TWh of new annual wind power capacity currently under construction in Norway by the end of 2017, and another 17.1 TWh of expected annual production has been granted approval to be constructed, mainly in the form of wind power [4]. The power levels required to charge this fleet may, however, constitute a significant strain on the existing power grid, as the necessary power levels can be higher than the rated power capacities of the lines and transformers in the power grid. NVE calculated in 2016 that an average power increase of 5 kW consumption in all households will overload >30% of the distribution grid transformers in Norway [3]. It is, therefore, a reason to believe that a large number of EVs charging simultaneously with similar power levels may cause overloading of grid components.

Public fast chargers are being built to strengthen the range and attractiveness of electric transportation. The potentially high amounts of power they can draw will pose an additional challenge to the grid, and a well-considered placement of the fast charging point will be valuable. If the voltage level drops too far, the charger may be able to mitigate this by offering a voltage-stabilising service by injecting reactive power [5].

In this study, we investigated the state of the current grid based on the smart meter measurements. Its EV hosting capacity was then assessed by modelling various EV penetration levels, and the implications of installing a fast charger at various locations are also looked into. Finally, the potential for reactive power injection at the fast charger's location as a means to reduce expected voltage drops in the system was assessed. All analyses were conducted using the load flow package MATPOWER in the MATLAB software.

The paper is organised as follows: Section 2 details underlying theory, with an emphasis on information that is distinct for Norway. Section 3 describes the data set being used, and how further information has been derived from the original data. Section 4 contains the methodology and model description, and Section 5 presents the results. The results are discussed in Section 6, and conclusions are given in Section 7.

2 EV penetration in Norwegian distribution grids

By the end of 2017, the EV market share in the private car sector in Norway had risen to 20% and it was registered more than 135,000 EVs in the country. More than 65,000 plug-in hybrid cars come in addition to these [6, 7]. With a total passenger car fleet of 2,662,910 vehicles at the end of 2017, the share of full-electric EVs approximates to 5.4% of all passenger cars in the country [8].

2.1 Isolée Terre (IT) and Terra Neutral (TN) grids in Norway

There are two main types of distribution voltage systems in Norway: IT (French) and TN grids. Power for a common 230 V single-phase load is drawn from an IT grid by connecting it between two 230 V phases, while the TN grid provides the same voltage by connecting the load between one of its 400 V phases and a neutral line, resulting in 230 V as seen from the load. More than 70% of the Norwegian distribution grid is built as an IT-grid [9]. As IT-grids usually only allows single phase power consumption, the maximal available power is effectively limited to 7.3 kW in most cases, due to the nominal voltage of 230 V and a maximally allowed current through one phase of 32 A.

2.2 EV-charging changes the consumption profile

The power drawn to charge an EV may effectively double or triple a given household's power use during the time of charging. Fig. 1 shows an excerpt of 8 days of hourly smart meter measurements of two households. The power series with the largest peak values stems from an end-user who is confirmed to charge an EV with a 7.3 kW charger. The other series belongs to an end-user with a

This is an open access article published by the IET under the Creative Commons Attribution License (http://creativecommons.org/licenses/by/3.0/)

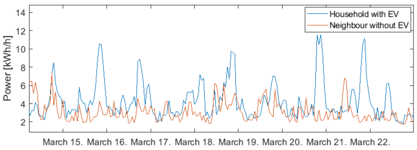

Fig. 1 *: Comparison between a household known to charge an EV regularly, and its neighbour without an EV. Each date on the x-axis begins at midnight*

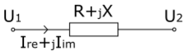

Fig. 2 *: Sample impedance*

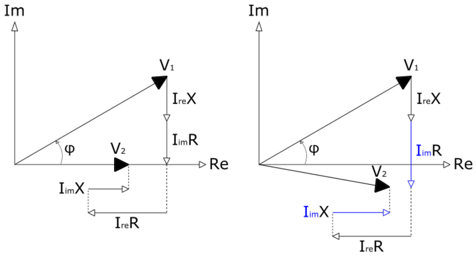

Fig. 3 *: Illustrating the difference in voltage magnitude due to an increase in the reactive current component*

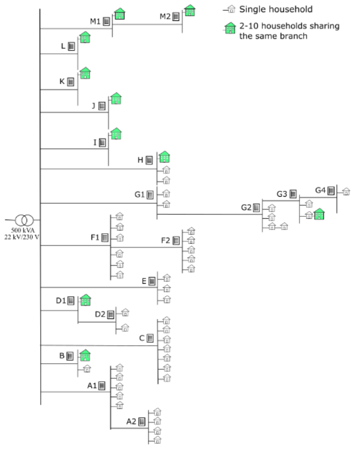

Fig. 4 *: Studied grid with its 54 consumers connected to the distribution transformer via 20 feeder cables A1–M2*

comparable base load profile, but without EV-charging. The five largest peaks all happen between 18:00 and 21:00.

2.3 Reactive power control in distribution networks

Reactive power flow in a network can be manipulated to an extent in order to stabilise the voltage level. This is explained in the following paragraphs, with the help of Fig. 2 and (1)–(3):

U_1 is the voltage at the beginning of the line, U_2 is the voltage at the end of the line, U_{drop} is the voltage drop over the impedance, and R and X are the active and reactive component of the load impedance. The difference in voltage in U_2 compared to U_1 can be outlined as follows:

$$U_2 = U_1 - U_{\text{drop}}, \tag{1}$$

$$U_2 = U_1 - (R + \mathrm{j}X)(I_{\text{re}} + \mathrm{j}I_{\text{im}}), \tag{2}$$

$$U_2 = U_1 - \mathrm{j}(I_{\text{im}}R + I_{\text{re}}X) - I_{\text{re}}R + I_{\text{im}}X\,. \tag{3}$$

With a lagging power factor of 0.98, giving us an angle of 11.5°, Q amounts to 20% of S. If the angle is leading, the absolute value of Q remains the same while the sign will be negative instead of positive. Reactive power is now injected to the system by the load, instead of delivered to the load from the system. This increase in Q will also increase I_{im}, which as seen in (3) will reduce the voltage drop due to the resulting voltage V_2 having a larger absolute value. This is illustrated in Fig. 3. The deliberate injection of Q to help stabilise voltage is called reactive power control and was in this study tested as a way to help increase the grid voltage stability. A side effect is larger transmission losses due to the increased total currents in the system. The effectiveness of reactive power control is highly dependent on the line impedances in the distribution network, both in terms of absolute values and the R/X ratio [10].

3 Data set

A single line diagram depicting the studied IT-grid can be seen in Fig. 4. It consists of the following main parts:

- A 500 kVA distribution transformer.
- 20 distribution feeder lines, A1-M2, branching out from the transformer.
- 54 end-user buses and their respective cables.

In reality, there are 95 end-users present in the system, but some of them live in various forms of shared housing such as row houses or apartment blocks, thus sharing the same connection line. These larger nodes have been aggregated into single loads, and are marked with a larger, colourised symbol in the single line diagram. After this aggregation, the total number of end-users is 54.

The following data set was provided by the distribution system operator (DSO):

- Hourly active power flow measurements for all end-users in the system for the year of 2012, which is considered as a 'zero EV' base case.
- All interconnections in the system and the types of cables being used.
- Smart meter measurements for a neighbourhood in 2016, in which one household regularly charges an EV.

The following information was derived from this data:

- Hourly reactive power flow based on the DSO's assumed power factor of 0.98.
- MVA ratings for all cables.
- The single line diagram is shown in Fig. 4.
- An empirical EV charging profile for a whole year.

It was assumed zero EV to be present in the grid when the data was collected in 2012. This is supported by the fact that the municipality as a whole had only 13 registered EVs dispersed over its 38,075 inhabitants that year [11, 12].

The external power grid was modelled as an infinite bus connected to the main feeder, acting as the generator in the system. The impedances and MVA rating of the transformer were assigned to a virtual cable connected in series between the transformer and the main feeder. This infinite bus acted as a slack bus with a constant voltage of 1 p.u. All end-users in the system were modelled as load buses. Finally, the bus bars connecting the transformer's feeder lines to the end-user branches were implemented in the model as load buses with zero active and reactive power consumption. The mentioned bus bars are denoted with letters A1–M2 in the single line diagram in Fig. 4.

This is an open access article published by the IET under the Creative Commons Attribution License
(http://creativecommons.org/licenses/by/3.0/)

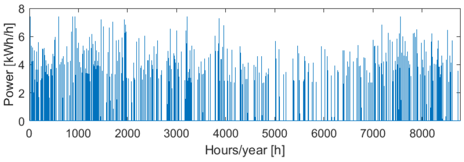

Fig. 5 *: Proposed EV charging profile*

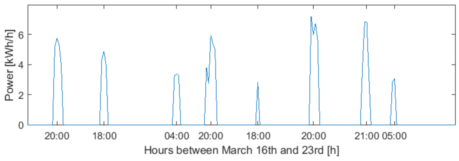

Fig. 6 *: Excerpt of eight consecutive days from the charging profile depicted in Fig. 5, with the power spikes marked with their respective time of day*

Before modelling the network, an EV charging pattern had to be acquired. As it was desired to run load flow analyses for every hour of the year and due to this study aiming at using actual measured EV charging patterns instead of an assumed charging pattern, it was desirable to acquire one or more data sets of measured residential EV charging profiles spanning the same length. Since this was not to be found, an EV charging profile has been derived from the smart meter readings from a household confirmed to regularly own and charge an EV with a 7.3 kW charger, by attempting to subtract the base household consumption from the total readings. This was done by constructing a sample household base load profile and subtracting this from the consumption profile seen in the household known to charge an EV.

NVE assumes an average consumption of 2667 kWh per EV per year in Norway [3]. In this study, it is assumed that an EV adds an extra 3000 kWh to the household consumption, which gives an average daily consumption of 8.22 kWh/day. A comparative base load has therefore been constructed by making an average load profile from the surrounding neighbours, which is 3000 kWh smaller than the EV-owning household is.

After subtracting the constructed average base load from the EV-owning household, small oscillations around the *x*-axis could be seen. This was interpreted as residual noise left over from the subtraction. To remove it, all values <2.7 kW were set to zero. This eliminated the noise left over from the subtraction with minimal effect on the total area, as approximately half of the values were below zero. Finally, all peaks >7.3 kW were clipped down to 7.3 kW, as this power level is considered the maximal household charging rate in a Norwegian IT-grid. Remaining values higher than this level is therefore considered residuals left over from the base household consumption. The resulting charging profile is shown in Fig. 5, and an excerpt of this graph is shown in Fig. 6, displaying eight days of energy consumption.

The area below the curve of the charging profile equals 3024 kWh. This is close to the expected yearly energy consumption for an EV, and it is therefore assumed that the consumption shown in the graph mainly stems from EV charging.

4 Methodology and model description

8784 individual load flow solutions were conducted – one for each hour of the (leap) year. By doing this, the grid could be remodelled as it was in its actual state in 2012, based on the load flow results. This provided a basis of comparison when the theoretical EV charging profiles were subsequently added on top of the actual measured values. The load flow results were found by using MATPOWER [13]. Due to the nature of load flow analyses, the power consumption in the system was assumed to be balanced.

4.1 Assigning EV owners to the system

Ten different EV penetrations from 10 to 100% with an incremental increase of 10% between each case were modelled. The peak voltage deviation and peak load ratio levels at all 20 feeder connections will be presented, along with a summary of any end-users experiencing a violation of the 10% voltage deviation limit or overloading with respect to the nominal power rating. A voltage deviation of 10% is considered as the lower limit for distribution systems according to the European Standard EN 50160.

The EV charging profile was added on top of the existing household consumption at various buses in order to model different EV-penetration levels. 100% EV penetration was in this study defined as equal to one EV per household. The buses containing aggregations of multiple household consumption profiles were set to take in an equivalent number of EV loads.

To construct the different EV penetration cases in a systematic order, the charging profiles were added in accordance with a delegation array that keeps track of where the load profiles should be added in all cases. In the 10% EV penetration case, the first ten locations in the delegation array were assigned their respective EV charging load. For 20% EV penetration, the first 19 locations in the delegation array were assigned their respective load etc. This ensured a cumulative development from one EV penetration percentage to another. The delegation array was made using a MATLABs random number generator *randperm*.

It is desirable to avoid adding identical EV charging patterns to all the end-users, as that would not happen in a realistic scenario. For each new end-user being assigned an EV charging load in addition to its base household consumption, the charging profile was, therefore, shifted forward in time before adding it to the respective end-user. To preserve a natural daily use pattern, the profile was only shifted a single hour back and forth in relation to its original pattern, before it was shifted 24 h forward in time for the next end-user.

4.2 Adding a fast charger to the model

To investigate the possible interaction between a fast charger and existing EV-loads, the system model developed for the 30% EV penetration was to be used as the base model. The fast charger was modelled as a constant 22 kVA load. This provides a consistent worst-case scenario for the fast charger part of this paper's data analysis.

The fast charger was modelled in three different ways:

- Adding the fast charger load to the existing system without changing any other variables.
- Assuming the fast charger replaces the five EV loads closest to its location.
- Repeating the last case while also examining the effects of 15 different power factors at each location.

4.3 Including reactive power control

While keeping the assumption that nearby EV-loads are substituted by the fast charger, each potential charger location is now also tested for 15 different power factors in order to see the potential effects on the voltage levels at its location. The power factor was varied from 0.98 lagging to 0.74 leading, with an increment of 0.02 between each. 0.98 is assumed by the local DSO to be the actual power factor observed in their grid today. A power factor of 0.74 corresponds to a −42.3° angle between the voltage and current phasors. The resulting reactive power injection will, in that case, be approximately equal to the active power consumption and is therefore considered the minimally acceptable power factor. Since the apparent power is held constant, a power factor of 0.74 will represent an active power consumption of 16.3 kW and reactive power consumption of −14.8 kVAR.

This is an open access article published by the IET under the Creative Commons Attribution License
(http://creativecommons.org/licenses/by/3.0/)

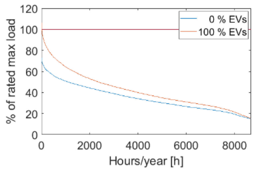

Fig. 7 : *Duration curve for the transformer loading for the base case model and for an EV penetration of 100%*

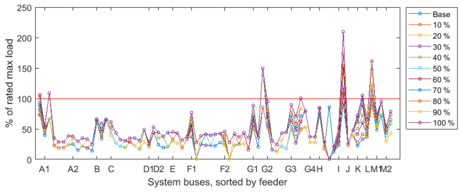

Fig. 8 : *Largest loading reached for all cables in the system for all ten EV penetration cases, expressed in per cent of nominal capacity*

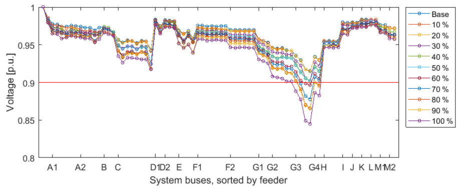

Fig. 9 : *Largest voltage deviations in p.u. reached for all cables in the system for all ten EV penetration cases*

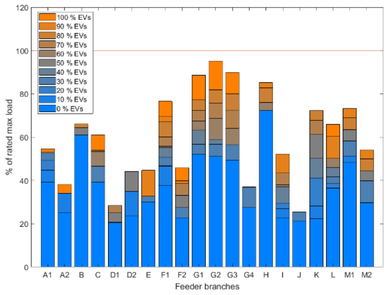

Fig. 10 : *Largest loading reached for the 20 feeder cables in the system for all ten EV penetration cases*

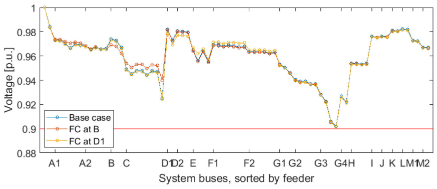

Fig. 11 : *Resulting worst voltage deviations throughout the year from placing a fast charger at location 'B' and 'D1'*

4.4 Finding an optimal fast charger location

Once all necessary data on how a base EV penetration and a fast charger placement at the potential locations would affect the voltage stability and power flows throughout the system was found, we weighed these voltage deviation levels and total power loss in the system against each other with a weighed-loss-voltage-factor (WLVF) as shown in (4). By doing this, a location for the fast charger that minimises the overall voltage drops and system power losses can be chosen

$$\mathrm{WLVF}_i = w_1 * V_{\mathrm{dev}\_i} + w_2 * P_{\mathrm{loss}\_i}, \tag{4}$$

$$w_1 + w_2 = 1. \tag{5}$$

P_{loss} is the per cent-wise increase in total system power losses when the feeder connection (FC) is placed at location i, compared to the base case. V_{dev} is the average voltage deviation observed at all 20 FCs when an FC is placed at location i, in comparison with the base case. The WLVF can then be computed with the weighing factors w1 and w2 varying between 1.0 and 0.0 in order to determine a suitable location.

5 Results and discussion

5.1 Unmodified base case and EV hosting capacity

A duration curve of the transformer loading throughout the year is shown in Fig. 7, displaying both the 0 and 100% EV-penetration case. There were no violations of the voltage or loading limits for any cables in the grid for the unmodified base case, and 12 h of overloaded hours for the 100% case.

5.2 EV hosting capacity

10 EV use cases were modelled – one for each cumulative 10% EV penetration. Fig. 8 displays the most extreme hour for the whole year with regard to power consumption for each case, expressed in terms of the respective power cables' nominal rating for all buses in the system. Fig. 9 displays the same results, with regard to the largest voltage level deviation at each bus connection instead of the cable loading. The end-users are sorted by the feeder connection buses to which they are connected, denoted with the letter codes on the x-axis.

An estimated EV penetration of 50% was possible before the first voltage deviation incident occurred, while the weakest distribution lines experienced overloading at an EV penetration of 20%. Fig. 10 depicts the same results as Fig. 8, but only for the feeder cables branching out from the transformer and not the cables connecting the end-users to them. It emphasises that neither of the 20 feeder cables was overloaded at any time during any of the ten EV penetration cases – only the smaller cables connecting the end-users to the feeder connections were. This indicates that in a case where the same EV charging loads had been wired directly to the feeders, the system as a whole could have managed the extra loading.

The distribution transformer experienced 12 h of overloading above its nominal power capacity during the 100% EV-penetration case, but these hours occurred during the coldest two days of the year. The cold temperature cools the transformer, and NVE assumes Norwegian distribution transformers to tolerate up to 120% of their nominal loading capacity during these conditions [3].

5.3 Fast charger implementation

Fig. 11 displays the worst voltage deviation for all buses in the system with the fast charger placed at the two locations where it caused the least and largest amount of voltage deviations in the system. The improvement is due to the assumption of the nearest 5 EVs to charge at the fast charger's location instead of at their respective household, thus offsetting the weaker end-user cables.

5.4 Reactive power compensation

By calculating the WLVF from (4) for all 20 investigated fast charger locations, 'G4' returned the worst results. Fig. 12 displays the voltage deviations in the system for three cases: the 30% EV-penetration case as the base case, a fast charger located at 'G4'

This is an open access article published by the IET under the Creative Commons Attribution License
(http://creativecommons.org/licenses/by/3.0/)

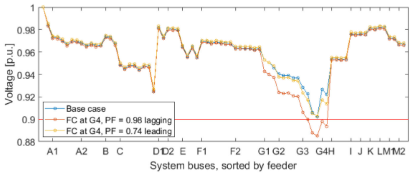

Fig. 12 : *Locating the fast charger at G4 gave the largest voltage deviations in the network (red line), but could be negated by injecting reactive power (yellow line)*

with a power factor of 0.98 lagging, and the same case but with the charger having a power factor of 0.74 leading, thus effectively injecting reactive power. In the base case and the case with power factor (PF) = 0.74, the voltage levels in the system remained within bounds, while it was 0.03 p.u. below the base case when the power factor was 0.98.

Due to the fast charger being connected directly to the feeder line G4 and the assumption of it replacing the five nearest EV-loads, there were no additional violations of the nominal permitted loading. Although still the least beneficial location for such a load, Fig. 12 indicates that reactive power injection can help support the voltage in weaker parts of the grid when necessary. For instance, new EV loads may be connected to an already stressed location, given they were equipped with the ability to inject reactive power when needed.

5.5 Limitations of the study and sources of error

All EV charging profiles used in this study stems from a measurement series of a single household for a single year. This measurement included the base load of the household, which had to be subtracted. One or more directly measured EV charging profiles over the course of a year would be superior to the one derived in this study, as no residual household consumption measurements would interfere the dataset, and no real charging data would have been lost as part of the subtraction process. Additionally, a larger sample could reduce the impact of potential outliers in the individual data set.

As described in Section 4.1, the simultaneity factor, which gave the maximum rate at which the EV-loads drew their semi-daily charging peak of 7.3 kW at the exact same time, was significantly altered by shifting the load profile back and forth between each assignment to a new household. This reduced the simultaneity factor from 100 to 33%. In a report in which NVE explored different EV-behaviour scenarios, a simultaneity factor of 70% was used as a worst-case scenario [3], while the 2017 survey by the Norwegian EV Association estimated a max simultaneity factor of 22% among its respondents [7].

6 Conclusion

This study explored the effects of increasing EV penetration levels in a Norwegian distribution grid, relying on real power measurements obtained from household smart meters and realistic load flow analyses with increasing EV penetration levels. The impact of a new fast charger in the grid has been assessed, and the optimal location for it has been proposed, minimising losses and voltage deviations. Finally, the potential for reactive power injection to reduce the voltage deviations caused by it has been investigated and discussed.

The EV hosting capacity was large, as all but six end-users stayed above the minimum voltage limit and below the nominal cable power rating at all hours of the year for the 100% EV-penetration case. The main transformer was overloaded for a 12 h at that point, but only during the time of year where it is expected to tolerate the load due to the low outside temperature. When restricting EV penetration to comply with the limitations of all end-users in the system, the distribution grid can tolerate a 50% EV penetration regarding voltage, and 20% EV penetration with regard to the rated power of the weakest cable.

Implementing a fast charger in the grid with a standard power factor of 0.98 lagging caused significant voltage deviations at several locations, the worst of which reached an extra voltage deviation close to 0.03 p.u. By assuming that the nearest 5 EV charging loads were replaced by the fast charger, the largest voltage deviations in the network were significantly reduced. Injecting reactive power at the location of the fast charger, therefore, gave significant results. A power factor of 0.74 leading made it possible to implement the fast charger in the weakest part of the grid without violating the minimum voltage level requirement of 0.9 p.u. By utilising the voltage stabilising properties of injecting reactive power, larger loads such as a fast charger or a large EV household charger might be installed in weaker parts of a power grid than would otherwise be possible.

7 References

[1] Ellingsen, L.A.-W., Singh, B., Strømman, A.H.: 'The size and range effect: lifecycle greenhouse gas emissions of electric vehicles', 2016

[2] IEA: '*Global EV outloook*' (2017)

[3] NVE – Norwegian Water Resource and Energy Directorate: 'Hva betyr elbiler for strømnettet?', 2016

[4] Norwegian Water Resource and Energy Directorate: 'Ny kraft: Endelige tillatelser og utbygging – 3. kvartal', 2017

[5] Knezovic, K.: 'Phase-wise enhanced voltage support from electric vehicles in a Danish low-voltage distribution grid', 2016

[6] Norwegian Electric Vehicle Association: 'Norwegian EV market', 2017. Available at https://elbil.no/english/norwegian-ev-market/, accessed 5 December 2017

[7] Norwegian Electric Vehicle Association, Elbilisten 2017, 2017

[8] Norwegian Public Roads Administration: 'Kjøretøybestanden i Norge', 2017. Available at www.vegvesen.no/_attachment/1899542/binary/118736/6?fast_title=Kj%C3%25, accessed 1 January 2017

[9] Hansen, E.H.: 'Elektroinstallasjoner', Classica, 2010

[10] Zecchino, A., Marinelli, A.: 'Analytical assessment of voltage support via reactive power from new electric vehicles supply equipment in radial distribution grids with voltage-dependent loads', *Int. J. Electr. Power Energy Syst.*, 2018, **97**, pp. 17–27

[11] Kommuneprofilen: 'Kommuneprofilen – personbiler etter type drivstoff', Kommuneprofilen, 2017. Available at http://www.kommuneprofilen.no/Profil/Samferdsel/Din/Region/samf_drivstoff_region.aspx, accessed 12 December 2017

[12] Kommuneprofilen: 'Kommuneprofilen – befolkningsstatistikk etter kommune', 2017. Available at www.kommuneprofilen.no/profil/Kommunefakta/Befol/kning_kommune.aspx, accessed 5 December 2017

[13] Zimmermann, R.D., Murillo-Sánchez, C.E., Thomas, R.J.: 'MATPOWER: steady-state operations, planning and analysis tools for power systems research and education', *IEEE Trans. Power Syst.*, 2011

This is an open access article published by the IET under the Creative Commons Attribution License
(http://creativecommons.org/licenses/by/3.0/)

Paper IX

Value Comparison of EV and House Batteries at End-user Level under Different Grid Tariffs

ENERGYCON2018

© 2018 IEEE. Personal use of this material is permitted. Permission from IEEE must be obtained for all other uses, in any current or future media, including reprinting/republishing this material for advertising or promotional purposes, creating new collective works, for resale or redistribution to servers or lists, or reuse of any copyrighted component of this work in other works.

Value Comparison of EV and House Batteries at End-user Level under Different Grid Tariffs

Sigurd Bjarghov, Magnus Korpås, Salman Zaferanlouei
Department of Electric Power Engineering
Norwegian University of Science and Technology
Trondheim, Norway
Email: {sigurd.bjarghov, magnus.korpas, salman.zaf}@ntnu.no

***Abstract*—With the introduction of real-time price signals through smart meters, the electric vehicle (EV) battery can become a powerful tool. Its relatively high charging power and capacity makes it attractive for both cost minimization and self-balancing. Focusing in particular on comparing EV and home batteries, the objective of this paper is to investigate the economic potential of utilizing PV and batteries at an end-user level. In simulations based on data from a single residence in Trondheim, Norway, a dynamic programming algorithm is used to minimize the electricity costs under four different grid tariff structures. This method guarantees to find the global optimum. Leveraging the variations in spot price and hourly grid tariff costs, the simulation results indicate reduced annual electricity cost. When utilizing an EV battery together with rooftop PV, the cost is reduced by 12.0 - 19.2 %, depending on the grid tariff structure, whereas a home battery installation together with PV reduces the cost by 8.9 - 14.4 %.**

***Keywords*—Battery optimization, Dynamic programming, Electric vehicle, Energy storage optimization, Photovoltaic, Optimal charging, Self-balancing, Smart grid**

NOMENCLATURE

η_{ch}	Charging efficiency of battery.
η_{dis}	Discharging efficiency of battery.
C_{el}	Total customer cost of electricity [€].
C_{low}	Energy price above P_{sub} during low load hours [€ct/kWh].
C_{peak}	(€ct/kWh) bought above P_{sub} kW during peak load hours [kWh].
$E_{bat,min}$, $E_{bat,max}$	Minimum and maximum energy capacity of battery [kWh].
E_{bat}	Energy capacity of battery [kWh].
E_{ddp}	Energy spent by EV for daily driving purpose [kWh].
F	Monthly fixed cost [€].
$P_{bat,max}, P_{bat,min}$	Maximum and minimum charge rate of battery [kW].
P_{bat}	Charging/discharging power of battery [kW].
P_{grid}	Power supplied by or delivered to the grid [kWh/h].
P_{load}	Residence load demand [kWh/h].
P_{PV}	Photovoltaic power production [kWh/h].
P_{sub}	Subscribed power [kW].
SOC	Battery state of charge [%].
SOC_{arr}	State of charge at EV arrival [%].
SOC_{dep}	State of charge at EV departure [%].
SOC_{max}, SOC_{min}	Maximum and minimum battery state of charge [%].
t	Time index [h].
$T, \Delta t$	Total number of discrete time intervals and time step.
$y(t)$, $z(t)$	Energy consumed above P_{sub} kW during low load hours and peak load hours [kWh].

I. INTRODUCTION

In June 2017, the climate and environment department of the Norwegian government published a climate law which states that Norwegian annual greenhouse gas emissions are to be reduced by 40 % of 1990 level by 2030 [1]. Road transport is the third largest emission sector in Norway, and is thus a focal point for the government's plan for emission reduction. The result has been a strong political will to increase EV adoption in Norway. Through tax exemption and other economical advantages, Norway has developed the largest EV share per habitant in the world, which complements the 96 % hydro power share in the electricity mix [2] [3]. This political will has resulted in more than 150 000 EVs on Norwegian roads as of May 2017, and do now represent 35 % of nationwide new car sales [4].

With the ongoing rollout of smart meters in Norway, new pricing structures for grid utility tariffs can be utilized to promote efficient use of the grid. Use of renewable energy is vital to this efficiency increase strategy, but also comes with new challenges. Meanwhile, PV and battery prices are plummeting [2], [5], which could be a driver for higher penetration of distributed energy storage. A price reduction of this magnitude raises the question once again whether rooftop PV together with battery on an end-user level can be economically profitable for the customer.

This paper investigates the interaction between PV and battery on end-user level, and compares the use of a dedicated home battery and an EV battery. The goal is to highlight to which extent the powerful EV batteries together with PV can be economically profitable. A dynamic programming optimization algorithm has been developed to calculate annual electricity costs for a residence in Trondheim. In addition, the simulations are performed with different grid tariff structures in order to determine which structures are suitable for more efficient use of the distribution grid. The economic operation of home battery with PV is studied in detail in [6]–[8]. This

978-1-5386-3669-5/18/$31.00 ©2018 IEEE

paper extends the study in [6] and compares an EV battery with a home battery, in order to show the economic potential of both installations.

Note that although the two batteries that are being compared differ greatly in size and performance, the basic idea of this paper is to see to which extent an EV battery solution can compete with a dedicated home battery solution. Thus, two batteries that exist on the market today have been chosen in this paper. Note that all prices were originally calculated in NOK, and have been converted to euro with an exchange rate of 9.5838 NOK per euro which was the exchange rate during the writing of this paper.

The paper is structured as follows. Section II describes the system model, whereas section III describes the dynamic programming optimization algorithm along with the simulated grid tariffs. Section IV shows the input data used in the model, and results and discussions are presented in section V. Conclusion and future work is then presented in section VI.

II. END-USER SYSTEM MODEL

A. *Residence model*

The power balance is calculated as seen in Fig. 1 and Eq. 1, and is considered loss free. The system model is deterministic, meaning that the load and PV production is known at all times. Therefore, P_{grid} is a function of P_{bat}.

$$P_{grid} = P_{load} + P_{bat} - P_{PV} \tag{1}$$

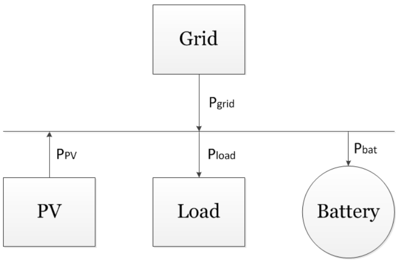

Fig. 1: Model of the residence. Positive power flow direction is indicated by arrows.

The grid is stiff, meaning that it has the balancing function, supplying and receiving power as a result of the balance equation. PV is modelled as in [9] based on [10].

III. DYNAMIC PROGRAMMING MODEL

A. *Optimal battery operation*

In order to assess the economic potential of EV battery and PV utilization, an optimization algorithm is used. By utilizing dynamic programming, the algorithm calculates the price for every single charge and discharge possibility, when the spot price, grid tariff, load and PV production is known.

The algorithm is generic, and can therefore be utilized for either a house battery or an EV battery. In the house battery setup, the optimization is run for T = 8760 periods. For the EV battery setup, the total time interval per optimization is T = 16 discrete time steps where Δt is one hour, due to the resolution of the load, PV and pricing data. After every 16 hour optimization, normal load balance is assumed. For weekends, the optimization is being run from Friday at 4 pm to Monday at 8 am. EV availability is shown in Tab. I.

TABLE I: EV availability

Availability	Weekdays	Weekend
Available	4 pm - 8 am	Always
Unavailable	8 am - 4 pm	Never

The function f is a description of the optimization target. The function is given by Eq. 2. $f(P_{bat})$ is then minimized

$$f(P_{bat}) = C_{el}P_{grid} \tag{2}$$

where P_{grid} is defined in Eq. 1.

Therefrom, minimize $f(P_{bat})$ as in Eq. 3.

$$\begin{aligned} SOC(t+1) &\leq SOC_{max} \\ SOC(t+1) &\geq SOC_{min} \\ P_{bat}(t) &\leq P_{bat,max} \\ P_{bat}(t) &\geq -P_{bat,max} \\ E_{bat}(t+1) &= E_{bat}(t) + \eta_{bat}P_{bat}(t)\Delta t \\ SOC(t+1) &= \frac{E_{bat(t+1)}}{E_{bat,max}} \end{aligned} \tag{3}$$

Note that

$$\eta_{bat} = \eta_{ch}, P_{bat}(t) \geq 0$$

$$\eta_{bat} = \eta_{dis}, P_{bat}(t) < 0$$

For $P_{grid} > 0$, both grid tariffs and energy price will be paid, both of which has taxes. For $P_{grid} < 0$, only the spot price will be received. As equation 1 shows, P_{grid} consists of three variables, of which two are known; P_{load} and P_{PV}. Thus, P_{bat} is decided for every hour to minimize the cost from 1 to T. The result are grids of nodes, where different possible SOCs for every time step in T are calculated. The goal is to find the path of SOCs that result in the lowest possible price for the given input. Fig. 2 illustrates how the dynamic programming with N time steps and M levels of SOC are calculated. Note that because the battery's maximum charging power $P_{bat,max}$, not all SOCs are reachable.

The EV battery state of charge at departure is set to SOC_{dep} = 90 % at 8 am on weekdays in order to assure the owner (almost) full range of the EV. On weekdays, E_{ddp} = 7 kWh are spent for driving [11], resulting in SOC_{arr} to be SOC_{arr} = SOC_{dep} - $\frac{E_{ddp}100\%}{E_{bat,max}}$ = 81 %.

B. *Grid tariffs*

1) Energy based tariff: The energy based tariff is the one broadly being used in Norway today, and is perhaps the simplest way of billing the customer. However, it creates no incentive for grid-friendly use. The grid tariff consists of an annual fixed cost and a variable cost which is based on kWh consumption.

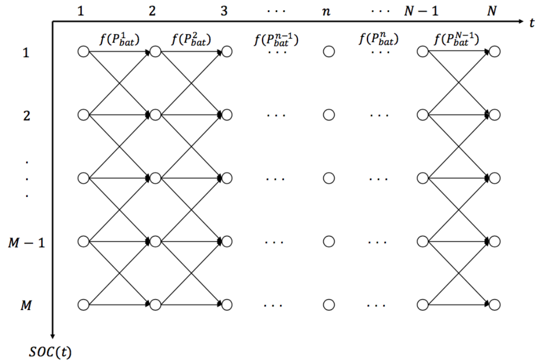

Fig. 2: Illustration of dynamic programming with N time steps and M levels of SOC.

2) Time-of-use tariff: While still being consumption based, the time-of-use tariff utilized daily load profiles to create time zones where grid use is more expensive. The tariff distinguishes between weekend and weekdays, as well as night, morning, afternoon and evening pricing. The prices are shown in Tab. II. A mid-level price is set for normal hours, which is doubled for peak load hours and reduced to half during low load hours.

TABLE II: Overview of different price zones with the time-of-use tariff

Day		**Hours**	**Price**
Weekdays	Night	23-05	1.26 €ct / kWh
	Standard	5-7, 10-18, 21-23	2.52 €ct / kWh
	Peak	7-10, 18-21	5.05 €ct / kWh
Weekend	Standard	00-24	2.52 €ct / kWh

3) Power based tariff: The power based tariff increases the price per kWh per kW used by the customer. This gives incentive for leveling the residence load as much as possible. The calculated price for the power tariff was 2.44 €ct/kWh/kW. Thus, when using less than one kW, the price per kWh is 2.44 €ct/kWh. Between 1-2 kW, it is 4.88 €ct/kWh etc.

4) Subscription based tariff: The subscription based tariff is a tariff consisting of two parts. The first part is a subscription fee, where a customer chooses a certain amount of kilowatts he wants to subscribe to, and pays a fixed monthly price for each subscribed kilowatt. The second part is an energy based cost, where all energy used at a power above the subscribed power has a certain price. This price is split into two prices, one for low and one for peak load hours. Peak load hours are 7-10 am and 6-9 pm, while the rest are low. The fixed price is as following 4:

$$F(x) = C_{Fixed} + P_{sub}C_{Power} \tag{4}$$

where P_{sub} is the subscribed power. The total annual price for this grid tariff is as described in equation 5.

$$C_{year}(P_{sub}, t) = 12F(P_{sub}) + C_{low}\sum_{t=1}^{T} y(t) + C_{peak}\sum_{t=1}^{T} z(t) \tag{5}$$

To achieve equal prices under this structure compared to the structure that exists today, the prices were calculated to be the following. C_{Fixed} = 9.4 €, C_{Power} = 9.4 €, C_{low} = 4.72 €ct/kWh and C_{peak} = 9.43 €ct/kWh.

IV. DATA INPUT

A. Load data

The load data are taken from a large residence in Trondheim. The data resolution is hourly, and is rounded to the closest 600 watts due to privacy reasons. The load heatmap is shown in Fig. 3, and shows the average electricity consumption per hour for each weekday for all of 2015. It should be mentioned that due to high amount of space heating, electricity consumption is much higher during winter.

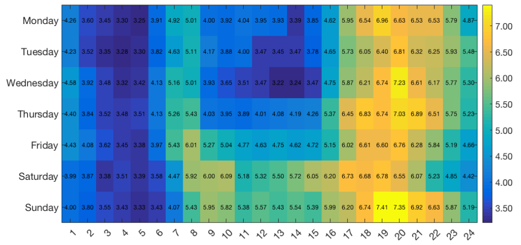

	1	2	3	4	5	6	7	8	9	10	11	12	13	14	15	16	17	18	19	20	21	22	23	24
Monday	4.26	3.60	3.45	3.30	3.25	3.91	4.92	5.01	4.00	3.92	4.04	3.95	3.93	3.39	3.85	4.62	5.95	6.54	6.96	6.63	6.53	6.53	5.79	4.87
Tuesday	4.23	3.52	3.35	3.28	3.30	3.82	4.63	5.11	4.17	3.88	4.00	3.47	3.45	3.47	3.78	4.65	5.73	6.05	6.40	6.81	6.32	6.25	5.93	5.48
Wednesday	4.58	3.92	3.48	3.32	3.42	4.13	5.16	5.01	3.93	3.65	3.51	3.47	3.22	3.24	3.47	4.75	5.87	6.21	6.74	7.23	6.61	6.17	5.77	5.30
Thursday	4.40	3.84	3.52	3.48	3.51	4.13	5.26	5.43	4.03	3.95	3.89	4.01	4.08	4.19	4.26	5.37	6.45	6.83	6.74	7.03	6.89	6.51	5.75	5.23
Friday	4.43	4.08	3.62	3.45	3.38	3.97	5.43	6.01	5.27	5.04	4.77	4.63	4.75	4.62	4.72	5.15	6.02	6.61	6.60	6.76	6.28	5.84	5.19	4.66
Saturday	3.99	3.87	3.38	3.51	3.39	3.58	4.47	5.92	6.00	6.09	5.18	5.32	5.50	5.72	6.05	6.20	6.73	6.68	6.78	6.55	6.07	5.23	4.85	4.42
Sunday	4.00	3.80	3.55	3.43	3.33	3.43	4.07	5.43	5.95	5.82	5.38	5.57	5.43	5.54	5.39	5.99	6.20	6.74	7.41	7.35	6.92	6.63	5.87	5.19

Fig. 3: Heat map of the 2015 household load. The matrix shows the average kW consumption for the specific hour at the specific weekday.

B. Battery specifications

Two batteries are used for these simulations. The most important one is an EV battery. The second one is a house battery for the comparison between the two. Their specifications are given in Tab. III. While most EVs in Norway as of 2017 are fairly small, bigger cars with bigger batteries are about to be released on the market. An EV battery with $E_{bat,max}$ = 80 kWh is chosen. The maximum power of an EV is normally above 100 kW, but a max limit of $P_{bat,max}$ 15 kW to reduce losses and keep inverter costs down is set. For the house battery, data based on the Tesla Powerwall will be utilized [12]. Note that the minimum and maximum limits of the batteries are set to 0 and 100 %, although it could be argued that a minimum limit of 5 % should be set due to lifetime concerns. In this paper this is not taken into account as the goal of this paper is to do an economic potential analysis, and technical details are secondary issues. It could also be argued that this is already done by the manufacturer to increase the amount of equivalent cycles the battery can perform before its end of life.

TABLE III: Battery specifications

	$P_{bat,max}$	E_{cap}	SOC_{max}	SOC_{min}	η_{dis}	η_{ch}
House Battery	7 kW	13.5 kWh	100 %	0 %	0.95	0.95
EV Battery	15 kW	80 kWh	100 %	0 %	0.95	0.95

C. PV production data

Irradiation and temperature data are taken from LMT, Landbruksmeteorologisk Tjeneste [13]. LMT is a governmental funded project operated by NIBIO (Norsk Institutt for Bioøkonomi) for measuring and publishing weather data from all over Norway. By using a PV production model based on [10], PV production data is created with MATLAB. To calculate the exact values, the PV panel Sanyo HIT-240HDE4 is used. The specification sheet [14] gives a $NOCT$ of 44 °C and an α_T of -0.3 %/°C. Nominal installed power P_{nom} is set to 7 kW. With 190 W/m^2, the installation is 36.84 m^2. The resulting produced power is shown in Fig. 4.

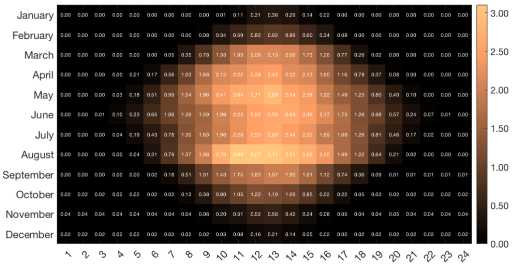

Fig. 4: Heat map of the 2015 PV production using the realistic model. The matrix average kWh production per hour for the different months.

D. Energy prices

Complete spot price data were downloaded from Nord Pool Spot's database [15], and has a one hour resolution. Fig. 5 shows the prices downloaded from Nord Pool Spot in heatmap. Tab. IV shows some key values from the figure.

TABLE IV: Average, minimum and maximum prices in 2015. All prices are presented in €ct per kWh.

Year	Mean	Variance	Min	Max
2015	1.98	0.049	0.11	6.14

As Fig. 5 shows, the prices are low at night, then rise in the morning due to higher demand. It has to be noted that the spot price for 2015 is historically low, and the lowest since 2005.

A general spot price contract from a local retailer is chosen, which contains a monthly cost, plus a small addition to the spot price to assure company revenues. The monthly cost is C_{fixed} = 3.92 €/month. In addition, a 0.645 €ct/kWh is added on every kWh bought from the spot market, which consists of a 0.26 €ct revenue margin and a 0.38 €ct green certificate cost. A 25 % tax (VAT) is added on all these costs.

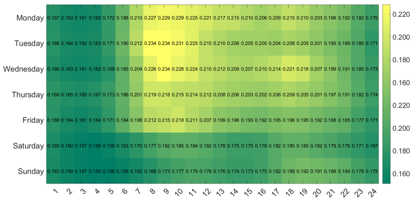

Fig. 5: Heat map of the 2015 spot price. The matrix shows the spot price in NOK/kWh for the specific hour at the specific weekday. (1€= 9.58 NOK)

E. Grid tariffs

Grid tariffs in Norway make up about one third of the electricity bill of a household customer. Today it is energy based and consists of a yearly fixed price and a fee for every kWh consumed as described in section III. The prices are regulated by NVE (governmental regulator). The load data used are as mentioned from Trondheim, which belongs to the distribution grid under the jurisdiction of Trønderenergi Nett AS. Their grid tariffs for 2015 are shown in Tab. V. The remaining three grid tariffs have price levels constructed to give the DSO the same income as with the energy based tariff before an optimization is run.

TABLE V: Overview of total grid tariff prices including consumer tax and VAT.

Year	Fixed annual cost	Variable cost	Consumer tax	VAT
2015	139.8 €	2.29 €ct/kWh	1.29 €ct/kWh	25 %

V. RESULTS AND DISCUSSION

A. Total customer cost

The results shown in Tab. VI and Fig. 6 the total annual customer costs. This includes grid tariffs, taxes, fees and energy prices. In other words, the actual costs that the customer has to pay. Fig. 6 shows the relative cost of each scenario, again compared to the basecase. Note that all scenarios with an EV battery, the cost of energy spent driving the EV was subtracted from the original sum, to avoid the results including the cost of daily transport. The values used were the average driving distance of a Norwegian car which was approximately 35 km/day. With an average efficiency of 0.2 kWh/km, this accumulates to 7.0 kWh/day. All numbers are taken from [11].

Even though there are some variations in the annual cost, there overall clear tendency shown in the results, is that the EV and PV battery solution is the highest saving solution, with savings from 3 to 7 hundred €(12.0-19.2 %) per year depending on tariff structure. The house battery and PV installations saved 8.9-14.4 %, when PV is included. The same tendency is observed when PV is not included - the EV battery is capable of saving quite a bit, whereas the house battery is only able to save a few percent.

TABLE VI: Total costs for customer for different scenarios and tariff structures. All numbers are given in €.

Structure	Basecase	Basecase incl. PV	House battery	EV battery	House battery incl. PV	EV battery incl. PV
Photo-voltaic	-	X	-	-	X	X
EV Battery	-	-	-	X	-	X
House Battery	-	-	X	-	X	-
Energy Based	3 733	3 319	3 717	3 538	3 311	3 167
Power Based	3 704	3 295	3 623	3 478	3 213	2 099
Time-of-use	3 697	3 264	3 610	3 390	3 186	2 988
Subscr. based	3 698	3 394	3 665	3 509	3 363	3 255

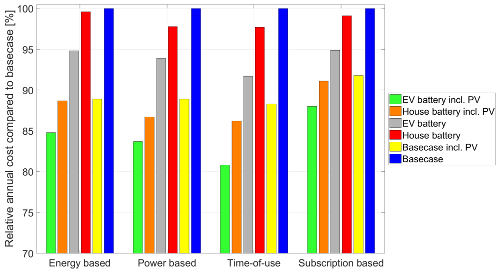

Fig. 6: Relative annual cost for different scenarios, all compared to the basecase cost.

Fig. 7 illustrates how the battery operates to minimize cost. The figure is an extraction of a day with high prices in 2015, shown for the house battery, and gives an indication of how the battery is charged during low price hours and discharged again during high price hours.

B. Battery SOC utilization

Fig. 8 illustrates how the batteries are being used in the case of a subscription based tariff. It also shows that the amount of energy passing through the battery is higher for an EV than a house battery. Although the EV battery is not always available, the increased power and energy capacity allows it to store more energy within its operating hours, which explains why the EV battery solution has higher savings. In addition, Fig. 8 also shows that the EV battery almost never is reduced below 40 kWh (50 % SOC). This implies that a battery half the size could provide close to equal cost reductions, and that this solution is not limited to EVs with big batteries.

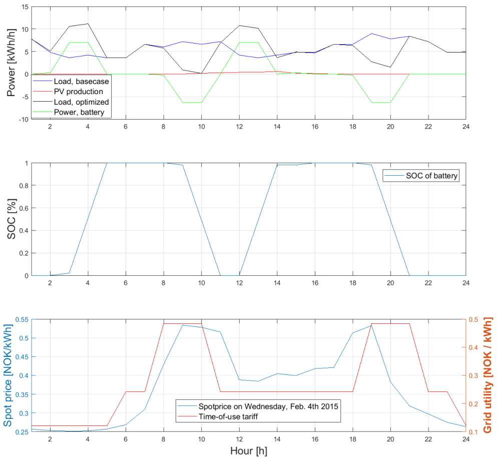

Fig. 7: Overview of basecase load, PV production, optimized load, house battery charge and discharge, SOC and spot price for October 20th, 2015.

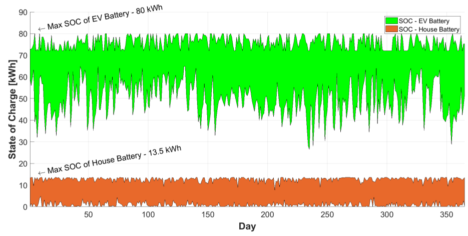

Fig. 8: SOC usage in kWh for both batteries.

C. Break even energy price

In order to determine which energy price is required for this investment to pay for itself, the net present value method is used. It is assumed that annual production remains at the 2015 level (5 439 kWh) for the lifetime of the PV panels. Discount rates of 3, 4 and 5 percent are analyzed to determine the break even cost of energy. According to [16], the cost of installing roof mounted PV in Norway is approximately 2 100 €per kWp. For the simulated 7 kWp installation, investment costs end up at 14 700 €. Even though the lifetime is guaranteed to be 25 years by most Norwegian PV merchants [16], the general statement is a lifetime of 30-40 years. 25 years is used as lifetime in these calculations. Because the primary use of an EV battery is to provide fuel for transport, the EV battery investment is considered to be zero. Due to few available house batteries at the market, with Tesla's Powerwall costing 8 400 €, break even calculations for PV and house batteries are not included. All assumptions made for these calculations are summarized:

Installed power photovoltaic	7 kWp
Cost per installed kWp	2 100 €/kWp
Lifetime	25 years
EV battery investment cost	0 €
Annual PV producton	5 453 kWh

The resulting break even price is shown in Tab. VII. The savings for the PV and EV battery system span from 444 - 710 €depending on grid tariffs, which with 5 453 kWh saves 8.65 - 13.00 €ct/kWh. In other words, those are the numbers which have to stand in comparison.

Three different installation cost scenarios are shown. The first one is calculated with today's prices in Norway [16]. The second one is with Norwegian prices, but includes subsidies from Enova (green project funding governmental organ). With 7 kW installed, the support provided by this governmental organ adds up to 1 956 €. For scenario two, the investment cost is therefore 12 651 €. The third scenario is calculated with German installation prices (1̃ 252 €/kWp) taken from [17], which adds up to 8 764 €.

TABLE VII: Break even energy cost for different discount rates. Note that the cost is the average cost saved per kWh produced by the PV, and includes all taxes and grid tariffs.

Scenario	Inv. cost	3 %	4 %	5 %
#1	14 607 €	15.39 €ct/kWh	17.15 €ct/kWh	19.01 €ct/kWh
#2	12 651 €	13.74 €ct/kWh	15.32 €ct/kWh	16.98 €ct/kWh
#3	8 764 €	9.01 €ct/kWh	10.13 €ct/kWh	11.23 €ct/kWh

D. Deciding economic factors

While today's conditions do not appear to provide economic reason to invest in PV and battery installations in Norway, several things can change in the future. The economic potential of this investment is still depending on:

- Future increase in energy prices [18]
- Future reduction in PV and battery prices [5] [2].
- Future grid tariff price and structure.
- Future electricity consumption behaviour [19].
- Degradation of battery and assumed battery investment cost.

VI. CONCLUSION

The presented results show that utilization of PV as of 2017 is on the verge of being economically profitable with Norwegian conditions due to high investment costs, low energy prices and semi-low irradiation, even with deterministic dynamic programming algorithms. However, the paper also shows that when Norwegian PV installation costs reach German levels (4̃0 % reduction), the investment will be profitable. Moreover, higher electricity prices e.g. due to raising CO2-prices will lead to even better profitability.

In general, the EV battery proved to provide more savings than a house battery due to capacity and power capabilities. Because an EV battery can be considered a "free" investment, net present value analysis of the system show better potential compared to a stationary battery which has very high investment costs compared to the savings provided. Still, the annual savings potential is fairly dependant on which grid tariff structure is being used, differing from 12.0 - 19.2 % for the PV and EV battery system compared to 8.9 - 14.4 % for the PV and home battery system.

For future work, it would be useful to study the economic potential under different scenarios for different EV availability profiles, load profiles and PV production profiles. Time resolution could also be increased in order to improve precision of PV and load data. In addition, the dynamic programming framework allows for including more technical details such as voltage, current, charging efficiency dependencies and battery degradation parameters. Another interesting aspect is to expand this model to a stochastic or rolling horizon dynamic programming algorithm, which could be used for simulating online operation under uncertainty.

ACKNOWLEDGMENT

We would like to thank Jørgen Erdal for his support to realize this model framework.

REFERENCES

[1] Lovdata, *Lov om klimamål (klimaloven)*, 2017, [Online; accessed 25-Oct-2017].

[2] IEA, "Global ev outlook 2016," http://bit.ly/1VK80Dx, 2016.

[3] SSB, "Klimagassutslippene økte i 2015," http://www.ssb.no/natur-og-miljo/statistikker/klimagassn/aar-forelopige, Oslo, Norway, May, 2016, [Online; accessed 11-December-2016].

[4] Elbilforeningen, "Elbilbestand, statistikk med antall registrerte elbiler i norge," https://elbil.no/elbilstatistikk/elbilbestand/, March 2017, [Online; accessed 08-May-2017].

[5] IEA, "A snapshot of global pv 2016," http://bit.ly/1NiTNea, 2016.

[6] J. Erdal, *En studie av økonomisk potensiale for PV-systemer og batterier i husstander for ulike nettariffer.* Trondheim, Norway: NTNU, Project thesis, 2016.

[7] I. Ranaweera and O.-M. Midtgaard, *Optimization of operational cost for a grid-supporting PV system with battery storage.* Trondheim, Norway: Renewable Energy, Volume 88 - Pages 262-272, April, 2016.

[8] Y. Levron, J. M. Guerrero, and Y. Beck, "Optimal power flow in microgrids with energy storage," *IEEE Transactions on Power Systems*, vol. 28, no. 3, pp. 3226–3234, Aug 2013.

[9] S. Bjarghov, *Utilizing EV Batteries as a Flexible Resource at End-user Level for Different Grid Tariffs.* Trondheim, Norway: NTNU, Master Thesis, 2017.

[10] I. Ranaweera, S. Sanchez, and O. M. Midtgård, "Residential photovoltaic and battery energy system with grid support functionalities," in *2015 IEEE 6th International Symposium on Power Electronics for Distributed Generation Systems (PEDG)*, June 2015, pp. 1–7.

[11] E. Figenbaum, M. Kolbenstvedt, and B. Elvebakk, *Electric vehicles - environmental, economic and practical aspects.* Oslo, Norway: Transportøkonomisk Institutt, GO, 2014.

[12] Tesla, "Tesla powerwall 2 data sheet," http://www.energymatters.com.au/wp-content/uploads/2016/11/tesla-powerwall-2-datasheet.pdf, 2017, [Online; accessed 8-May-2017].

[13] NIBIO and LMT, *Lov om klimamål (klimaloven)*, 2017, [Online; accessed 31-Oct-2017].

[14] Sanyo, "Sanyo hit-240hde4 - hybrid solar models," http://bit.ly/2xsWzaz, 2017, [Online; accessed 1-May-2017].

[15] NordPool, "Historical market data - spot price," http://www.nordpoolspot.com/historical-market-data/, [Online; accessed 29-January-2017].

[16] Accenture and WWF, *MOT LYSERE TIDER Solkraft i Norge – Fremtidige muligheter for verdiskaping.* Oslo, Norway: Accenture - Consultant firm and WWF - World Wide Fund for Nature, 2016.

[17] S. F. P. S. Strom, "Photovoltaik-kosten," http://bit.ly/2y9wRMO, [Online; accessed 2-June-2017].

[18] Statnett, *Langsiktig markedsanalyse Norden og Europa 2016–2040.* Statnett - Norwegian TSO, October 2016.

[19] H. Sæle, Ø. Høivik, and D. E. Nordgård, "Evaluation of alternative network tariffs - for residential customers with hourly metering of electricity consumption," http://bit.ly/2xvDqVr, 2016.

Appendix

Appendix A

Permutation Matrix and Reordering

Reordering is usually carried out with a permutation matrix such that multiplying a vector by it directly permutes its coefficients [120]. A new reordering format is proposed to permute vector of variables and consequently, the coefficient matrix associated with: Let $\Xi = (\xi_{i'=1}, \ldots, \xi_{i'=n})$ be new order of (permutation of) numbers $(1, 2, \ldots, n)$. Thus, the permutation matrix can be defined as:

$$\mathbf{P} \in \mathbb{R}^{n\times n} \quad where \quad p_{i',j} = \begin{cases} 1 & j = \xi_{i'} \\ 0 & \text{otherwise} \end{cases} \tag{A.1}$$

If we have a linear algebraic equation $\mathbf{AX} = \mathbf{B}$, where $\mathbf{A} \in \mathbb{R}^{n\times n}$ is the coefficient matrix, $\mathbf{X} \in \mathbb{R}^{n\times 1}$ is the vector of variables, and $\mathbf{B} \in \mathbb{R}^{n\times 1}$ is the righthand side, then permutation matrix properties can be expanded in Table A.1. These properties are basics rules used in the reordering section (section 2.1.3).

Table A.1: Properties of Permutation Matrix

Operation	Description
$\mathbf{P} \times \mathbf{X}$	Permutation of rows of the vector of variables: $[x_{\xi_1}, \dots, x_{\xi_n}]$
$\mathbf{P} \times \mathbf{A}$	Permutation of rows of the coefficient matrix: $[a_{\{\xi_{i'=1}, j=1\}}, \dots, a_{\{\xi_{i'=n}, j=n\}}]$
$\mathbf{A} \times \mathbf{P}$	Permutation of columns of the coefficient matrix: $[a_{\{i=1, \xi_{j'=1}\}}, \dots, a_{\{i=n, \xi_{j'=n}\}}]$
$\mathbf{P} \times \mathbf{P}^\top = I$	Multiplication of a permutation matrix into the transpose of permutation matrix is an identity matrix, this means that permutation matrices are orthogonal: $\mathbf{P}^{-1} = \mathbf{P}^\top$.